Investigation of the Effects of Mechanical Stress on the Permeability of Engineering Materials to Certain Cryogenic and Storable Propellants Used in Launch Vehicles

ANNUAL SUMMARY REPORT

Contract NAS 8-11322
Control No. DCN 1-4-50-01100-01(1F)
CPB 02-1152-64

Reporting Period:

30 June 1964 to 30 June 1965

NATIONAL AERONAUTICS AND SPACE ADMINISTRATION
GEORGE C. MARSHALL SPACE FLIGHT CENTER
Huntsville, Alabama

Prepared by:

P. J. Lare
W. R. DeBoskey
A. Divecha
H. Hahn

MELPAR, INC.
RESEARCH DIVISION
MATERIALS LABORATORY
7700 Arlington Boulevard
Falls Church, Virginia

September 1965

Investigation of the Effects of Mechanical Stress on the Permeability of Engineering Materials to Certain Cryogenic and Storable Propellants Used in Launch Vehicles

Annual Summary Report

Contract: NAS 8-11322
Control No.: DCN 1-4-50-01100-01 (1F)
CPB 02-1152-64

Reporting Period: June 30, 1964 to June 30, 1965

Melpar, Inc.
Research Division
Materials Laboratory
7700 Arlington Boulevard
Falls Church, Virginia

F. J. Lare
Metallurgical Engineer

W. R. DeBoskey
Sr. Metallurgist

A. Divecha
Sr. Metallurgist

H. Hahn
Research Leader

Approved by:
J. L. Pentecost
Manager
Materials Laboratory

FOREWORD

This report was prepared by Melpar, Inc., Falls Church, Virginia, under NASA Contract No. NAS 8-11322 for the George C. Marshall Space Flight Center of the National Aeronautics and Space Administration. The work was administered under the technical direction of the Propulsion and Vehicle Engineering Laboratory, Materials Division of the George C. Marshall Space Flight Center with Mr. John G. Austin acting as project manager.

TABLE OF CONTENTS

TABLE OF CONTENTS (Continued)

LIST OF ILLUSTRATIONS

LIST OF ILLUSTRATIONS (Cont.)

LIST OF TABLES

LIST OF TABLES (Continued)

LIST OF TABLES (Continued)

1. INTRODUCTION

This report covers research performed during the first year under contract NAS 8-11322 for "An Investigation of the Effects of Mechanical Stress on the Permeability of Engineering Materials to Liquid Hydrogen and Other Propellants Used in Launch Vehicles."

The principal objectives of the past year's effort have included the design, development, and qualification of apparatus and procedures for the measurement of permeability rates of fluids through stressed materials. Twelve materials (ten plastics and two metals) were selected by the sponsoring agency for initial investigation. Three basic pieces of permeability apparatus have been developed for the various permeating fluids. These fluids include liquid hydrogen, liquid nitrogen, liquid oxygen, monomethylhydrazine, and nitrogen tetroxide. In addition to permeation tests, the previously mentioned twelve materials have been characterized in terms of their mechanical properties at room and liquid nitrogen temperature, as well as in terms of their compatibility with the permeating fluids, particularly with monomethylhydrazine. While metal diaphragms were subjected to major fractions of their biaxial yield stress during testing, polymeric materials -- due to their low yield strength and broad plastic range -- were stressed in excess of their yield strength.

The sensitivity of the apparatus and instrumentation, depending upon the fluid under consideration, permits the measurement of permeation rates in the range of approximately 10^{-10} to 10^{-17} SPU.* This range may be broadened by altering diaphragm configuration, instrumentation, and/or test procedures.

* One permeability unit (SPU) is defined as the number of cubic centimeters of gas at STP (0°C, 1 atmos.) passing through one square centimeter of material, one centimeter thick, under a pressure gradient of one centimeter Hg (10 torr) in one second.

Preliminary permeability screening of all polymeric materials together with chemical compatibility tests have eliminated many of the materials from further testing, and preclude their use as bladder materials or in fluid containers. Lack of compatibility with monomethylhydrazine, high imperfection count, and poor properties at cryogenic temperature were found to be common to many of the film polymers.

An intensive schedule of permeability tests for the second year of research includes primarily reinforced composites, laminates, honeycomb structures, and adhesive bonds. The number of permeating agents has been reduced to four with the elimination of nitrogen tetroxide.

No basic changes in apparatus or procedures are contemplated in future tests.

2. LITERATURE SURVEY

2.1 General Considerations

It is well known that gases can permeate most solid and colloidal membranes. Essentially, the mass transfer of a gas from one surface of a membrane to the other involves the following steps:

a. Adsorption on the barrier surface

b. Solution in the membrane

c. Diffusion

d. Dissolution

e. Evaporation at the opposite surface

Any one of the phenomena enumerated above may be rate controlling in permeation. However, when (c) above is the rate-controlling factor, the permeation phenomenon can be treated by Fick's Law for undimensional diffusion, where

$$J = -D \frac{\partial c}{\partial x} \qquad (1)$$

and Henry's Law for solubility which states that

$$S = kp \qquad (2)$$

where S - solubility

k - solubility constant

p - gas pressure

c - concentration within the membrane

D - diffusion constant

$\frac{\partial c}{\partial x}$ - concentration gradient

If D is independent of concentration, for the stationary state, then

$$\frac{\partial c}{\partial x} = \frac{\Delta c}{\delta} = \frac{S\Delta p}{\delta} \tag{3}$$

where δ is the thickness of the membrane. Combining equations (3) and (1), gives the relationship

$$J = -D\,S\,\Delta p/\delta \quad \text{or} \quad -Dkp\,\frac{\Delta p}{\delta} \tag{4}$$

and since P = DS, it follows that steady state permeability is a function of the pressure difference, the area, and the thickness of the membrane.

The above treatment is basically applicable in case of amorphous polymers in which the gas transport is diffusion-controlled. However, certain factors, physical and chemical, have to be taken into account which determine k and D.

2.2 Factors Affecting Permeability of Gases Through Polymers

2.2.1 Temperature

Barrer[1] has examined the effect of temperature (0 to 65°C) on the permeability and diffusivity of gases through numerous polymeric materials using the standard Arrhenius type of equation:

$$A = A_0 \exp -\left(\frac{Q}{RT}\right) \tag{5}$$

where A - diffusivity, or permeability

Q - activation energy for the process

R - gas constant

and T - absolute temperature

Solubility of a gas in a polymer such as polyethylene has also been shown to be temperature dependent and can be expressed as

$$S = k_o \exp\left(- \frac{\Delta H}{RT} \right) \qquad (6)$$

where k_o is a constant and ΔH is the apparent heat of solution.[2] It should, however, be mentioned that permeability P is more temperature dependent than solubility.

2.2.2 Crystallinity

The degree of crystallinity in polymers is perhaps the most important factor which determines permeability. In a completely amorphous polymer, permeation is a simple diffusion-controlled process. However, the flow process is more complicated in a micro-crystalline polymer such as polyethylene. It has been established that diffusivity and solubility decrease as the degree of crystallinity increases, suggesting that solubility of gases in the crystallites is negligible. Michaels and Parker[3] propose that the polymer structure may be thought of as consisting of crystallites randomly distributed in an amorphous phase. Impedance to permeation is then dependent upon the geometry and orientation of the impermeable (crystalline) phase. The permeating gas molecules have to, of necessity, bypass crystallites and diffuse through amorphous region of the polymer. Thus crystallites tend to reduce the chain mobility and increase the energy barrier for diffusion. Physically, the above phenomenon can be explained by the following equation[3]

$$D = D_a/\tau \qquad (7)$$

where D_a is the diffusion constant in a completely amorphous polymer (e.g. polyethylene), and τ is the tortuosity factor. Hence, permeability, diffusivity and solubility are related by

$$P = DS = \frac{D_a}{\tau} \quad X_a) \qquad (8)$$

and

$$S = S_a \; X_a$$

where X_a is the amorphous volume fraction of the polymer and subscript (a) refers to the amorphous phase.

Other factors that affect polymer permeability include pressure, the size and shape of the diffusing gas species and composition of the gaseous medium. For example, pressures of up to several atmospheres usually have little effect on permeability, diffusivity or solubility. However, it has been reported[4] that the "permeability at low temperatures is lower than at high temperatures at low partial pressures but at higher pressures the order is reversed. At each pressure there is a temperature at which the permeability is a minimum." See figure 1.

As already mentioned, the rate at which a gas permeates in a polymeric material is dependent upon the size of the molecular diameter of the gas. Thus, Van Amerogen[5] has shown that helium with a diameter of 1.9 Å will diffuse faster than hydrogen which has a diameter of 2.4 Å. In a mixture of gases, each gas will act individually depending upon the partial pressure of each component gas.

E0853

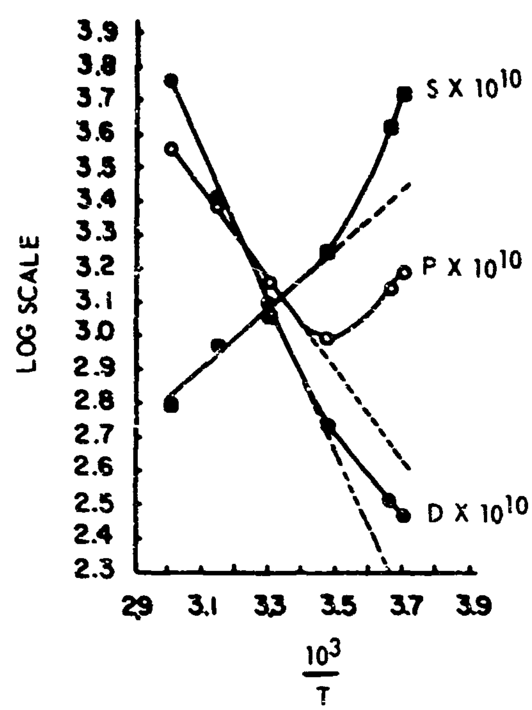

Figure 1. Variation of P, D, and S with Temperature

2.2.3 Effect of Stress on Permeability

The role of stress in permeability has thus far received little experimental attention. Though permeability appears to increase with stress, the relative contribution to permeation by extended pores and "true" increase in permeability is not known.

Barrer[6] considered the problem from a theoretical point of view, based on a simplified model. He calculated the effect of elastic displacement, i.e., elastic strain, upon the potential energy barrier for diffusion in a simple two-dimensional square methane lattice. The results show that the effect of elastic strains is to reduce the activation energy for diffusion considerably. It may be noted that the effect of the heats of solution are very small, and hence are neglected.

2.2.4 Effect of Polymer Composition on Permeability

The composition of the polymer itself has been shown to be a very prominent factor affecting permeability. Thus, in a simple hydrocarbon polymer such as polyethylene, its structure uniquely determines its permeability to gaseous mediums. When other atoms are introduced into the chain structure, diffusivity (D) and solubility (S) change appreciably. As a result, permeability (P) which is a product of D and S is also affected. For example, addition of one chlorine atom per ethylene unit reduces D and P. Successive additions of chlorine atoms to the polyvinyl chloride chain greatly reduce the permeability and hence, vinylidene chloride and vinylidene-acryonitrile copolymers (Saran) have the lowest permeabilities.[7]

Toth and Barber[8] measured hydrogen and nitrogen permeabilities in polymers such as Tedlar, Mylar, etc., and in electrodeposited silver and nickel. As expected, the permeability values of the polymers were much higher than those of the metals (see table 1).

2.3 Review of Experimental Data

Though the process of permeation has been studied since as early as 1866, the experimental methods used today to measure diffusion of gases through solids and membranes are basically unchanged. For example, a rigidly-supported membrane is brought into contact with the diffusing gaseous material. The chamber or vessel on one side of the membrane is evacuated so that the pressure is almost zero, or very small, compared to the gas pressure on the other side of the membrane. The rise in pressure in the evacuated chamber may be measured by a McLeod gauge as a function of time which, in turn, is a measure of permeability.

The conventional method of measuring permeability is due to Barrer[1] -- the so-called "Time Lag" method. (See figure 2.) The pressure rise on the low pressure side is measured as a function of time. By this method, it is possible to determine D directly, using the following equation:

$$L = \frac{h^2}{6D} - \frac{c_o h^2}{2Dc_1} \qquad (9)$$

where h - the thickness of the membrane

L - time lag

For a detailed description and derivation of this equation see reference 9.

Table 1. Unstressed Room Temperature Permeability of Selected Materials (Taken from Toth)[8]

Material	Membrane Thickness,	Permeability P* x 10^{-9} at STP	
		Hydrogen Gas	Nitrogen Gas
Mylar A	2	8.6	1.1
		13.0	1.6
Seilon UR 29E Polyurethane	5	50.0	7.1
		54.0	9.0
Tedlar BG-30-WH	2	5.7	3.8
		6.9	2.7
H Film**	1	23.0	1.0
		24.0	1.4
Electrodeposited Silver	10	less than 0.04	less than 0.04
Electrodeposited Nickel	7	less than 0.03	less than 0.03

*P in units of $cm^3/sec\ cm^2\ cm$

** Manufactured by duPont

E0854

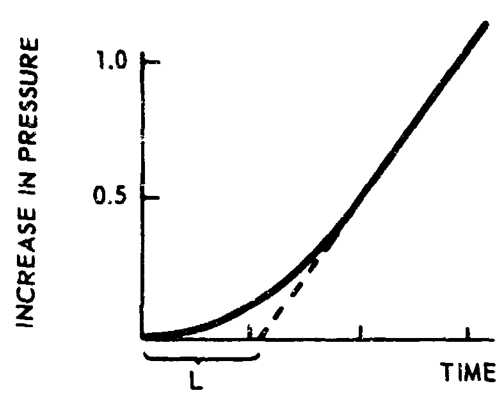

Figure 2. Establishment of a Steady State in Diffusion Through a Membrane. Time Lag Defined by L.

ıce permeation is a highly sensitive process, care must be exercised in measuring the thickness and density of the test material. In the case of polymers, these measurements and previous fabrication history assume vital importance.

Permeability and diffusion characteristics of literally hundreds of polymers and metals have been studied. The purpose of this section is to present, in a concise fashion, some of the more important data obtained by various investigators in this field.

Barrer[1] determined permeability constants P of numerous polymer–gas systems in a limited (0 to 65°C) temperature range. Typical values of P are presented in table 2. He also obtained temperature coefficients of permeability as defined by the equation

$$P = P_o \exp\left(\frac{-Q}{RT}\right) \text{ (see table 3)} \qquad (10)$$

It may be noted that activation energies for the diffusion in organic membranes are comparatively low and lie in the range of 6 to 12 k cal/mole.

Due to its importance in the packaging industry, the permeability of polyethylene has been a subject of many investigations. Generally speaking, the permeation of gases through polyethylene has been related to the volume fraction of crystalline material by measurement of polymer density.[10 11 12] However, the mechanism of flow of gases is not known precisely. In addition, it is quite difficult to reconcile data generated by different investigators.[13]

Harvey Alter,[14] from results of previous investigators and his own experiments, found that the density of a polyethylene material is sensitive to its thermal and processing history. Thus, it is possible that a

Table 2. Permeability Constant P* for Various Gas-Polymer Systems (Taken from Barrer[1] and Jost[9])

System	Temp. °C	P x 10^6
He - Neoprene (vulcanized and with filters)	0	0.0022
He - Neoprene (raw, unvulcanized)	21.6	0.0039
H_2 - Polystyrene - Butadiene polymer	19.9	0.0084
H_2 - Butadiene - methyl methacrylate	20.0	0.023
H_2 - Neoprene (vulcanized commercial polychloroprene)	17.5	0.0085
N_2 - Neoprene	27.1	0.00137
N_2 - Butadiene methyl methacrylate polymer	21.2	0.0028
N_2 - Polystyrene - butadiene polymer	20.0	0.0029

*P in units of cc/sec/cm^2/mm/cm Hg

Table 3. Heats of Activation, Q, of Permeability Constant (in cal/mole) for Various Polymers (Taken from Barrer[1] and Jost[9])

Membrane Q (cal/mole)	He	H_2	N_2
Rubber (vulcanized)	6300	6000	-
Rubber (unvulcanized)	6400	6500	-
Neoprene (vulcanized)	8000	8300	10,500
Butadiene acrylonitrite	-	8200	9,800
Butadiene methyl methacrylate	-	-	9,500
Butadiene polystyrene	-	-	7,900
Chloroprene	-	8300	-

single sample of the polymer may have varying densities, depending upon the rate of crystallisation. In the course of this work, the density of each specimen was measured individually before experimentation. Data obtained by Harvey Alter and other workers[3 11 12 14 15] are presented in figure 3, for comparison.

The effect of temperature and molecular diameter of gases on permeation and diffusion was investigated by Waack et al.[16] It was found that for all the polymers tested, permeability increased in the order N_2, O_2, CO_2, indicating that permeability increases with decreasing molecular diameter. In addition, permeation and, hence, diffusivity increase with increasing temperature.

Several polymeric films were evaluated for hydrogen permeability in the temperature range of -100 to 200°F (table 4).[17] It is readily seen that permeability decreases rapidly with temperature in every case. Figures 4, 5, and 6 are the plots of permeability versus the reciprocal of temperature obtained by using the Arrhenius equation. Note that this relationship is valid in all cases over a part of the temperature range with the exception of Teflon for which the curve is non-linear. Evidently, the mechanism of permeation undergoes a change at the temperature at which the nonlinearity is observed. An attempt to correlate this temperature with the glass transition temperature proved unsuccessful.

As in the case of hydrogen gas, oxygen and nitrogen permeability also reduce drastically with temperature, as shown in figure 7.[18] Extrapolating the curve into the cryogenic range, the permeability would decrease further but at a much slower rate.

E0855

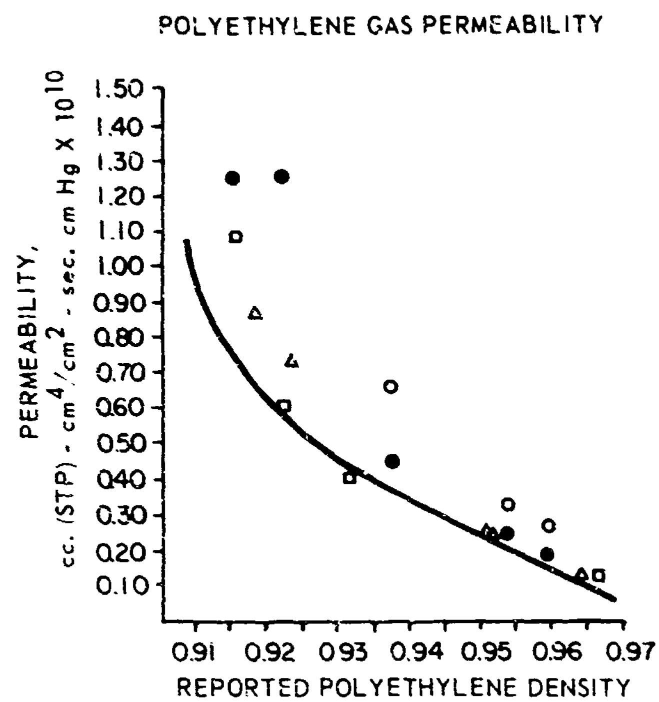

Data of Harvey Alter; (O) Data of Myers et al.;[11] (●) Data of Myers et al.;[12] (□) Data of Michaels and Parker;[3] (▲) Data of Brandt.[15]

Figure 3. **A Comparison of Reported Permeabilities of N_2-Polyethylene System at 25°C**

Table 4. Hydrogen Permeability Values at Selected Temperatures

Permeability $\frac{\text{std cc cm}}{\text{sec cm}^2 \text{ cm Hg}} \times 10^{-11}$

Material	200°F	150°F	100°F	50°F	0°F	-50°F	-100°F
H-Film	-	58	29.0	14.0	5.4	1.7	0.17
Mylar	50	23	9.4	3.4	0.97	0.16	-
Tedlar	100	36	9.6	2.1	0.32	-	-
Polyethylene	-	-	97.0	25.0	4.7	0.75	0.05
Kel-F (Kx8105)	170	66	19.0	5.0	0.96	-	-
Teflon FEP	-	300	135.0	52.0	14.0	2.4	0.15
Kel-F (Kx8205)	172	61	19.0	5.2	1.1	0.13	-

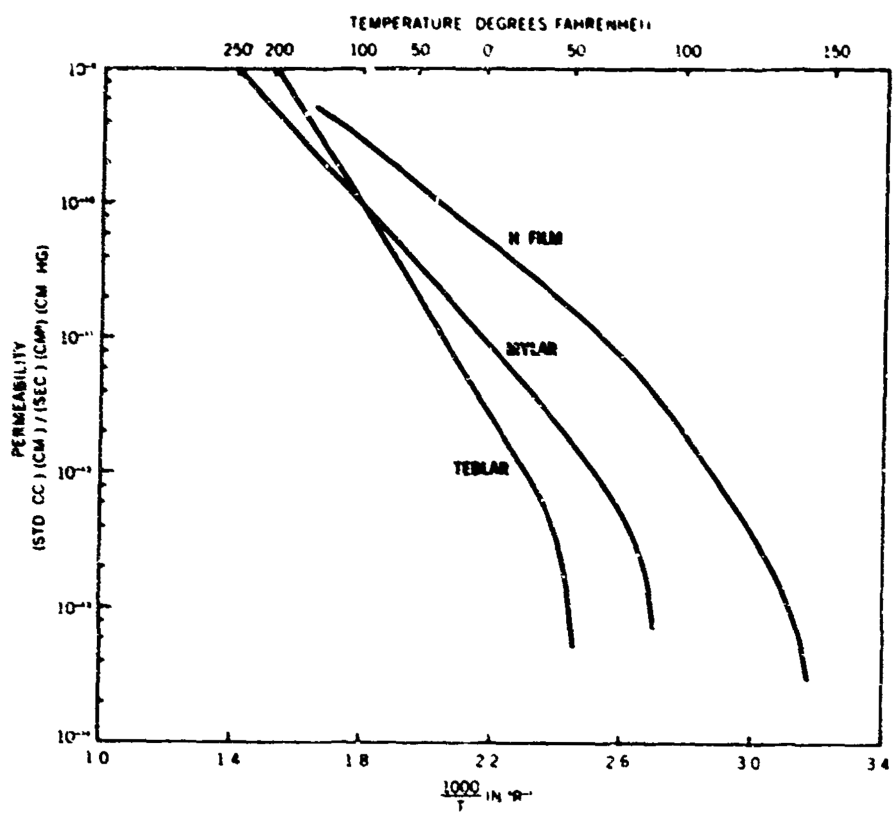

Figure 4. Hydrogen Permeability of H-Film, Mylar, and Tedlar

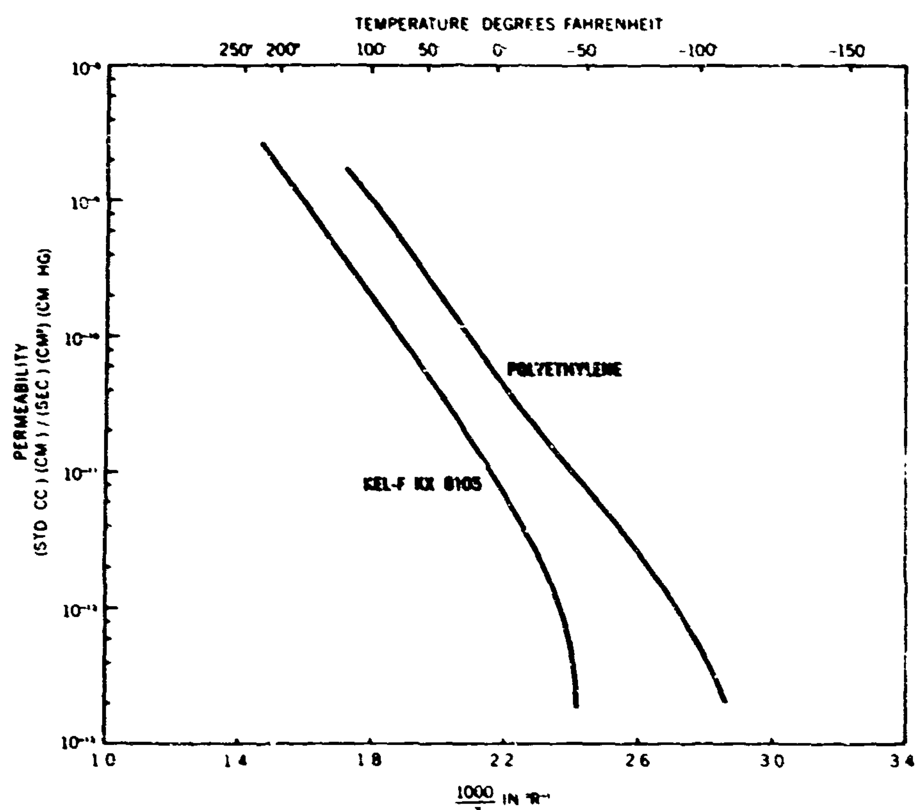

Figure 5. Hydrogen Permeability of Polyethylene and Kel-F (Kx8105)

E1428

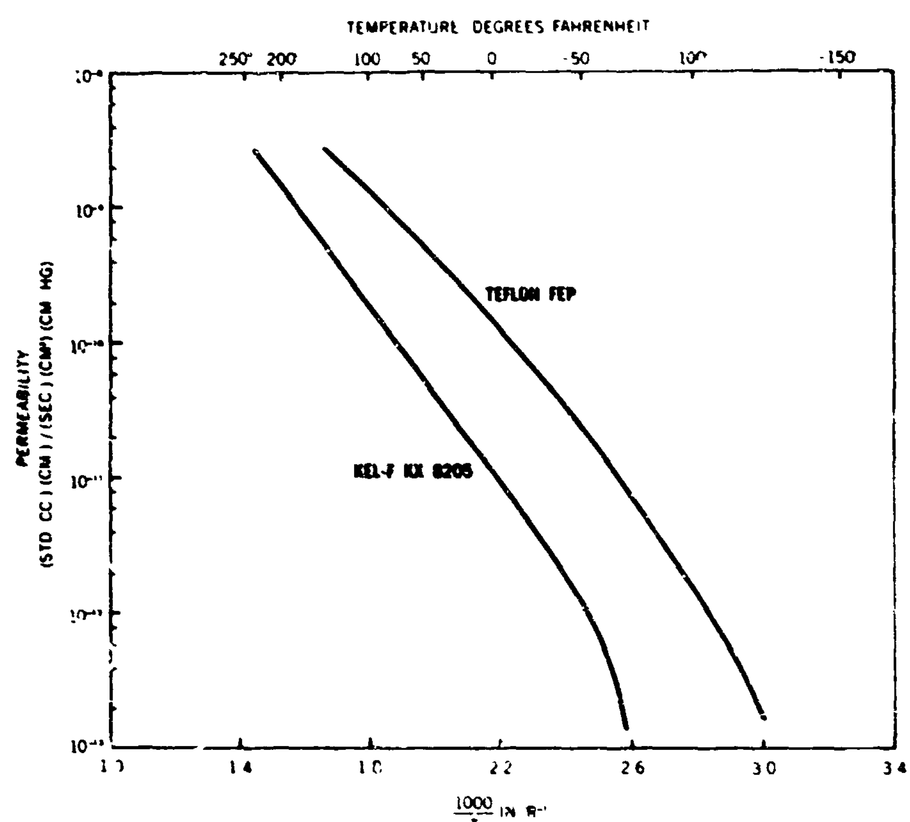

Figure 6. **Hydrogen Permeability of Teflon FEP and Kel-F (Kx8205)**

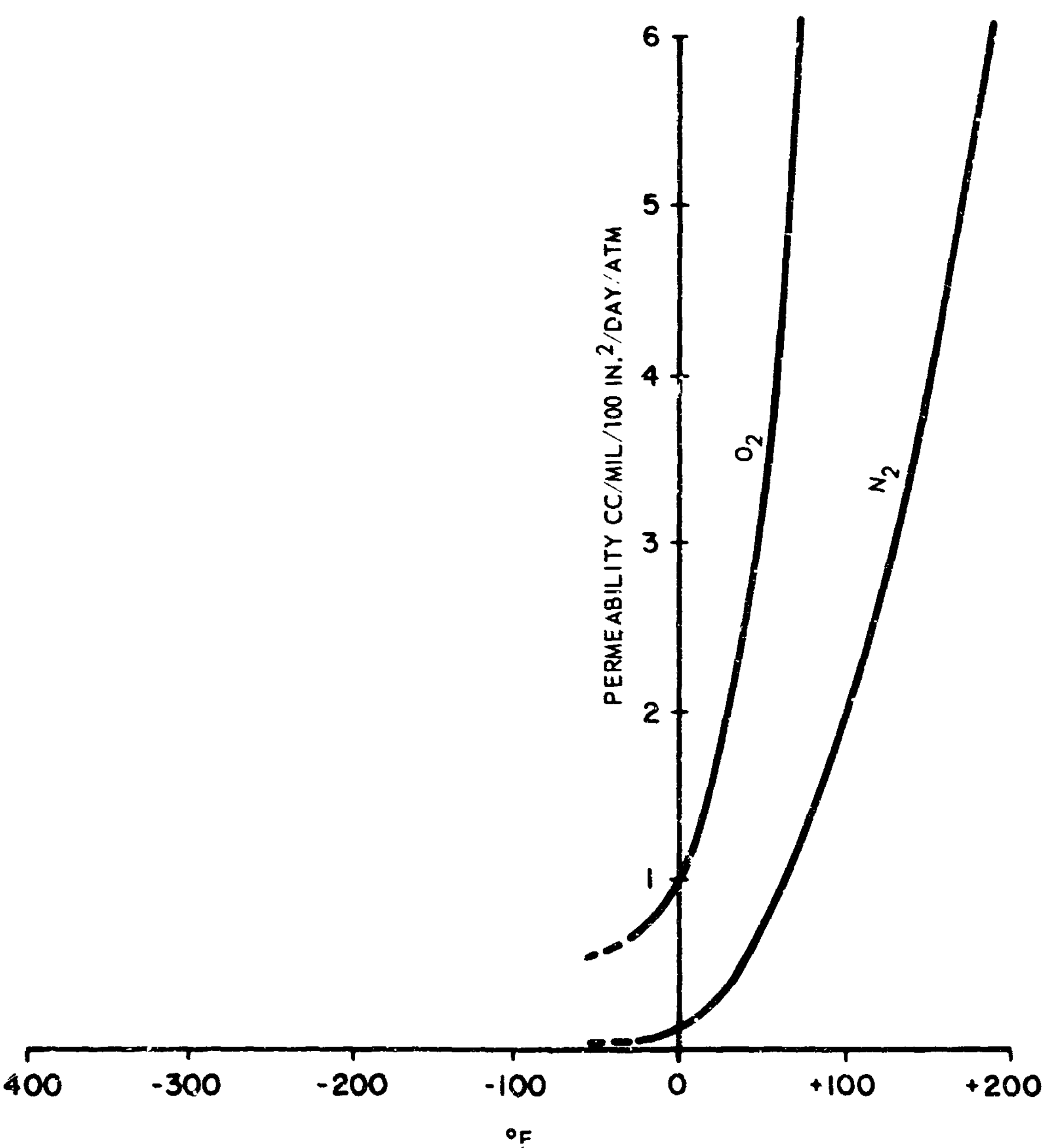

Figure 7. Oxygen and Nitrogen Permeability of Mylar

Permeation of gases through metals has been studied extensively.[19, 20] Of particular interest is the work of J. K. Gorman and W. R. Nardella[21] who measured permeation rates U* of hydrogen through several metals of interest commonly used for vacuum envelopes (i.e., nickel, OFHC copper, Kovar, stainless steel, Monel, Inconel, etc.). The results of this investigation (see table 5) indicates that the permeation process is strongly temperature-dependent. The low value of copper (-37×10^{-2}) at 1000°K is probably related to its comparatively low hydrogen solubility. It may be noted that the value of U for stainless steel is much lower than iron and cold drawn steel probably because of the presence of chromium in the former alloys.[21]

Table 5. Hydrogen Permeation Through Metals

Sample	U at 727°C (1000°K)	U at 427°C (700°K)
Nickel	3.32	19.1
Copper	0.37	0.74
Kovar	0.55	1.75
Stainless Steel, 303	0.60	1.80
Stainless Steel, 304	0.58	1.45
Iron	4.17	68.70
Cold-drawn Steel	3.70	57.4
Monel	1.77	11.0
Inconel	1.20	3.26

3. TEST APPARATUS

3.1 Cryogenic Chambers

A schematic diagram of the two systems fabricated is shown in figure 8. The nitrogen-oxygen and hydrogen systems differ principally in the design of the dewar chamber, the former being the one-stage type and the latter being the two-stage type.

The fluid chambers have been designed for 0 to 300 psig operation. The high pressure is to ensure the attainment of near yield stresses in the metal diaphragm specimens.

3.1.1 Liquid Hydrogen System

The hydrogen system (figure 9) and its control console (figure 10) are housed in a remote building (figure 11) designed and constructed especially for this purpose. The test cell housing the apparatus is fire- and explosion-proof and essentially all operations (while the system is charged with fluid) may be performed remotely. The control console and all recording instruments are separated from the LH_2 system by the test cell wall.

3.1.2 Liquid Nitrogen System

The nitrogen system is shown in figure 12. This system is located in the remote permeability test facility on the outside wall of the operation's area. This location was chosen to concentrate all test equipment in one location wherein explosion and fire are not a problem. To facilitate construction, manual valves were installed for all control and operations.

3.2 Room Temperature Chamber

The room temperature chamber for permeability studies of monomethylhydrazine and nitrogen tetroxide is illustrated in figures 13 and 14.

E0860

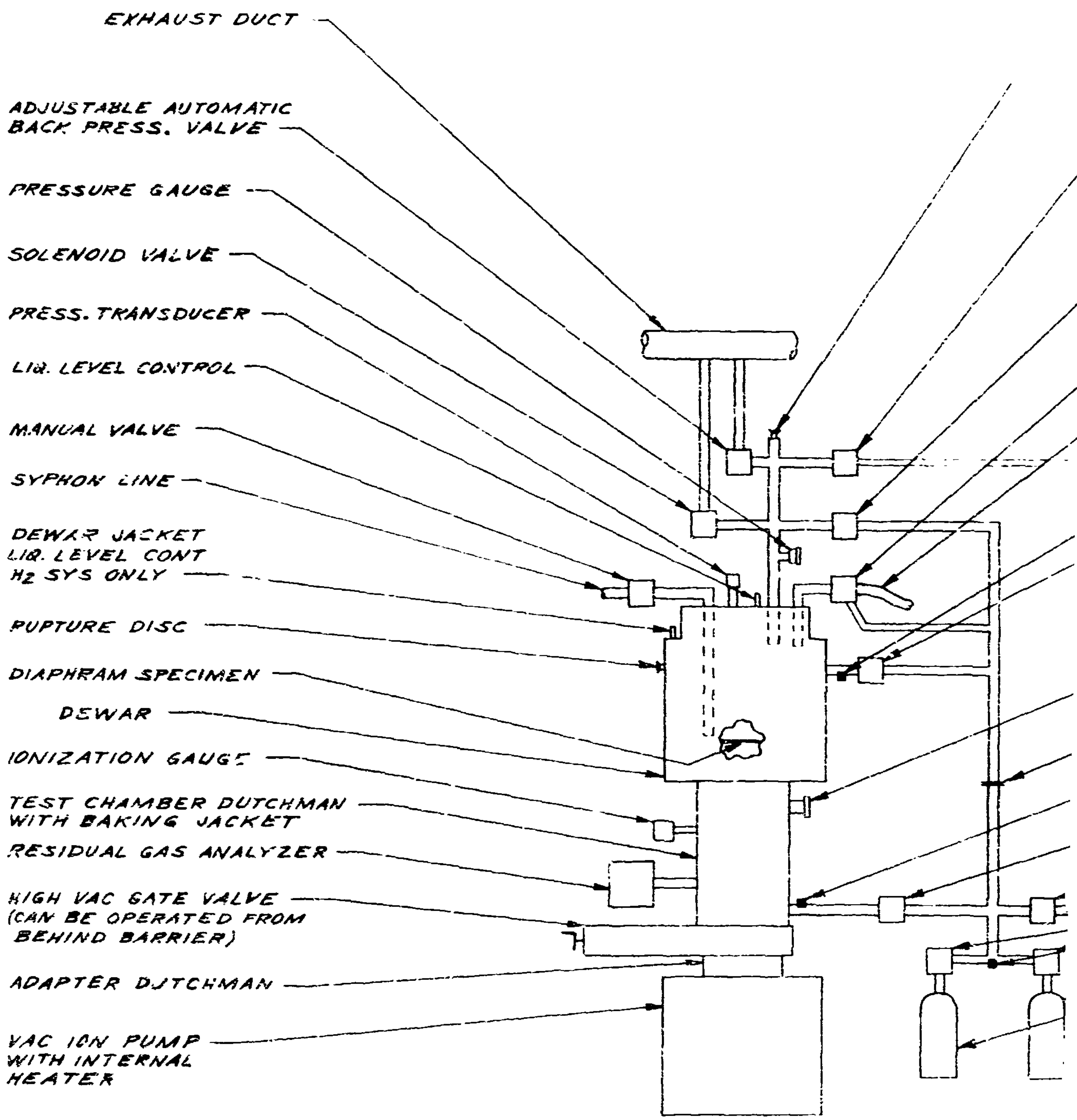

EXHAUST DUCT
ADJUSTABLE AUTOMATIC BACK PRESS. VALVE
PRESSURE GAUGE
SOLENOID VALVE
PRESS. TRANSDUCER
LIQ. LEVEL CONTROL
MANUAL VALVE
SYPHON LINE
DEWAR JACKET LIQ. LEVEL CONT H2 SYS ONLY
RUPTURE DISC
DIAPHRAM SPECIMEN
DEWAR
IONIZATION GAUGE
TEST CHAMBER DUTCHMAN WITH BAKING JACKET
RESIDUAL GAS ANALYZER
HIGH VAC GATE VALVE (CAN BE OPERATED FROM BEHIND BARRIER)
ADAPTER DUTCHMAN
VAC ION PUMP WITH INTERNAL HEATER

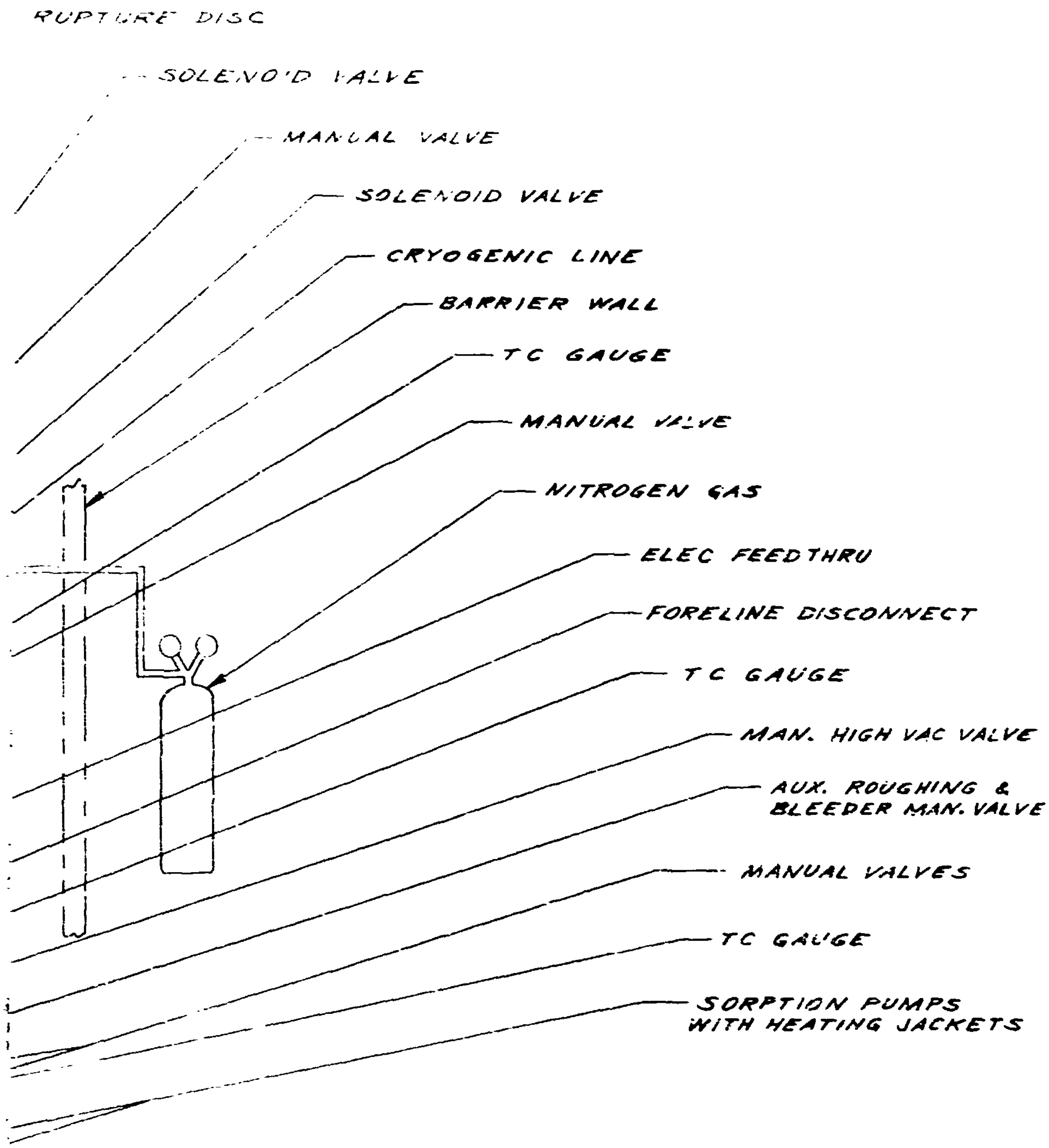

Figure 8. Schematic Diagram of Cryogenic Permeability Apparatus

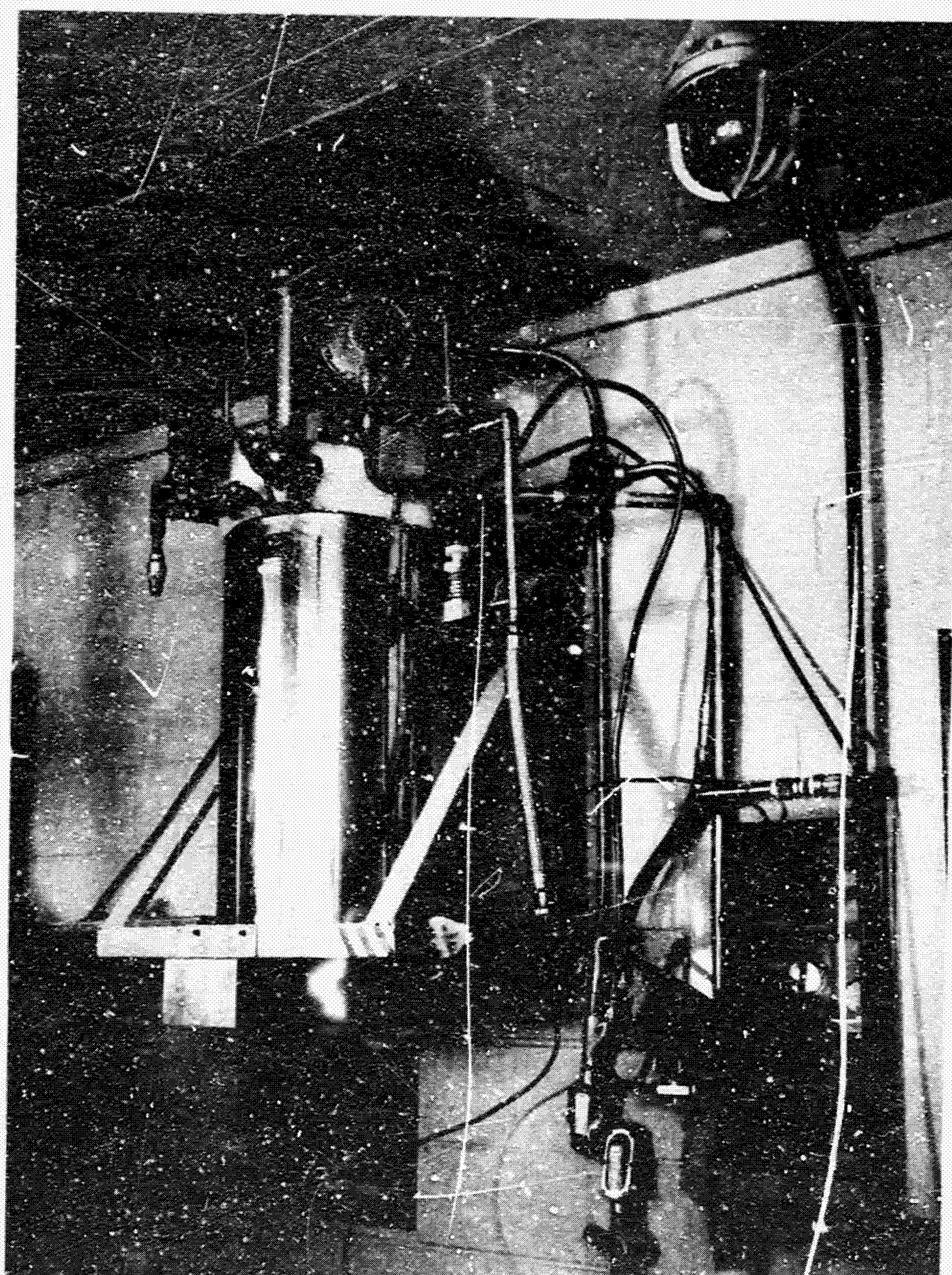

Figure 9. LH_2 Permeability Chamber in Test Cell

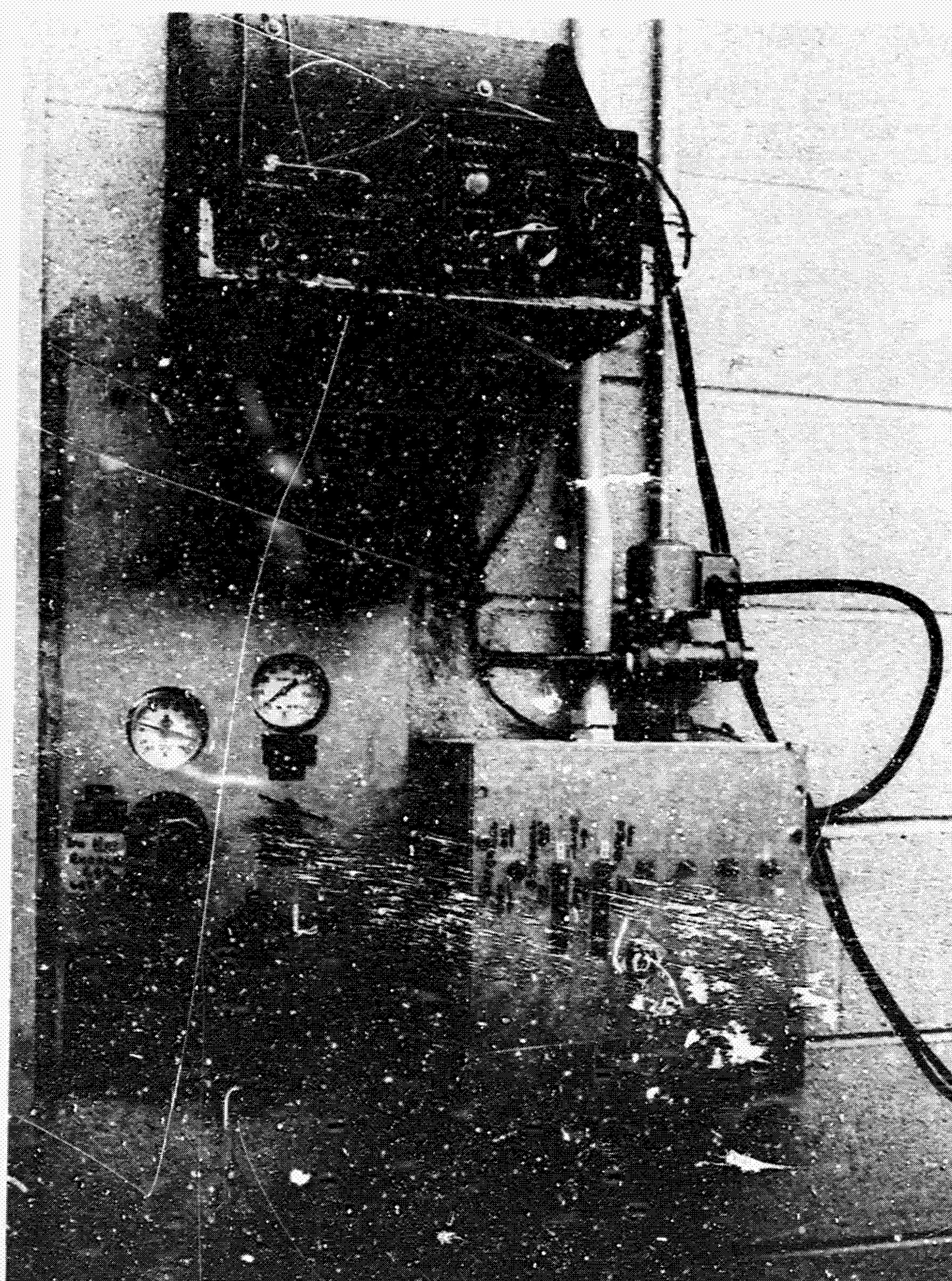

Figure 10. LH_2 System Control Console

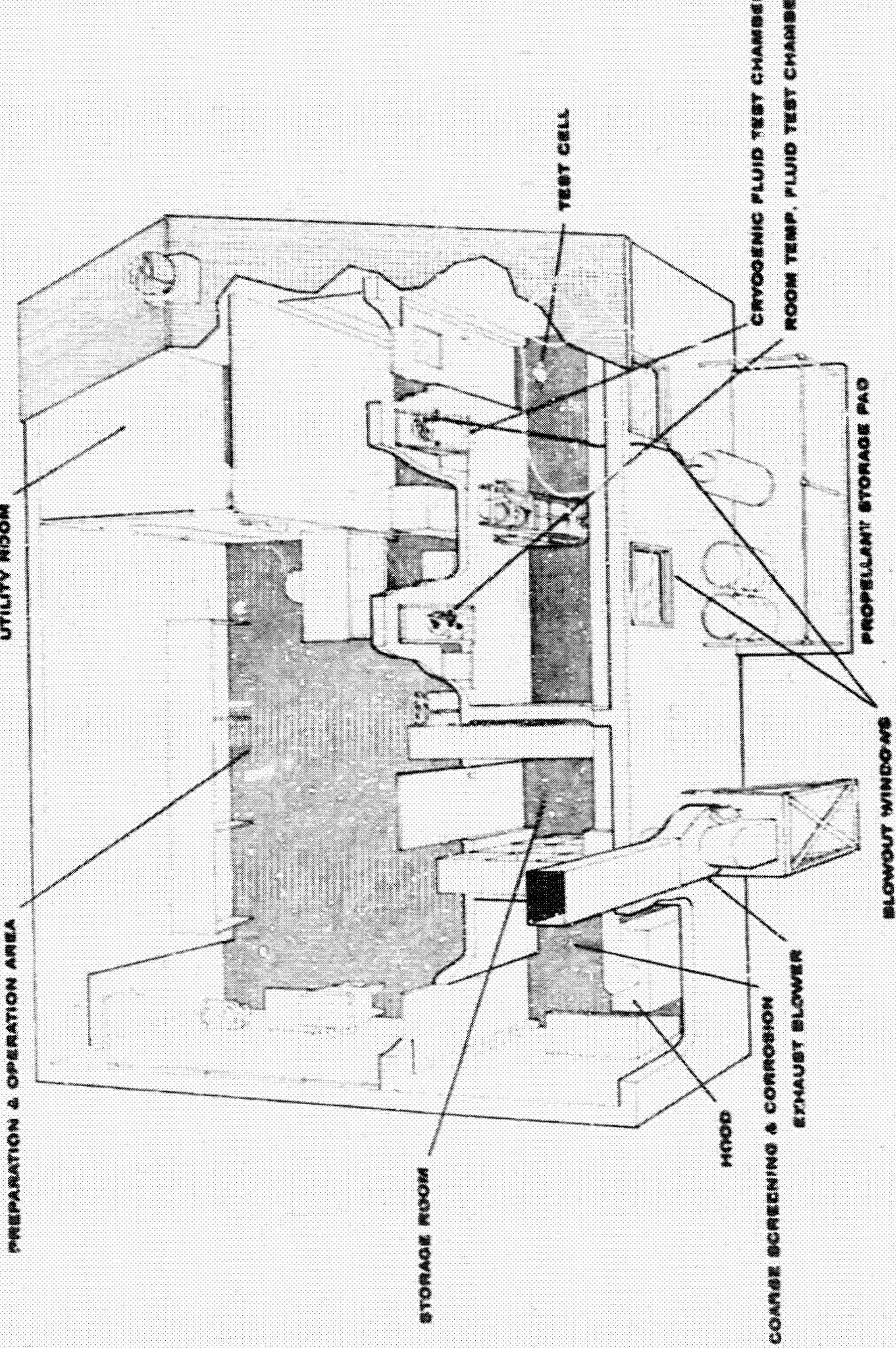

Figure 11. Permeability Test Facility

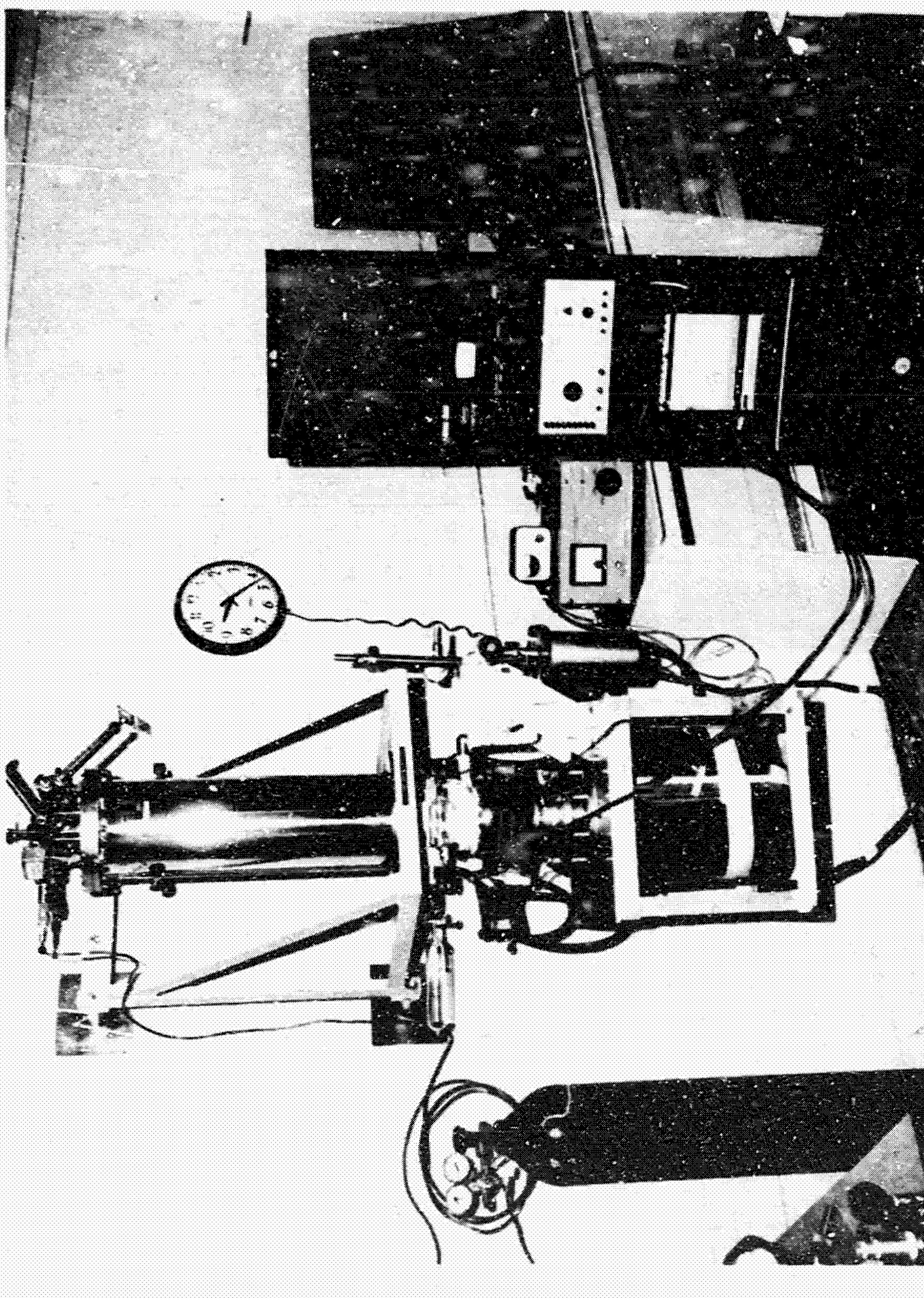

Figure 12. LN_2 Permeability Apparatus

R535046

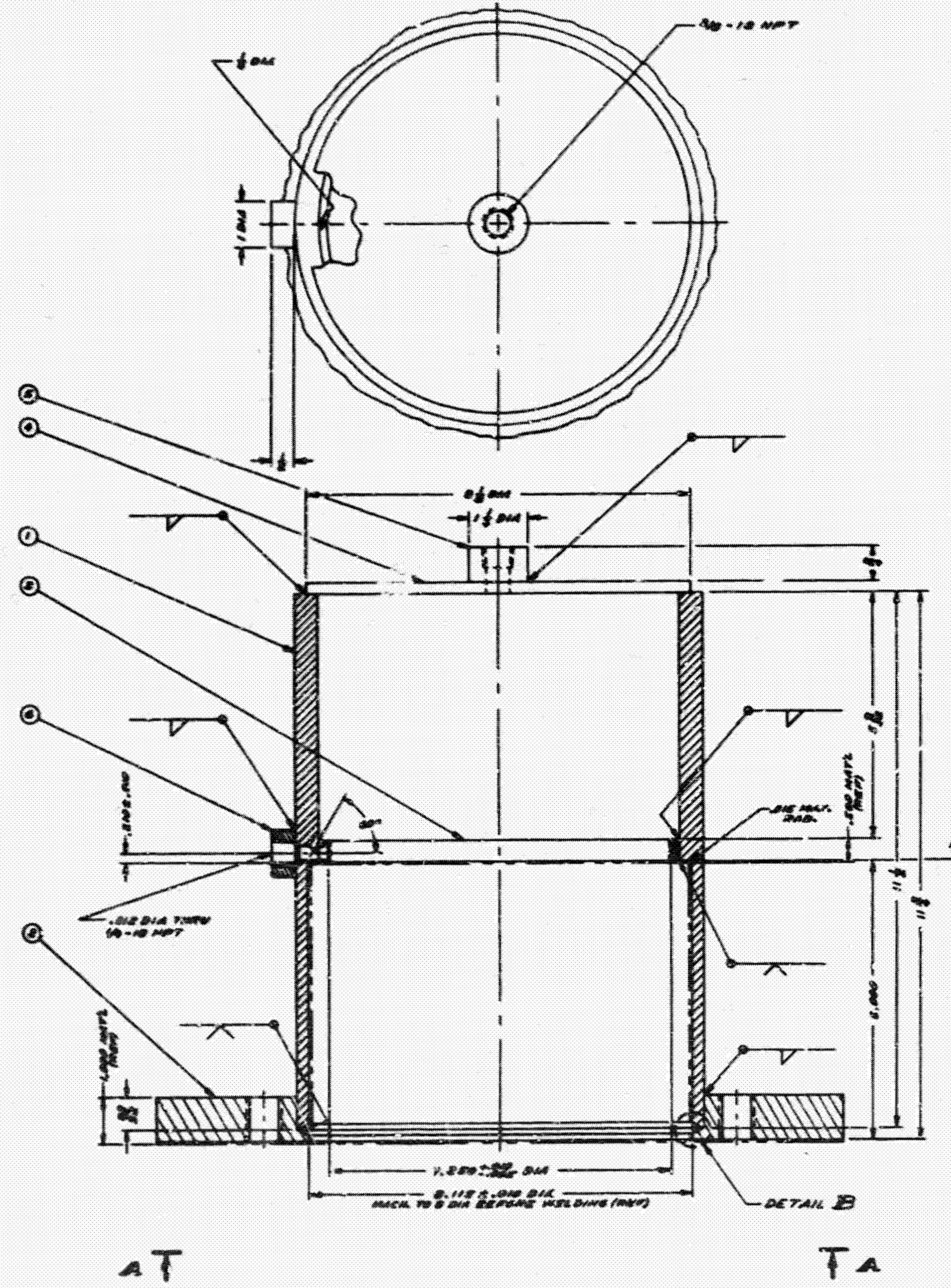

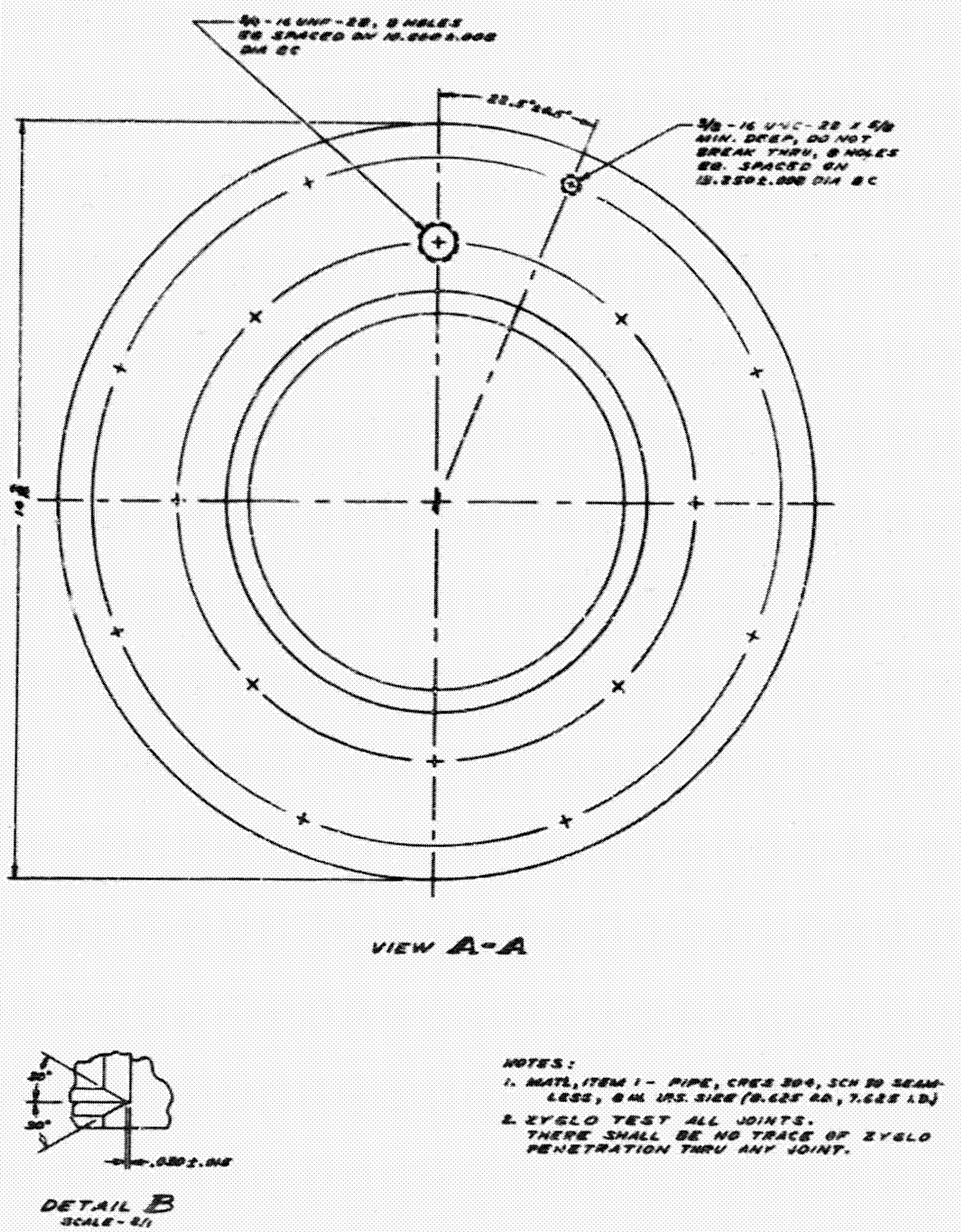

Figure 13. Room Temperature Permeability Chamber

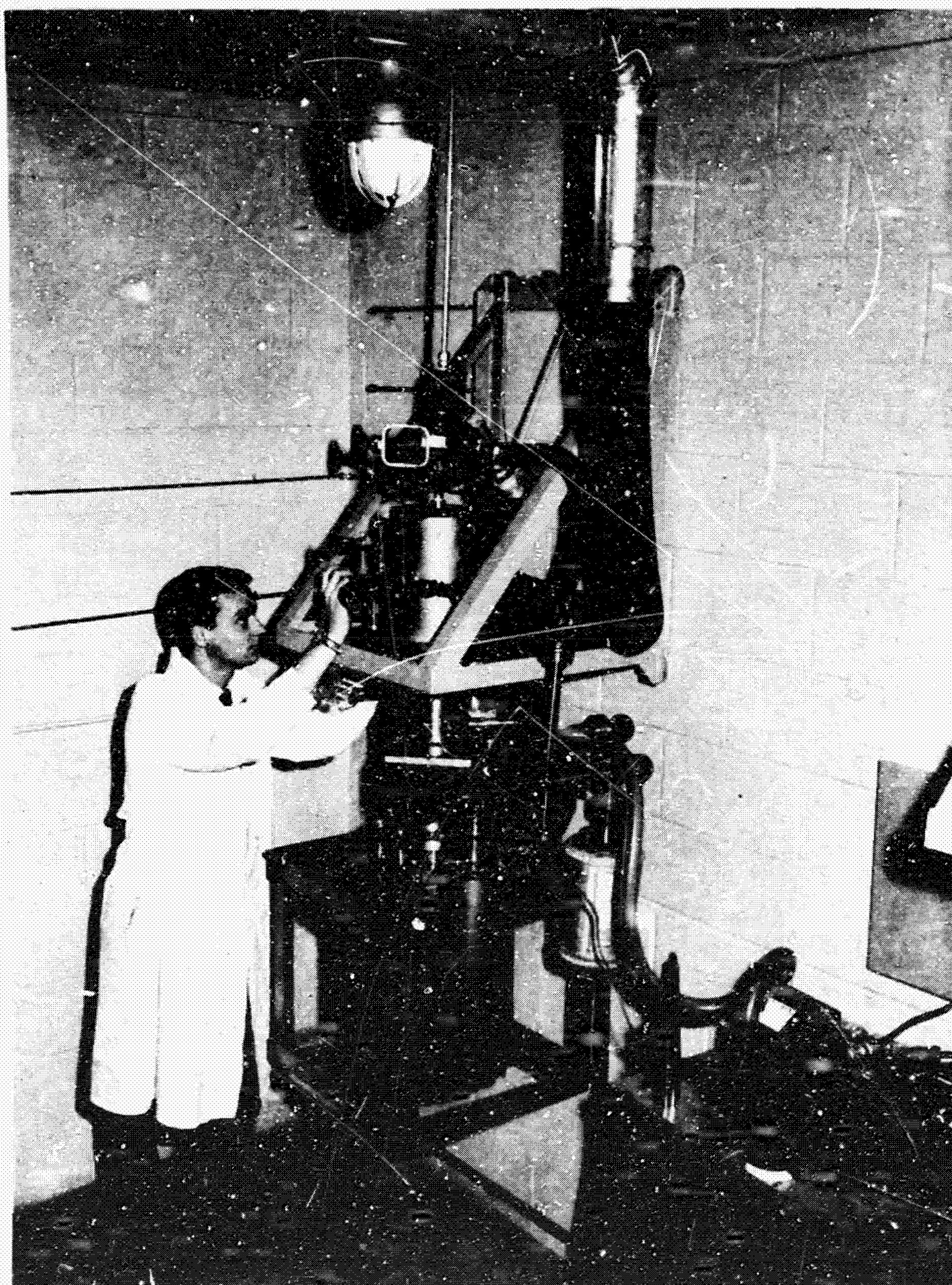

Figure 14. Room Temperature Permeability Apparatus

This chamber differs from the cryogenic chambers in that the dewar jacketing is eliminated. The test fluids are charged by pressurizing the supply sources and are drained by gravity. Upon removal of the test fluid, the system may be flushed with either a Freon MF solvent or acetone which may be followed by gaseous nitrogen and/or Freon 12 purging and evacuation.

For safety, the system is located in the test cell of the remote permeability test facility. The MMH supply is located outside the building on the concrete platform and the N_2O_4 supply, in the test cell.

3.3 Vacuum System

The vacuum system, shown schematically in figure 15, consists of a set of bakeable sorption pumps, a 300-1/sec ion pump with internal heaters, a hand operated 6-inch ultrahigh vacuum gate valve, a Granville Philips valve, a bakeable dutchman accommodating an ionization gauge, residual gas analyzer, and a twelve terminal feedthrough (for thermocouple and strain gauges). The system is portable through the use of a hydraulic lift and serves all three permeability test chambers.

Sorption and ion pumping was selected in order to eliminate possible interference with mass spectrometer readings due to breakdown of pumping fluids. A small mechanical pump is used for preliminary system evacuation during startup after specimen changes or test chamber moves.

3.4 Diaphragm Mounting Fixtures

3.4.1 Metal Diaphragm

The design of the metal diaphragm clamping fixture and high vacuum seal is illustrated in figure 16. Aluminum O-rings were used for both the

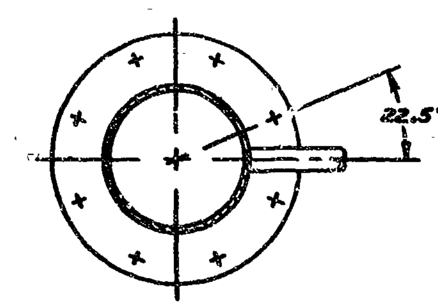

SECTION A-A

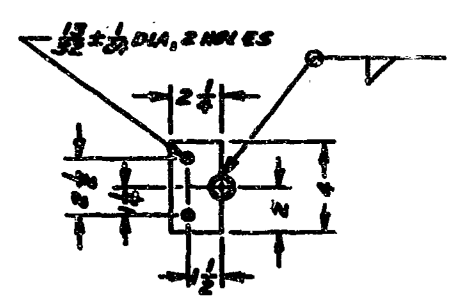

SECTION B-B
DETAILS OF SUPPORT PLATE
MAT'L- CRES, 1/4 THICK
2 REQ'D TOL- ± 1/32

PUMP & LO
MANIFOL
SUPPORT P

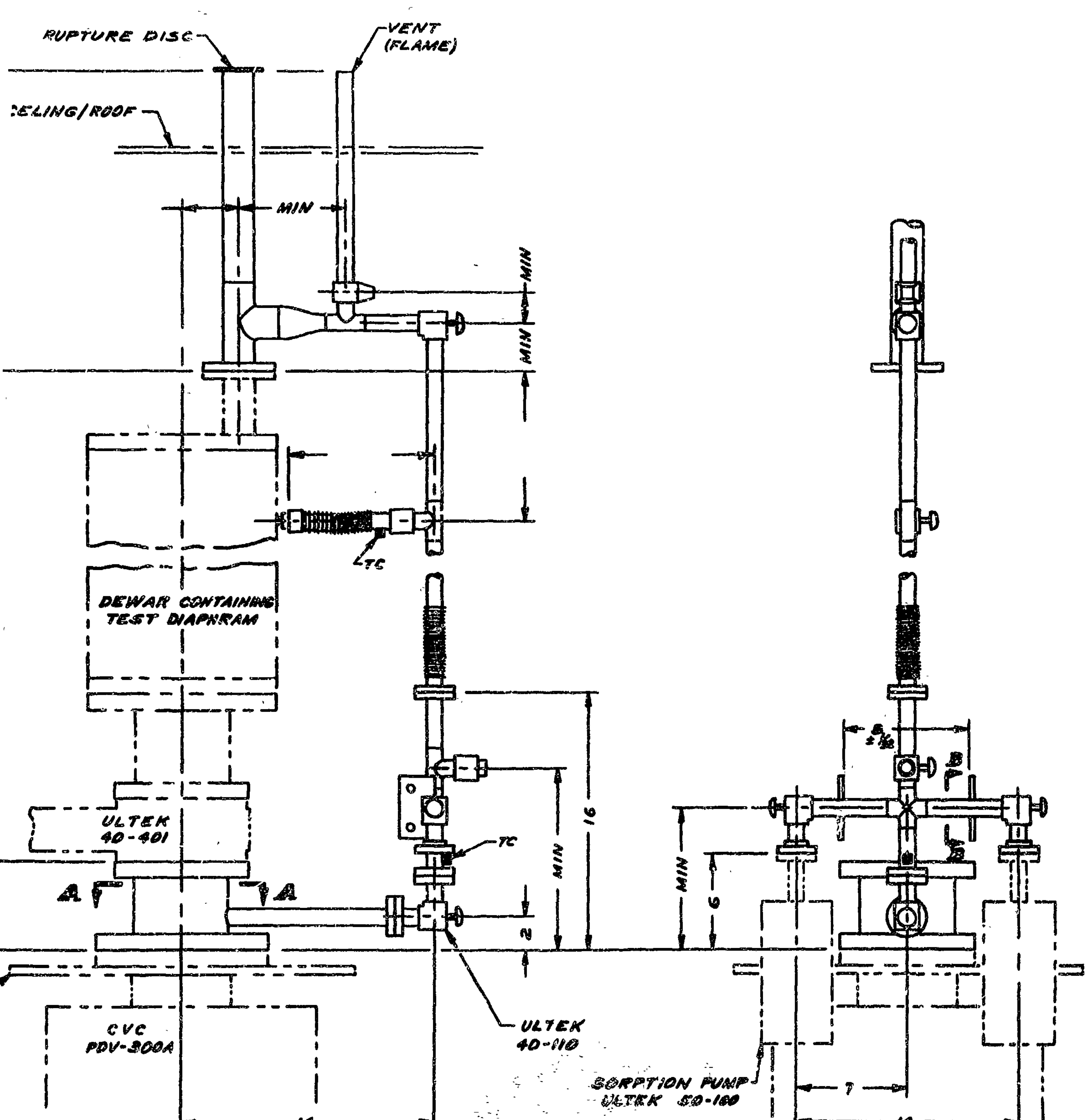

Figure 15. Schematic Diagram of the Vacuum System

R448230

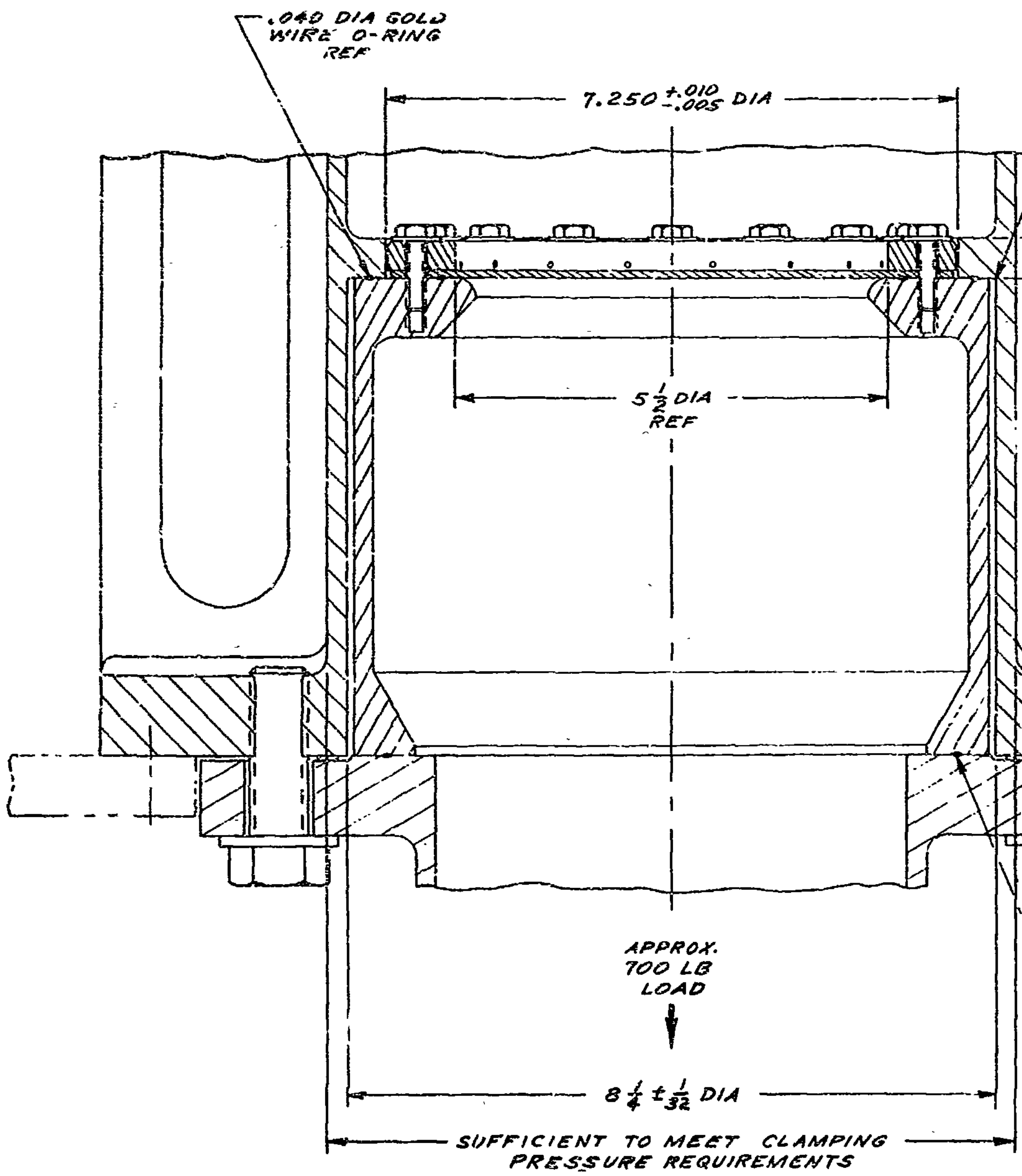

.040 DIA GOLD
WIRE O-RING
REF
7.250 +.010 -.005 DIA
5 1/2 DIA
REF
APPROX.
700 LB
LOAD
8 1/4 ± 1/32 DIA
SUFFICIENT TO MEET CLAMPING
PRESSURE REQUIREMENTS

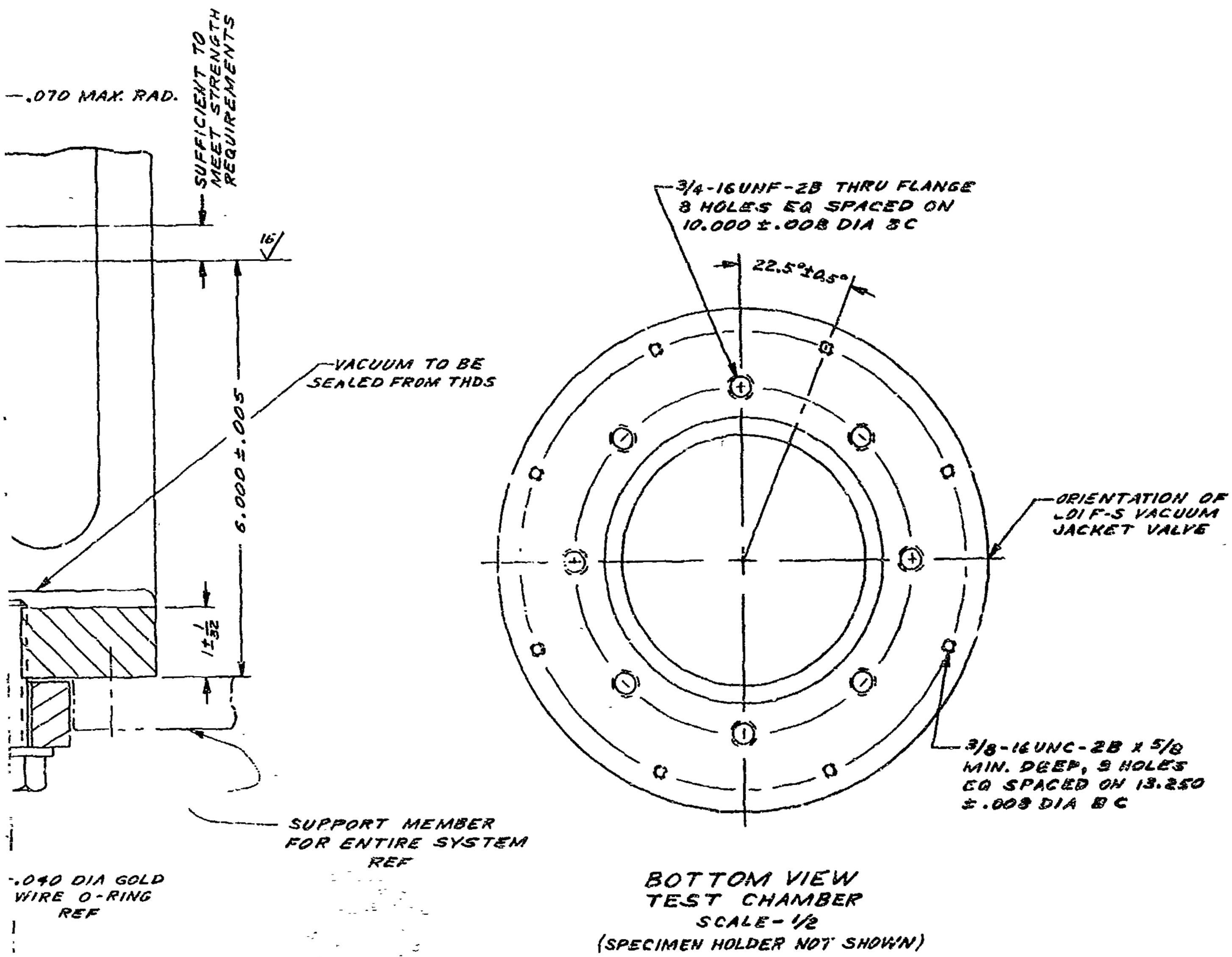

Figure 16. Diaphragm Clamping Fixture

seal to the vacuum system and the diaphragm seal, as shown. The low vacuum seal between the diaphragm clamping fixture and the wall of the test chamber was accomplished by using a gasket made of reinforced Teflon.

3.4.2 Polymeric Diaphragm

The design of the polymeric diaphragm clamping fixture is illustrated in figures 17 and 18. Essentially, the polymeric film material is sandwiched between the two components of the clamping fixture. Drilled through the support are twenty-six 1/4-inch holes. Mating holes are provided in the clamping plate for pressurization.

The high vacuum seal is achieved by compressing the polymeric material approximately 75% by using a thin metal ring between the clamping plate and the polymeric specimen. (See section 5.2.5 for seal development details.) The uniform metal ring, 11-mil thickness by 35-mil width by 5.5-inch diameter, was a previously compressed 25-mil wire diameter aluminum O-ring.

3.5 Experimental Procedure

The testing procedure used in the program consisted, first, of installing the diaphragm specimen in the diaphragm clamping fixture. The vacuum system, specimen holder, and test chamber were then assembled. The system below the specimen was evacuated to a pressure in the 10^{-7} to 10^{-8} torr range by means of sorption and ion pumping.

After initial pumpdown, the background vacuum and residual gas constituents were monitored and recorded. Nitrogen gas and/or Freon 12 gas was then applied to the upper side of the test specimen at predetermined pressure levels to check the high vacuum seal and the system residual gas

R449637

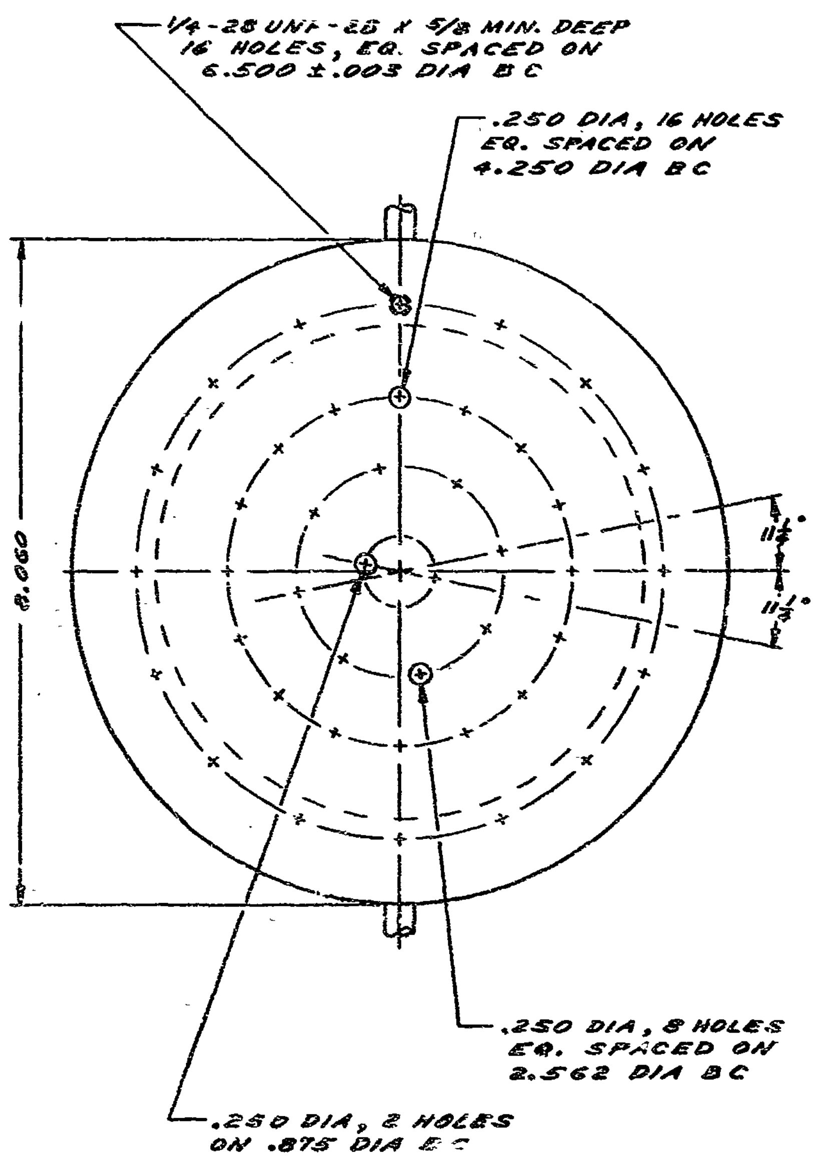

1/4-28 UNF-2B X 5/8 MIN. DEEP
16 HOLES, EQ. SPACED ON
6.500 ±.003 DIA BC
.250 DIA, 16 HOLES
EQ. SPACED ON
4.250 DIA BC
8.060
11¼°
11¼°
.250 DIA, 8 HOLES
EQ. SPACED ON
2.562 DIA BC
.250 DIA, 2 HOLES
ON .875 DIA BC

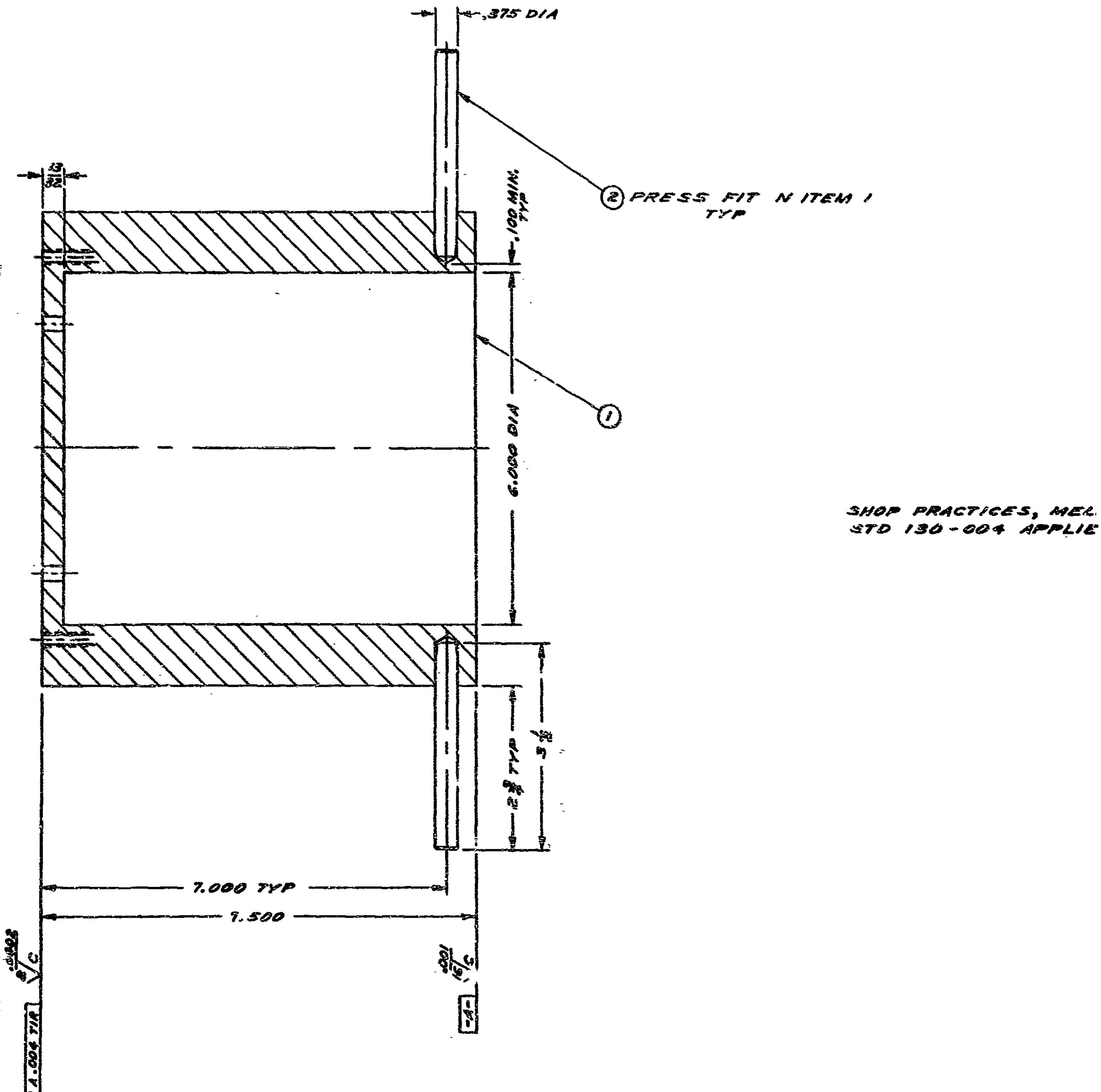

Figure 17. Plastic Specimen Support

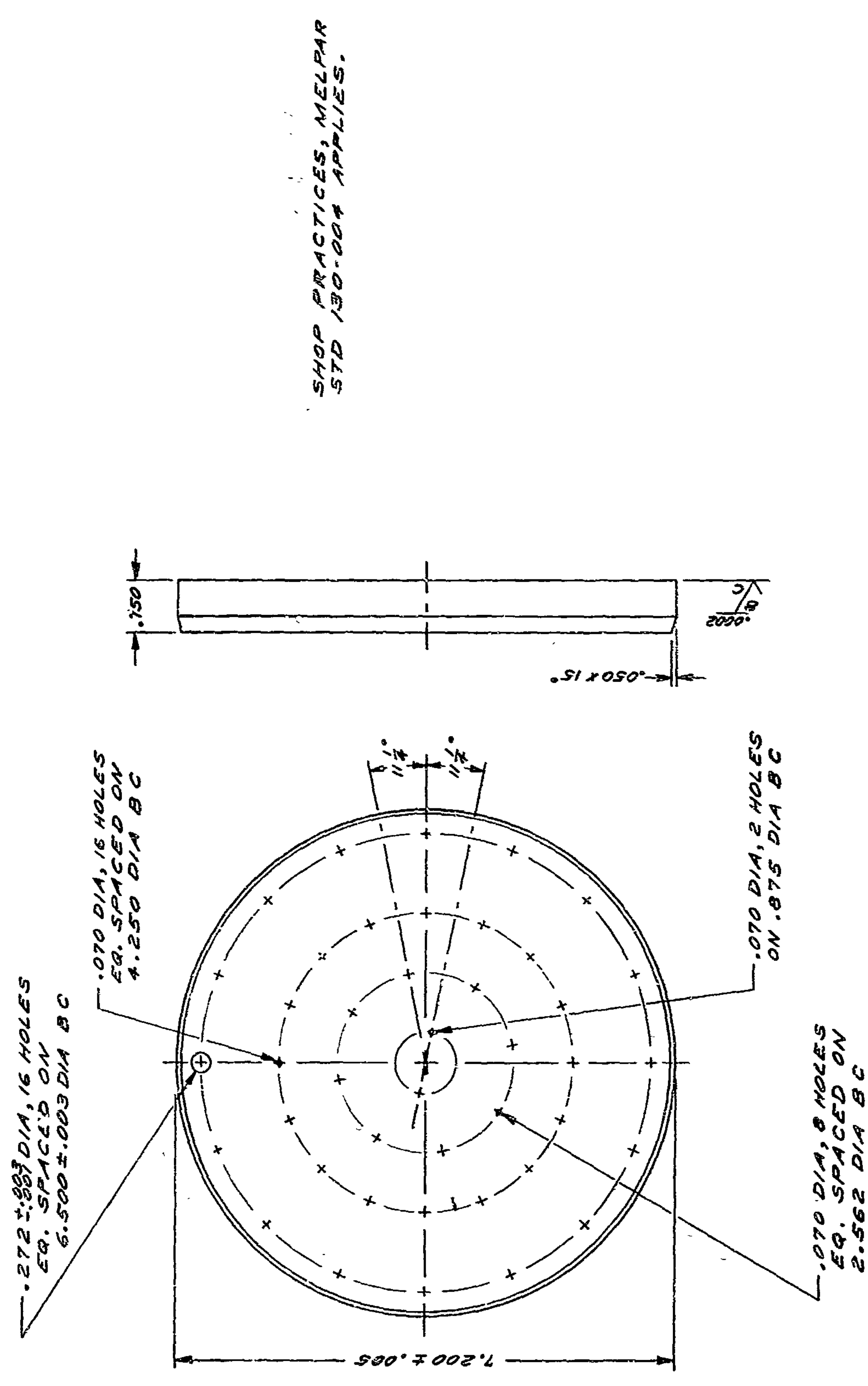

Figure 18. Plastic Specimen Clamp Plate

background over the approximate pressure range to be tested with the test fluid. Both the mass spectrometer and ionization gauges were used in their most sensitive range. Peak height changes and pressure rise in the dutchman (with the 6-inch gate valve closed) were the indicators used to ascertain the degree of permeation, if any.

After completion of background monitoring and seal check, the system was filled with the test fluid. The two amounts of fluid utilized in each single test included 3 liters of MMH or N_2O_4, 6 to 13 liters of LN_2, or approximately 10 liters of LH_2. Predetermined test fluid overpressures were then applied. Again, peak height changes (in some cases appearance) and pressure rise in the dutchman (with the 6-inch gate valve closed) were the indicators used to ascertain the degree of permeation, if any.

3.6 System Calibration

Calibration of the residual gas analyzer sensitivity was accomplished using a calibrated* N_2 leak. By using controlled holdup times of the known leak, distinct recorder output trace discontinuity is observed. A typical curve for a 10-second holdup period is reproduced as figure 19. The number of chart units represented by the discontinuity was correlated to the holdup time. (See figure 20.) It should be noted that the initial condition of the surfaces within the system apparently affect the sensitivity. That is, with repeated test runs, the discontinuity height tends to seek a lower level after long-time system pump out. From knowledge of the known leak rate, 2×10^{-7} cc/sec at STP, the sensitivity was

*Calibration traceable to NBS

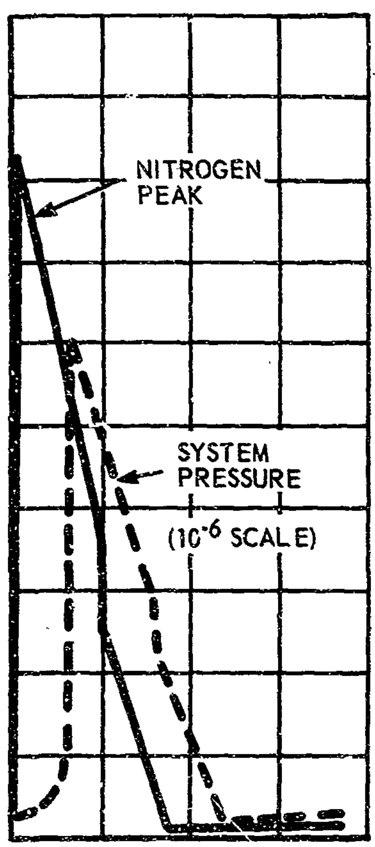

Figure 10. Nitrogen Peak and System Pressure Traces Showing 2 x 10^{-6} cc STP Nitrogen Gas Burst

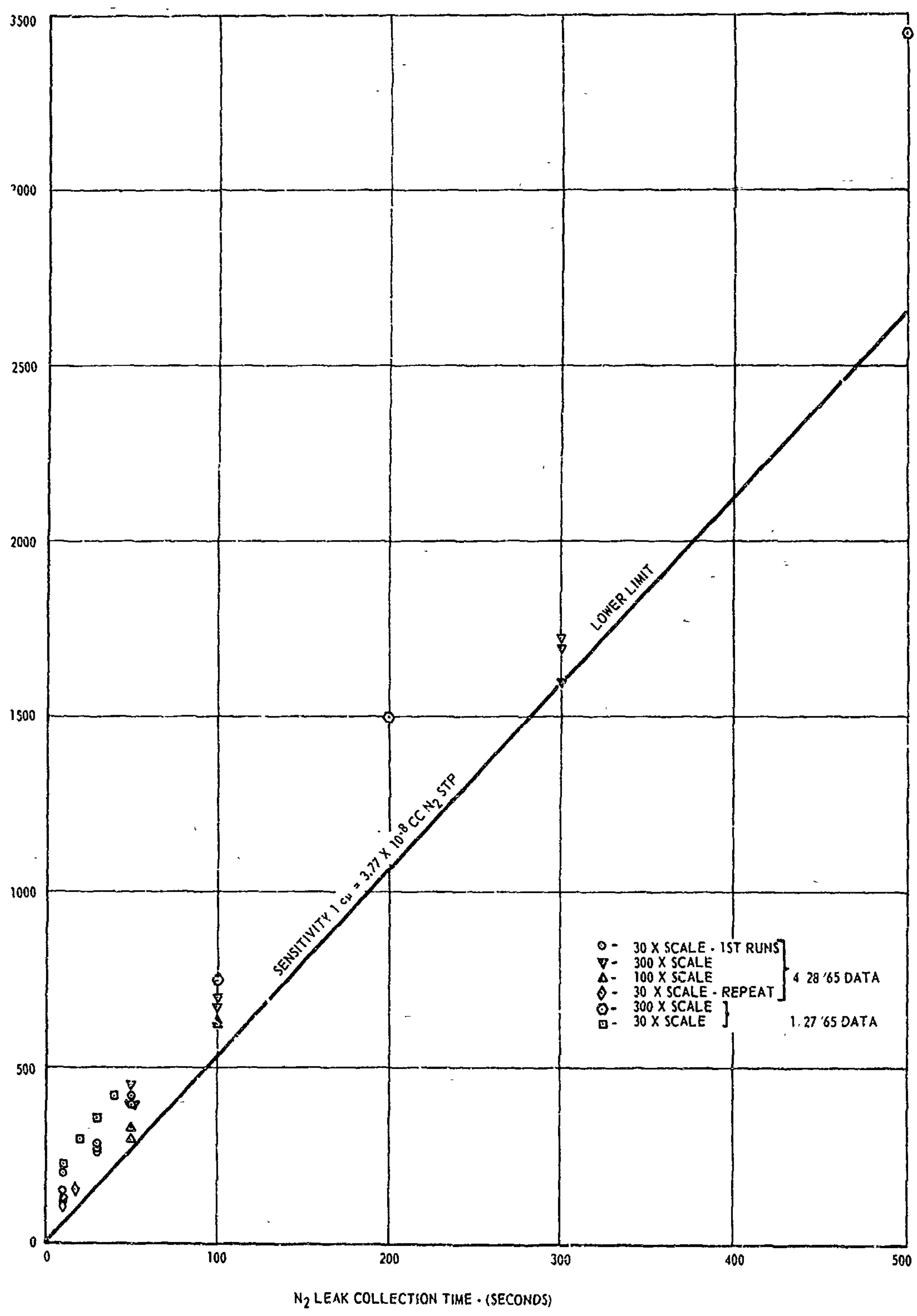

Figure 20. Residual Gas Analyzer Sensitivity

calculated for the probable lower limit of the data presented in figure 20.

3.7 Technique for Measuring Deflection of Polymer Diaphragms in Permeability Apparatus

Some of the polymeric materials to be evaluated for this program are very ductile in comparison with metals, even at cryogenic temperatures. Strain measurement of materials which elongate more than 4 or 5% at -320°F or lower are somewhat problematic, particularly when high vacuum requirements have to be satisfied. A detailed survey indicated that no strain gauges are available which reliably measure high elongations at low temperatures in ultrahigh vacuum.

As a result, optical measurement was selected. However, the location of the diaphragm in the system and the surrounding cryogenic dewar chamber make it almost impossible to view it directly. Consequently, the method described below was selected.

Research in optics during the past few years has resulted in a new instrument called a fiberscope. It operates on the following basic principles:

a. Smooth filaments or fibers of transparent materials, such as glass, conduct light efficiently by total internal reflections.

b. Individual fibers in a cluster or bundle conduct this light independently.

The fiberscope itself consists of aligned flexible bundles of single or multiple glass or quartz fibers (about 25-microns diameter) fitted with suitable lenses at either end, and these tranfer images along flexible paths. Fiberscopes are available in lengths up to 4 meters and, depending upon requirement, may be sheathed in flexible or semi-rigid envelopes.

The upper dutchman of the vacuum system had been modified to provide a glass window in the manner shown in figure [illegible]. A nylon thread was attached to the diaphragm center. As the diaphragm is stressed, the thread deflects vertically downward. A marker on the thread facilitates monitoring this movement when viewed through the fiberscope. Thus, actual deflection of the diaphragm can be monitored.

The fiberscope used in this program has a field of view 1-inch in diameter. The focusing distance for sharp image is approximately 1.75 inch from the objective lens. Since the fiberscope has a built-in light source, no illumination inside the chamber is necessary.

The fiberscope was preferred over the simpler telescopic viewing because:

a. The distance between the lens of the telescope and the object to be viewed is quite large (of the order of 10 feet or more). In the present setup, where all operations are performed remotely, telescope arrangement is impractical from the viewpoint of safety and ease of operation.

b. Through a small opening in the barricade wall, the fiberscope may be introduced in the optical window for viewing inside the system. Due to its flexibility and small size, the fiberscope may be used on all three systems without time-consuming adjustments

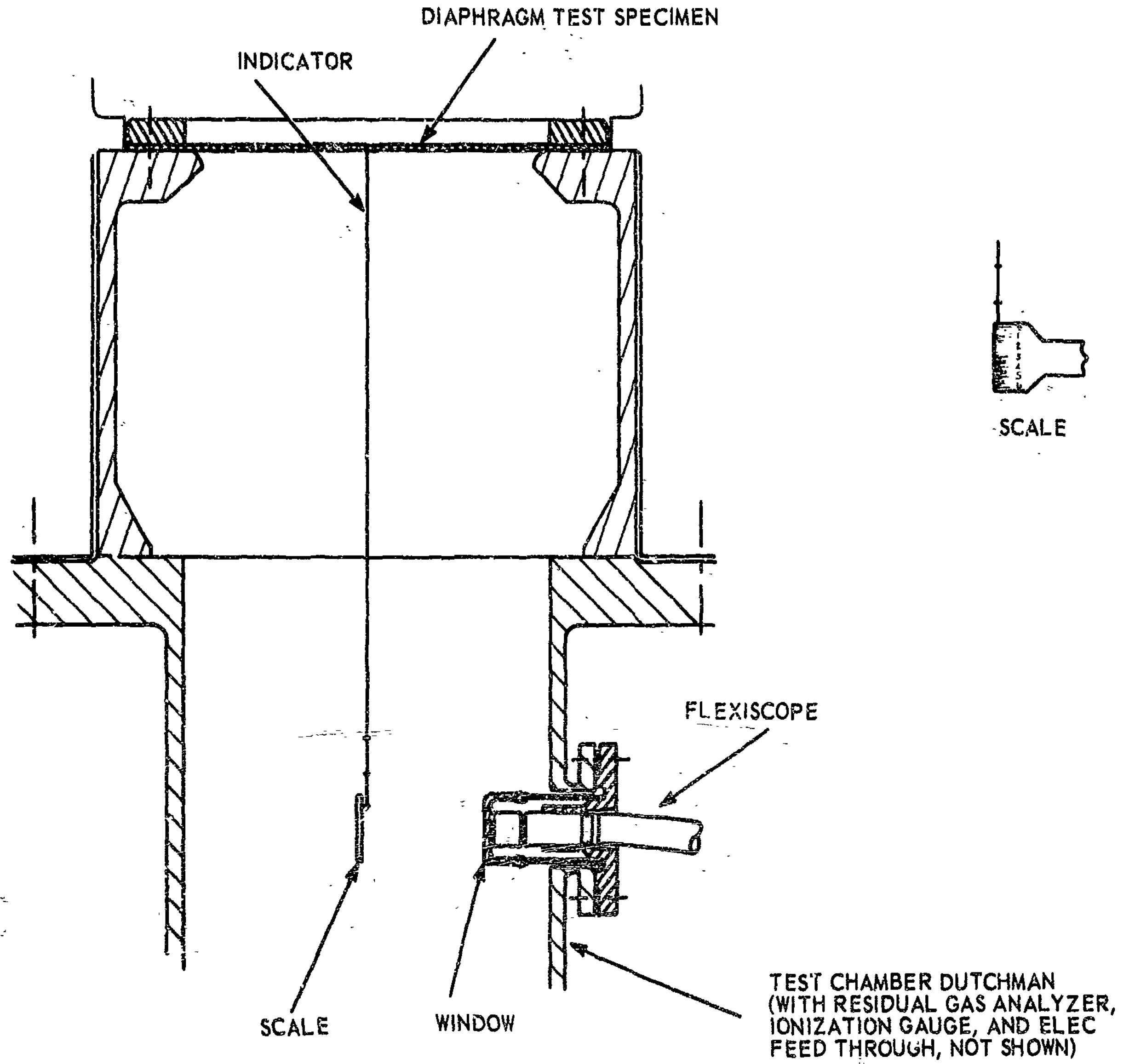

Figure 21. Optical Measurement of Diaphragm Deflection by Fiberscope

4. DIAPHRAGM MATERIALS

4.1 Source and History

The selection of materials for evaluation was based on the work statement of the present contract. General information regarding each metallic and non-metallic material in the "as received" condition supplied is presented below in brief. Wherever possible, permeability values are also included.

2024 T6 Aluminum Alloy: The alloy was procured in 12 and 20 mil thicknesses in T-3 condition. The properties of this material are presented in table 6.

304 Stainless Steel (United States Steel Company): The alloy was obtained in three thicknesses, namely 8, 12, 15 mils. Available data on the mechanical properties are presented in table 7.

Teflon (FEP Type A, E.I. DuPont): Teflon FEP-fluorocarbon film was formerly referred to as film made of Teflon 100X perfluorocarbon resin. The film is a fully fluorinated copolymer of ethylene and propylene, and exhibits an outstanding combination of chemical, electrical, thermal and physical properties. Table 8 presents the values for the properties readily available from literature.

Mylar (Type A, E.I. DuPont): Mylar has been used in ultra-low temperature applications both as a structural as well as a dielectric material. In the aluminum metallized form* it has been used as a lightweight heat insulator for low temperature storage vessels. It is an excellent general-purpose

* Metallized Mylar (1-micron aluminum on 2-mil Type S Mylar) was obtained from National Metallizing Company.

Table 6. Mechanical Properties of 2024 T6 Aluminum Alloy

Property	RT	Temperature °F	-423
Yield Strength (psi)	47,000		94,000
Ultimate Tensile Strength (psi)	60,000		105,000
Elastic Modulus (psi) x 10^6	10.5		12.5

Table 7. Mechanical Properties of 304 Stainless Steel (Full Hard)

Property	RT	Temperature °F	-423
Yield Strength (psi)	140,000		230,000
Ultimate Tensile Strength (psi)	185,000		285,000
Elastic Modulus psi x 10^6	24.5		28.6

Table 8. Properties Data on Teflon

Available Film Thicknesses: 0.0005 to 0.040 inches

Tensile (psi)

	LH_2 -420°F	LN_2 -320°F	LO_2 -297°F	R. T. 77°F
FEP 0.040* (50% crystallinity)	20.2×10^3	14×10^3	13.5×10^3	2×10^3
FEP (compression molded)		16×10^3	15.5×10^3	3×10^3
TFE 0.125*	19.5×10^3	16.5×10^3	13×10^3	3.8×10^3

Modulus of Elasticity (psi)*

	LH_2 -420°F	LN_2 -320°F	LO_2 -297°F	R. T. 77°F
FEP 0.040 inch	3,120,000	1,040,000		160,000

Thermal Expansion (%)

	LH_2 -420°F	LN_2 -320°F	LO_2 -297°F	R. T. 77°F
Teflon (extruded and annealed)	-2100×10^{-3}	-1900×10^{-3}		0

Thermal Conductivity

FEP 1.35 Btu/hr/ft^2/°F/in

Permeability

	Density	Transmission Rate cc/100 in^2/24 hr Air	Transmission Rate cc/100 in^2/24 hr N_2O_4
TFE° 0.0100 inch	2.186 gm/cc	20.0	275.9
FEP° 0.0106 inch	2.138 gm/cc	30.0	81.8

*Calculated from Stress-Strain Graphs in Cryogenic Data Handbook.

plastic material in the temperature range -20°C to 150°C and is noted for its toughness, flexibility, and low permeability to oxygen, water and organic vapors. Below -60°C the material becomes embrittled and its use as a gasket or flexible liner becomes limited. However, at the lower temperatures the mechanical properties of Mylar, as indeed with most plastic materials, increase and higher modulus of elasticity and strength-to-weight ratio values than observed at room temperature are obtained. Some of the data on Mylar properties that has been obtained and is considered pertinent for this report are given in table 9.

<u>Tedlar (Type 200SG40TR, E.I. DuPont)</u>: One of the unique properties of Tedlar is low permeability to gases, particularly oxygen. It is also noted for its good mechanical strength and chemical resistance. Because Tedlar contains no plasticizers, it is a film with good aging properties that remains tough and flexible over a broad temperature range. More than sufficient information about its room temperature properties is available and on hand. Unlike Mylar, the metallized form of Tedlar* is used as a heat insulation material in cryogenic applications but specific cryogenic properties data is lacking. At present, Tedlar is available only in thin films, 0.5 to 2.0 mils, although three surface variations of Tedlar film are manufactured.

Typical engineering properties for this material are presented in table 10. There is a lack of cryogenic data.

---

* Metallized Tedlar (1 micron aluminum on 2 mil Type 200SG40TR Tedlar) was obtained from National Metallizing Company.

Table 9. Properties Data on Mylar

Available Thicknesses: 0.00015 to 0.015 inch

Tensile (psi)	LH_2 -420°F	LN_2 -320°F	R. T. 77°F
Mylar A - 0.003 inch	--	44×10^3	--
0.004 inch		31×10^3	21×10^3
0.010 inch	38.5×10^3	37×10^3	19×10^3
Modulus of Elasticity (psi)			
Mylar - 0.004 inch	--	1,900,000	1,100,000
Thermal Expansion (linear)			20×10^{-6}/°F
Thermal Conductivity			
cal/cm/sec/°C			3.63×10^{-4}
Permeability at Room Temperature			N_2
cc/100 sq in. 24 hr/mil			1.0

Table 10. Properties Data on Tedlar

Property	Typical Value
Burst Strength	19 to 70 psi
Moisture Vapor Transmission	157 to 205 $g/100M^2$ (hr)(mil)(53 mm Hg)
Oxygen Permeability	3.2 cc/100 sq in 24 hr/mil
Hydrogen Permeability	58.1 cc/100 sq in 24 hr/mil
Nitrogen Permeability	0.25 cc/100 sq in 24 hr/mil
Tensile Modulus	310 to 250 x 10^3 psi
Ultimate Tensile	7.0 to 18.0 x 10^3 psi
Ultimate Yield	6000 to 4900 psi
Temperature Range (continuous use)	-100°F to 225°F

Nylon-Based Adhesives (FM 1000, Bloomingdale Rubber Company): FM-1000, an unsupported film, is designed for structural bonding of both sandwich and all metal constructions. Cryogenic data on this material is presented in table 11.

Polyurethane Foam (Type H-602N, Nopco Chemical Company): Nopcofoam H-602N is a fluorocarbon-blown urethane foam insulation dimensionally stable at subzero temperatures. The physical properties obtained from Nopco Chemical Company are presented in table 12.

Silicone Rubber (Raybestos Manhattan Co.): The major suppliers of silicone rubber, for example, General Electric and Dow Corning, can offer a variety of grades and thicknesses of silicone rubber. From the general literature, it is known that silicone rubber has been used frequently in cryogenic engineering applications, particularly as a gasket material. It retains its toughness and flexibility over a wide temperature range: -150°F to 500°F and retains its rubber-like properties in environments where natural rubbers fail. Some general data obtained from commercial sources are given in table 13.

Polyethylene (E.I. DuPont): As a family, the polyethylene resins have many outstanding properties. They exhibit good chemical resistance to most acids, bases, and salts that attack metals. Polyethylene, however, is attacked by strong oxidizing acids such as nitric acid and is affected by many hydrocarbon solvents such as benzene and xylene. As a packaging material, but not necessarily as an engineering material, the gas permeability properties of polyethylene are considered excellent. The material is relatively impermeable to water but permeable to air, oxygen and CO_2. The high density

Table 11. Cryogenic Test Data on Nylon-based Adhesives

Adhesive	Tensile Shear Strength* psi Room Temperature	-423°F
302 S. S. Bonded to Tedlar		
Narmco 3135	1100 to 1300	--
EC-1469 (3M)	1000 to 1200	1000
302 S.S. Bonded to Mylar		
AF 110 (3M)	260 to 430	--
Narmco 3135	1000 to 1900	1100 to 1200
EC 1469 (3M)	140 to 430	1200
5024 Aluminum Bonded to Mylar		
XL 967045 (3M)	880 to 1000	720 to 1000
3M Weatherband	64 to 67	630 to 1000

*In most cases failure occurred at the adhesive-plastic interface.

Table 12. Properties Data on Polyurethane Foam

	Parallel to Rise	Perpendicular to Rise
Tensile Strength	35 psi	29 psi
Compressive Strength	40 psi	21 psi
Shear Strength	30 psi	21 psi
Flexural Strength	40 psi	29 psi
Flexural Modulus	1500 psi	800 psi
Overall Density	2 lbs/cu ft	

Table 13. Properties Data on Silicone Rubber

Material	Tensile Strength psi	Elongation	Compression Set 20 hr 300°F
Class 500 Extreme Low Temp	800 to 1500	200 to 600%	20 to 50%
Class 400 General Purpose	800 to 1100	250 to 500%	15 to 35%
Class 300 "O" Rings and Seal	800 to 1100	80 to 200%	10 to 20%
Class 700 Extreme High Temp	800 to 900	180 to 250%	20%

Typical Values for All Class Materials

Thermal Conductivity 0.18 Btu-ft/ft^2-hr-°F

Thermal Expansion 200 to 380 x 10^{-6} in/in/°C forms of polyethylene, however, are more impermeable to oxygen and other gases and, because of their superior mechanical and durability properties, are often preferred in cryogenic engineering applications. A wide selection of film thicknesses and density grades of polyethylene is available. Some of the typical properties of the polyethylenes are presented in table 14.

Polyvinyl Chloride (Vitafilm D-80, Goodyear): The use of polyvinyl chloride in cryogenic engineering applications is limited due to the presence of small amounts of plasticizers in the material that cause embrittlement at low temperature. As a class, the polyvinyl chlorides are one of the cheapest and most widely used of the engineering plastics. The mechanical properties, flexibility and chemical resistance are often a function of the plasticizers used and the method of fabrication. Nearly any degree of flexibility of the material can be obtained by controlling the compounding, filler concentration and final processing. Cryogenic data are meager at present and more will have to be obtained. Typical room temperature properties of polyvinyl chloride are readily available, a sample of which appears in table 15.

4.2 Mechanical Property Evaluation

4.2.1 Mechanical Properties of Metal Diaphragm Materials at Room Temperature and -320°F

The tensile properties of 304 stainless steel (0.008, 0.012 and 0.015 inch) sheet and 2024 T6 aluminum alloy (0.012 and 0.020 inch) sheet were determined at room temperature and at -320°F. The tensile specimens were fabricated in accordance with ASTM CE8-52T. All testing was performed on the Instron tensile testing machine with a strain rate of 0.02 in./in./min. The data are presented in tables 16 through 20. During testing at liquid nitrogen temperature, it was found that the specimens occasionally fractured

Table 14. Properties of Polyethylene

Property	Low Density	Medium Density	High Density
Tensile Strength (psi) D 638, D 651	1000-2300	1200-3500	3100-5500
Thermal Conductivity (10^{-4} cal/sec/sq cm/°C/cm) C 177	8.0	--	11-12.4
Thermal Expansion (10^{-5}/°C) D 696	16-18	--	11-13
Tensile Modulus (10^5 psi) D 638	0.17-0.35	0.25-0.55	0.6-1.5
Temperature Resistance (°F)	-70 to 200	-70 to 220	-50 to 250
Permeability to Gases cc/100 sq in/mil/24 hr/ atmos/25°C/0%RH			
CO_2	2900	990	580
N_2	180		42
O_2	550	280	185

Table 15. Properties of Polyvinyl Chloride

Property		Polyvinyl Chloride Rigid	Non-Rigid
Tensile Strength (psi)		7,000 to 10,000	1,400 to 5,600
Temperature Resistance (°F)		--to 150 to 200	-50 to 150 to 200
Permeability to Gases 10^{-6} g/24 hr/m^2/mm/cm Hg at 21°C, 50% RH	CO_2	970	970
	O_2	150	150
Availability		0.001 to 0.010 inch	
Thermal Conductivity (10^{-4} cal/sec/sq cm/°C/cm) C177		3.0 to 7.0	3.0 to 4.0
Thermal Expansion (10^{-5}/°C) D696		5 to 18.5	7 to 25
Tensile Modulus (10^{-5} psi) D638		3.5 to 6	--

Table 16. Tensile Properties of .008 in. 304 Stainless Steel

Direction	Temp.	No.	Ultimate Tensile Strength (psi)	Yield Strength (psi) .2% Offset	Elongation (%)	Remarks
Trans.	LN_2	1	284,000	186,000	22.0%	
		2	284,000	187,000	28.0%	
		3	--	--	--	
		Avg	284,000	186,500	25.0%	
	Ambient	1	219,000	161,000	1.5%	
		2	219,000	161,000	1.6%	
		3	218,000	161,000	1.8%	
		Avg	218,667	161,000	2.45%	
Long.	LN_2	1	291,000	176,000	25.0%	Broke at machine mark
		2	271,000	181,000	--	
		3	--	--	--	
		Avg	281,000	178,000	25.0%	
	Ambient	1	207,000	172,000	--	Broke at gauge mark
		2	207,000	168,000	1.2%	
		3	206,000	155,000	1.2%	
		Avg	206,667	165,000	1.2%	
45°	LN_2	1	277,000	180,000	25.0%	
		2	276,000	179,000	24.0%	
		3	--	--	--	
		Avg	276,500	179,500	24.5%	
	Ambient	1	208,000	159,000	1.2%	
		2	210,000	155,000	1.2%	
		3	211,000	156,000	1.3%	
		Avg	209,667	156,667	1.23%	

Table 17. Tensile Properties of .012 in. 304 Stainless Steel

Direction	Temp.	No.	Ultimate Tensile Strength (psi)	Yield Strength (psi) .2% Offset	Elongation (%)	Remarks
Trans.	LN_2	1	287,000	187,000	6.0%	
		2	284,000	198,000	7.0%	
		3	--	--	--	
		Avg	285,500	192,500	6.5%	
	Ambient	1	171,000	121,000	2.8%	
		2	170,500	119,000	3.0%	
		3	170,200	124,000	2.5%	
		Avg	170,567	121,333	2.8%	
Long.	LN_2	1	273,000	182,000	27.0%	
		2	274,000	181,000	26.0%	
		3	--	--	--	
		Avg	273,500	181,500	26.5%	
	Ambient	1	159,000	120,000	2.0%	
		2	158,500	113,000	2.0%	
		3	157,200	117,000	2.2%	
		Avg	158,000	116,667	2.1%	
45°	LN_2	1	268,000	176,000	27.0%	
		2	271,000	174,000	27.0%	
		3	--	--	--	
		Avg	269,500	175,000	27.0%	
	Ambient	1	163,000	119,000	2.3%	
		2	163,000	121,000	2.5%	
		3	162,500	120,000	2.4%	
		Avg	162,833	120,000	2.4%	

Table 18. Tensile Properties of .015 in. 304 Stainless Steel

Direction	Temp.	No.	Ultimate Tensile Strength (psi)	Yield Strength (psi) .2% Offset	Elongation (%)	Remarks
Trans.	LN_2	1	273,000	172,000	32.0%	
		2	276,000	165,000	29.0%	
		3	--	--	--	
		Avg	274,500	168,500	30.5%	
	Ambient	1	198,000	131,000	3.2%	
		2	197,000	129,000	3.2%	
		3	196,500	133,000	3.0%	
		Avg	197,000	131,000	3.1%	
Long.	LN_2	1	274,000	171,000	30.0%	
		2	273,000	174,000	30.0%	
		3	--	--	--	
		Avg	273,500	172,500	30.0%	
	Ambient	1	184,000	145,000	1.5%	
		2	185,000	147,000	1.7%	
		3	184,500	142,000	2.5%	
		Avg	184,333	144,667	1.9%	
45°	LN_2	1	267,000	158,000	34.0%	
		2	266,000	162,000	32.0%	
		3	--	--	--	
		Avg	266,500	160,000	33.0%	
	Ambient	1	189,000	133,000	2.6%	
		2	189,000	133,000	2.6%	
		3	189,500	134,000	2.4%	
		Avg	189,167	133,333	2.5%	

Table 19. Tensile Properties of .012 in. 2024 T6 Aluminum

Direction	Temp.	No.	Ultimate Tensile Strength (psi)	Yield Strength (psi) .2% Offset	Elongation (%)	Remarks
Trans. (Heat Treatment Batch #1)	LN_2	1	84,900	69,200	6.5	Broke in gauge mark
		2	84,000	70,600	5.5	Broke in gauge mark
		3	85,000	71,800	8.5	
		Avg	84,600	70,500	6.8	
	Ambient	1	73,600	60,800	6.5	
		2	72,900	60,000	7.0	
		3	72,600	62,000	7.0	
		Avg	73,000	60,933	6.8	
Long. (Heat Treatment Batch #1)	LN_2	1	85,800	74,000	10.0	
		2	85,600	75,200	9.5	
		3	85,500	75,000	11.0	
		Avg	85,600	74,733	10.2	
	Ambient	1	73,100	63,100	5.5	
		2	73,400	63,500	6.0	
		3	73,300	62,700	6.0	
		Avg.	73,300	63,100	5.8	
Trans. (Heat Treatment Batch #2)	Ambient	1	71,500	62,000	5.5	
		2	71,600	62,200	5.5	
		3	71,200	61,300	5.0	
		Avg.	71,400	61,833	5.3	
Long. (Heat Treatment Batch #2)	Ambient	1	71,200	60,100	7.0	
		2	74,000	65,600	5.5	
		3	74,300	66,900	6.0	
		Avg.	73,200	64,200	6.2	

Table 19 Cont'd. Tensile Properties of .012 in. 2024 T6 Aluminum

Direction	Temp.	No.	Ultimate Tensile Strength (psi)	Yield Strength (psi) .2% Offset	Elongation (%)	Remarks
45^o (Heat Treatment Batch #2)	LN_2	1	83,200	58,300	20.0	
		2	81,300	58,600	12.0	
		3	80,600	58,100	12.0	
		Avg.	81,700	58,333	14.6	
	Ambient	1	70,000	48,000	13.0	
		2	70,000	49,800	12.0	
		3	70,500	52,000	11.0	
		Avg	70,200	49,933	12.0	

Table 20. Tensile Properties of .020 in. 2024 T6 Aluminum

Direction	Temp.	No.	Ultimate Tensile Strength (psi)	Yield Strength (psi) .2% Offset	Elongation (%)	Remarks
Long.	LN_2	1	87,600	79,000	7.5	
		2	87,100	77,500	7.5	
		3	87,300	78,200	8.0	
		Avg	87,333	78,233	7.6	
	Ambient	1	74,000	65,300	4.9	
		2	73,600	64,900	5.4	
		3	75,000	68,000	5.7	
		Avg	74,200	66,133	5.3	
Trans.	LN_2	1	86,400	73,700	7.5	
		2	84,900	70,400	12.5	
		3	84,600	68,600	11.3	
		Avg	85,300	70,900	10.4	
	Ambient	1	72,300	60,500	6.4	
		2	73,200	61,000	6.7	
		3	72,800	61,900	5.7	
		Avg	72,766	61,133	6.3	
45°	LN_2	1	83,100	68,000	12.5	
		2	83,800	74,500	10.0	
		3	84,000	71,000	10.0	
		Avg	83,633	71,167	10.8	
	Ambient	1	73,400	53,300	5.5	
		2	72,500	61,100	6.7	
		3	73,000	64,200	5.1	
		Avg	72,967	62,867	5.7	

in the grips due to greatly increased ductility and tensile strength. Consequently, the coupon width was reduced from 0.500 to 0.400 inch to cause failure in the gauge length.

Since the 2024 aluminum alloy sheet was received in the T3 condition, the tensile coupons were heat treated to the T6 condition by heating in a Hotpack air/vacuum oven at 375° ± 4°F for 8 hours. Although the properties of the transverse and longitudinal coupons showed that the heat treatment was successful, the 0.012-inch thick tensile specimens exhibited significantly lower yield strength and elongation. A second heat treatment of new coupons was executed and the tensile properties were in agreement with those of the first heat treatment.

4.2.2 Mechanical Properties of Polymeric Diaphragm Materials at Room Temperature

Tensile properties of polymeric materials (Mylar, polyethylene, Teflon, and silicone rubber) in the "as received" condition were determined at room temperature. The resulting values are reported in tables 21 to 24.

Tensile specimens were obtained by using an ASTM D-412 Type C die as recommended for thin film plastic materials. As in the case of metallic specimens, all testing was performed on the Instron machine. All materials were stained at a rate of 0.5 in./in./min except for silicone rubber. The latter was strained at a rate of 12 in./in./min.

Table 21. Tensile Properties of Mylar at Room Temperature

Direction	No.	Ultimate Tensile Strength (psi)	Tensile Modulus (psi)	Yield Strength (psi) 2% Offset	Elongation (%)	Film Thickness (in.)
Trans.	1	23,500	360,000	12,600	85	.005
	2	22,800	400,000	12,800	80	.005
	3	23,500	370,000	12,400	100	.005
	Avg.	23,267	376,667	12,600	88.3	.005
Long.	1	24,000	353,000	12,400	122	.005
	2	22,500	373,000	12,000	105	.005
	3	23,250	400,000	11,600	115	.005
	Avg	23,250	375,333	12,000	114	.005
45°	1	26,900	366,000	12,200	95	.005
	2	26,900	393,000	12,400	100	.005
	3	25,750	350,000	12,400	90	.005
	Avg	26,517	369,000	12,333	95	.005
Trans.	1	22,100	380,000	12,600	60	.002
	2	25,250	450,000	12,600	80	.002
	3	23,800	406,000	12,200	75	.002
	Avg	23,717	412,000	12,467	71.7	.002
Long.	1	22,500	350,000	13,200	100	.002
	2	21,100	380,000	13,000	80	.002
	3	22,600	373,000	12,800	100	.002
	Avg	22,067	367,667	13,000	93.3	.002
45°	1	16,000	366,000	14,400*	150	.002
	2	16,500	346,000	14,300	145	.002
	3	--	380,000	14,500	--	.002
	Avg	16,250	364,000	14,400	147.5	.002

*Ultimate Yield Strength

Table 21 Cont'd. Tensile Properties of Mylar at Room Temperature

Direction	No.	Ultimate Tensile Strength (psi)	Tensile Modulus (psi)	Yield Strength (psi) 2% Offset	Elongation (%)	Film Thickness (in.)
Trans.	1	19,500	380,000	11,200	70	.0005
	2	19,000	370,000	11,600	60	.0005
	3	19,200	390,000	12,000	60	.0005
	Avg	19,233	380,000	11,600	63.3	.0005
Long.	1	18,300	400,000	12,200	65	.0005
	2	17,500	400,000	12,800	50	.0005
	3	19,800	340,000	12,000	60	.0005
	Avg	18,533	380,000	12,333	58.3	.0005
45°	1	15,200	340,000	13,400*	50	.0005
	2	15,200	370,000	13,450	45	.0005
	3	14,400	313,000	13,100	40	.0005
	Avg	14,933	341,000	13,167	45	.0005

*Ultimate Yield Strength

Table 22. Tensile Properties of Polyethylene at Room Temperature

Direction	No.	Ultimate Tensile Strength (psi)	Tensile Modulus (psi)	Yield Strength (psi) 2% Offset	Elongation (%)	Film Thickness (in.)
Trans.	1	1,575	16,600	960*	940	.006
	2	1,600	16,600	970	915	.006
	3	1,430	15,300	940	755	.006
	Avg	1,535	16,167	957	870	.006
Long.	1	1,740	9,600	580	515	.006
	2	2,200	13,000	520	675	.006
	3	1,940	11,200	600	660	.006
	Avg	1,960	11,667	567	617	.006
45°	1	1,995	10,800	620	792	.006
	2	1,910	11,500	540	760	.006
	3	2,160	11,500	560	870	.006
	Avg	2,022	11,267	573	807	.006
Trans.	1	2,320	18,333	1,410	910	.004
	2	2,310	20,000	1,475	850	.004
	3	2,050	19,285	1,500	725	.004
	Avg	2,228	19,206	1,462	828	.004
Long.	1	2,875	14,090	775	570	.004
	2	3,100	15,000	850	770	.004
	3	2,975	13,750	775	590	.004
	Avg	2,983	14,280	800	643	.004
45°	1	2,775	12,857	750	880	.004
	2	2,975	13,571	750	940	.004
	3	2,725	11,428	650	930	.004
	Avg	2,825	12,619	717	917	.004

*Ultimate Yield Strength

Table 22 Cont'd. Tensile Properties of Polyethylene at Room Temperature

Direction	No.	Ultimate Tensile Strength (psi)	Tensile Modulus (psi)	Yield Strength (psi) 2% Offset	Elongation (%)	Film Thickness (in.)
Trans.	1	2,460	24,000	1,375	785	.002
	2	2,400	20,000	1,340	790	.002
	3	2,075	18,300	1,310	695	.002
	Avg	2,312	20,767	1,341	757	.002
Long.	1	2,975	15,000	800	380	.002
	2	2,750	15,000	850	340	.002
	3	3,250	19,286	950	350	.002
	Avg	2,992	16,429	867	357	.002
45°	1	3,560	13,900	1,050	740	.002
	2	2,975	11,100	950	530	.002
	3	2,925	14,000	950	620	.002
	Avg	3,153	13,000	983	630	.002

Table 23. Tensile Properties of Teflon at Room Temperature

Direction	No.	Ultimate Tensile Strength (psi)	Tensile Modulus (psi)	Yield Strength (psi) 2% Offset	Elongation (%)	Film Thickness (in.)
Trans.	1	2,875	56,600	1,850	410	.005
	2	2,875	58,300	1,875	400	.005
	3	2,750	51,600	1,825	400	.005
	Avg	2,833	55,500	1,850	403	.005
Long.	1	3,500	--	--	453	.005
	2	3,960	48,750	1,975	520	.005
	3	3,575	57,300	1,975	470	.005
	Avg	3,678	53,000	1,975	481	.005
45°	1	3,290	55,000	1,900	460	.005
	2	3,325	60,000	1,950	460	.005
	3	3,180	60,000	1,900	440	.005
	Avg	3,265	58,333	1,917	453	.005

Table 24. Tensile Properties of Silicone Rubber at Room Temperature

No.	Ultimate Tensile Strength (psi)	Tensile Modulus (psi)	Yield Strength (psi) 2% Offset	Elongation (%)	Film Thickness (in.)
1	1,540	10,500	--	990	.0315
2	1,570	10,570	--	990	.0315
3	1,190	9,330	--	840	.0315
Avg	1,433	10,133	--	940	.0315

4.3 Compatibility Evaluation

Longitudinal and transverse tensile coupons were fabricated from each polymeric material having anisotropic mechanical properties. The ends of each coupon were heat-sealed to form a ring (except in the case of silicone rubber) in order to facilitate handling and to minimize adherence when exposed to MMH. Identification of each coupon was made by a series of slits in the grip position of the coupon. From this point on, the coupons were handled with Teflon-coated tweezers. The coupons were ultrasonically cleaned in 190-proof ethanol (when applicable) to remove moisture and fingerprints and subsequently rinsed in fresh ethanol. Then the coupons were oven-dried at 100°F on clean lens paper. After drying, the rings were packaged in open polyethylene bags which were, in turn, placed in desiccators (properly identified by material and direction) for at least 16 hours. The coupons were then weighed to the nearest tenth of a milligram and the thickness measured. Three rings of each material were placed in weighing bottles (80 ml capacity), having ground glass caps, and covered with MMH. Figure 22 shows the glassware employed in the exposure tests.

After exposure (up to 500 hours) the coupons were washed in de-ionized water, ultrasonically cleaned in 190-proof alcohol (when applicable), rinsed in fresh ethanol, oven-dried at 100°F on clean lens paper, and desiccated for 16 hours. The coupons were then reweighed and remeasured. Finally, the coupons were tensile tested in the same manner as described in section 4.2.2 of this report.

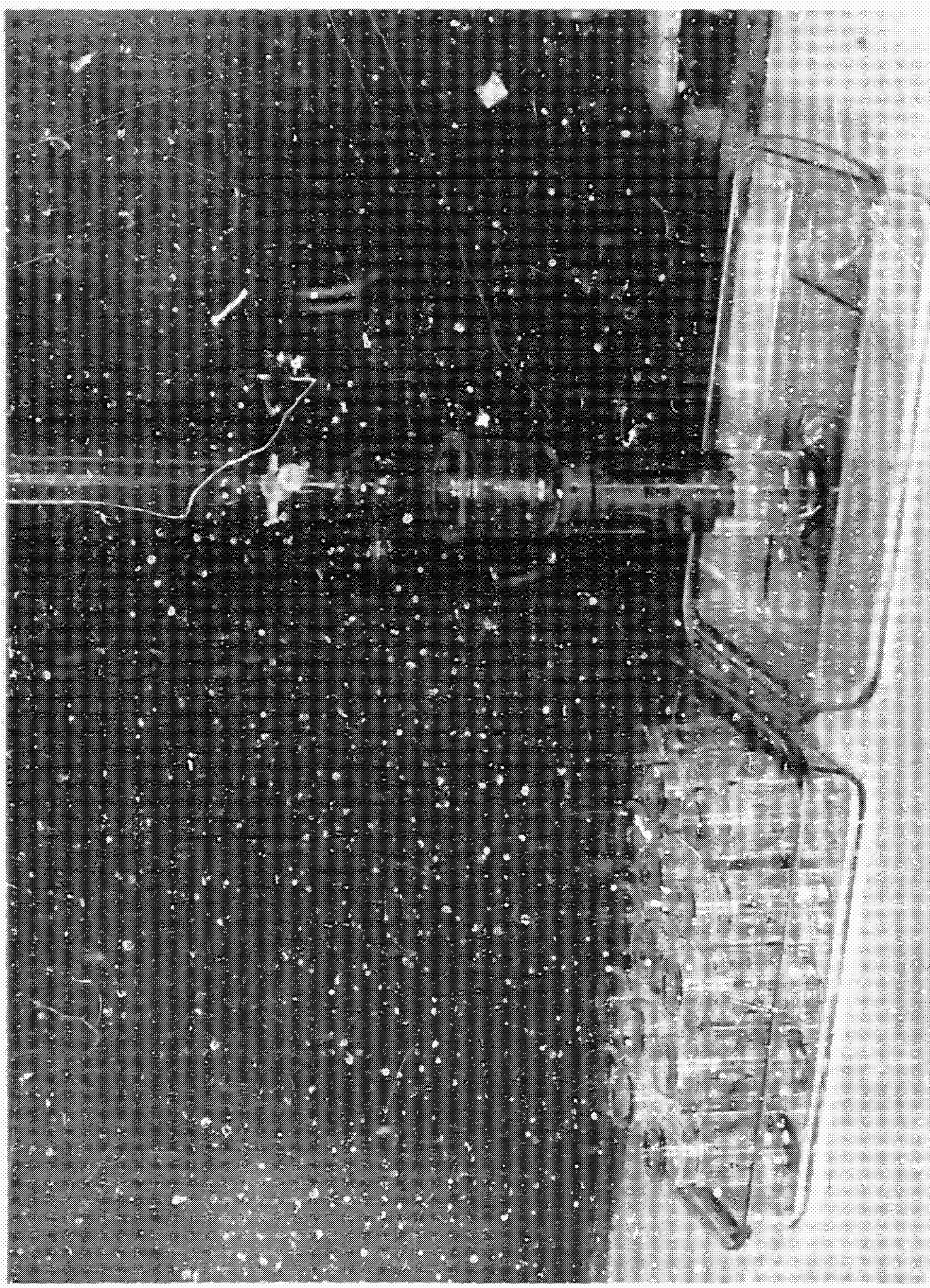

Figure 22. Exposure of Polymers to Monomethylhydrazine

Tables 25 through 32 summarize the effect of monomethylhydrazine on all polymeric diaphragm materials evaluated under this program with the exception of polyurethane foam. In addition to the data given in the tables, a brief résumé of observations made during the compatibility testing is presented below.

Teflon (from table 25): The results show that while no change in weight or dimensions of the Teflon specimens occur, some degradation in mechanical properties such as modulus, yield strength and ductility is indicated after long-time (100 and 500 hour) exposures. But in view of the overall results of table 25, it may be said that Teflon is not significantly affected by MMH.

Mylar (from table 26): After one-hour exposure to MMH, the ultimate strength and elongation of Mylar A decreased significantly. Also, Mylar A reacted with MMH as indicated by the generation of gas and discoloration of the solution to slightly yellowish. After 10 hours, gas generation was still in evidence, and the solution had a yellowish color. The coupons shattered into flakes when brought into contact with de-ionized water. After 100 hours, the solution appeared to be slightly darker than the 10-hour exposure solution; also, gas generation had ceased. The coupons were almost completely dissolved with some fragments settled at the bottom of the solution.

Tedlar (from table 27): Tedlar was found to behave similarly to Teflon. Though some change in modulus and yield strength is observed, Tedlar is resistant to MMH, and even after 500 hours the change in weight or dimensions is negligible.

Table 25. Effect of Monomethylh

Sample No.	Orient. of Tens.Cpn.	Exposure Time (hrs)	Coupon Weight (g)		Δ Wt. (g)	Coupon Thickness(in.)		Δ
			Before	After		Before	After	
1	Trans.	0	.5207	.5209	+.0002	.0051	.0051	
2	Trans.	1	.5205	.5207	+.0002	.0054	.0055	+.
3	Trans.	1	.5243	.5245	+.0002	.0051	.0051	
4	Trans.	1	.5169	.5171	+.0002	.0051	.0055	+.
5	Long.	0	.5234	.5233	-.0001	.0054	.0054	
6	Long.	1	.5329	.5330	+.0001	.0054	.0054	
7	Long.	1	.5330	.5330	0	.0054	.0054	
8	Long.	1	.5385	.5385	0	.0054	.0054	
9	Trans.	10	.5140	.5139	-.0001	.0053	.0053	
10	Trans.	10	.5180	.5178	-.0002	.0052	.0052	
11	Trans.	10	.5208	.5206	-.0002	.0053	.0053	
12	Long.	10	.5224	.5223	-.0001	.0054	.0053	-.(
13	Long.	10	.5267	.5266	-.0001	.0053	.0053	
14	Long.	10	.5321	.5320	-.0001	.0054	.0054	
15	Trans.	100	.5192	.5191	-.0001	.0052	.0052	
16	Trans.	100	.5215	.5214	-.0001	.0054	.0053	-.(
17	Trans.	100	.5218	.5214	+.0001	.0053	.0053	
18	Long.	100	.5340	.5339	-.0001	.0054	.0054	
19	Long.	100	.5110	.5110	0	.0052	.0052	
20	Long.	100	.4937	.4937	0	.0051	.0051	
21	Trans.	500	.5203	.5202	-.0001	.0055	.0055	(
22	Trans.	500	.5444	.5442	-.0002	.0056	.0056	(
23	Trans.	500	.5530	.5529	-.0001	.0057	.0058	+.(
24	Long.	500	.5264	.5264	0	.0055	.0055	(
25	Long.	500	.5438	.5437	-.0001	.0056	.0056	(
26	Long.	500	.5253	.5251	-.0002	.0055	.0055	(

(1) 0.2% Offset

e on Teflon

Ult. Str. (psi)	(1) Yield Str. (psi)	Elong. % in 1"	Modulus (psi)	R E M A R K S
3,870	-	470	-	MMH showed no discoloration
3,880	1,570	479	57,500	No apparent surface reaction
3,640	1,550	444	50,600	
3,730	1,460	475	68,500	
2,970	1,480	340	62,500	MMH showed no discoloration
4,570	1,520	545	57,800	No apparent surface reaction
4,500	1,620	532	57,600	
-	1,640	519	58,000	
3,700	1,720	440	79,500	MMH showed no discoloration
4,060	1,730	485	66,000	No apparent surface reaction
3,620	1,620	427	65,000	
4,050	1,510	491	58,400	MMH showed no discoloration
3,900	1,600	466	60,000	No apparent surface reaction
3,800	1,600	455	55,800	
3,650	1,850	465	39,000	MMH showed no discoloration
3,340	1,900	415	36,000	No apparent surface reaction
3,800	1,900	475	38,000	
3,800	1,750	440	45,000	MMH showed no discoloration
2,930	1,800	350	42,000	No apparent surface reaction
3,580	1,900	405	44,000	Note slight change in yield strength
				and modulus
2,300	1,400	275	49,000	MMH showed no discoloration
2,550	1,600	320	56,000	No apparent surface reaction. Note
2,580	1,650	315	48,000	slight change in yield strength
				and modulus
2,725	1,550	370	46,000	MMH showed no discoloration
2,460	1,550	300	49,000	No apparent surface reaction
2,650	1,500	355	46,000	Note slight change in yield strength
				and modulus

Table 26. Effect c

Sample No.	Orient. of Tens.Cpn.	Exposure Time (hrs)	Coupon Weight (g) Before	After	Δ Wt. (g)	Coupon Thickness Before	Afte
1	Trans.	0	.1290	.1292	+.0002	.0021	.002
2	Trans.	1	.1299	.1263	-.0036	.0021	.002
3	Trans.	1	.1298	.1299	+.0001	.0020	.002
4	Trans.	1	.1303	.1288	-.0015	.0021	.002
5	Long.	0	.1319	.1321	+.0002	.0021	.002
6	Long.	1	.1317	.1298	-.0019	.0019	.002
7	Long.	1	.1298	.1301	+.0003	.0020	.002
8	Long.	1	.1314	.1293	-.0021	.0020	.002
9	Trans.	10	.1283	A	A	.0020	A
10	Trans.	10	.1292	A	A	.0020	A
11	Trans.	10	.1276	A	A	.0020	A
12	Long.	10	.1282	A	A	.0020	A
13	Long.	10	.1299	A	A	.0021	A
14	Long.	10	.1316	A	A	.0021	A
15	Trans.	100	.1300	B	B	.0021	B
16	Trans.	100	.1292	B	B	.0020	B
17	Trans.	100	.1309	B	B	.0021	B
18	Long.	100	.1305	B	B	.0021	B
19	Long.	100	.1310	B	B	.0021	B
20	Long.	100	.1305	B	B	.0021	B

methylhydrazine on Mylar

Δ t (in.)	Tensile Properties at Room Temp. Ult. Str. (psi)	Yield Str. (psi)	Elong. % in 1"	Modulus (psi)	REMARKS
0	22,400	11,700	83.0	493,000	MMH turned sl. yellowish
0	17,200	11,000	31.5	488,000	Notable gas generation
+.0001	17,100	11,200	30.0	445,000	Note decrease in ultimate
0	16,700	11,700	29.0	485,000	strength and ductility
0	21,000	11,000	74.7	460,000	MMH turned sl. yellowish
+.0002	15,300	11,300	18.8	425,000	Notable gas generation
-.0001	16,000	11,500	25.0	440,000	Note decrease in ultimate
.0001	15,000	11,700	16.5	375,000	strength and ductility
A					MMH turned yellow
A					Gas generation throughout test
A					A-material shattered during transfer
					from MMH to water
A					
A					
A					
B					MMH turned yellow
B					B-coupons were almost completely
B					dissolved. Fragments of material
					remained undissolved
B					
B					
B					

Table 27. Effe

Sam-ple No.	Orient. of Tens. Cpn.	Exposure Time (hrs)	Coupon Weight (g) Before	After	Δ Wt. (g)	Coupon Thickness(Before	Afte
1	Trans.	0	.1305	.1308	+.0003	.0019	.002
2	Trans.	1	.1250	.1250	0	.0020	.002
3	Trans.	1	.1218	.1219	+.0001	.0020	.001
4	Trans.	1	.1244	.1246	+.0002	.0021	.002
5	Long.	0	.1280	.1281	+.0001	.0020	.002
6	Long.	1	.126	.1267	+.0002	.0019	.002
7	Long.	1	.1369	.1378	+.0009	.0021	.002
8	Long.	1	.1350	.1350	0	.0019	.002
9	Trans.	10	.1388	.1407	+.0019	.0023	.002
10	Trans.	10	.1246	.1260	+.0014	.0020	.002
11	Trans.	10	.1360	.1373	+.0013	.0023	.002
12	Long.	10	.1264	.1265	+.0001	.0020	.002
13	Long.	10	.1340	.1340	0	.0022	.002
14	Long.	10	.1224	.1225	+.0001	.0020	.002
15	Trans.	100	.1442	.1453	+.0011	.0024	.002
16	Trans.	100	.1251	.1258	+.0007	.0020	.002
17	Trans.	100	.1193	.1200	+.0007	.0020	.002
18	Long.	100	.1461	.1470	+.0009	.0024	.002
19	Long.	100	.1270	.1272	+.0002	.0020	.002
20	Long.	100	.1310	.13-6	+.0006	.0020	.002
21	Trans.	500	.1174	.1172	-.0002	.0020	.002
22	Trans.	500	.1460	.1459	-.0001	.0025	.002
23	Trans.	500	.1298	.1296	-.0002	.0023	.002
24	Long.	500	.1279	.1277	-.0002	.0023	.002
25	Long.	500	.1207	.1205	-.0002	.0021	.002
26	Long.	500	.1254	.1254	0	.0022	.002

(1) 0.2% offset

t (in.)	Ult. Str. (psi)	Yield Str (1) (psi)	Elong. % in 1"	Modulus (psi)	R E M A R K S
)001	11,900	4,800	249	280,000	MMH showed no discoloration
0	10,900	4,600	183	225,000	Surface of Tedlar does not etch
)001	11,600		216	245,000	Note slight decrease in modulus
)001	12,600	4,400	250	210,000	
0	7,950	4,520	335	195,000	MMH showed no discoloration
0002	7,730	4,650	285	167,500	Surface of Tedlar does not etch
)001	8,430	4,750	294	197,500	
0002	8,840	4,700	248	190,000	
0	11,900	4,300	290	164,000	MMH showed no discoloration
0	11,800	3,500	223	168,000	Surface of Tedlar does not etch
0001	11,500	4,000	235	188,000	Note decrease in modulus
0	8,430	4,550	335	187,500	MMH showed no discoloration
0	8,100	4,600	292	197,500	Surface of Tedlar does not etch
0	8,030	4,350	313	180,000	
0	12,600	5,950	280	168,000	MMH showed no discoloration
0	12,400	5,300	225	152,000	Surface of Tedlar does not etch
0	11,400	5,000	210	164,000	Note slight change in yield strength
					and modulus
0	9,670	5,800	320	164,000	MMH showed no discoloration
0	7,000	5,400	231	140,000	Surface of Tedlar does not etch
0	8,500	5,400	320	124,000	Note slight change in yield strength
					and modulus
)001	10,800		230		MMH showed no discoloration
)001	8,900	4,600	120	164,000	Surface of Tedlar does not etch
)001	9,600	5,000	160	184,000	Note slight change in yield strength
					and modulus
0	6,500	5,200	180	168,000	MMH showed no discoloration
)001	6,400	4,800	210	168,000	Surface of Tedlar does not etch
0	6,400	5,000	180	184,000	Note slight change in yield strength
					and modulus

Table 26. Effect of Monomethyl

Sam-ple No.	Orient. of Tens.Cpn.	Exposure Time (hrs)	Coupon Weight (g) Before	Coupon Weight (g) After	Δ Wt. (g)	Coupon Thicknes Before	Af
1	Long	0	.0640	.0641	+.0001	.0013	.00
2	Long.	1	.0653	.0654	+.0001	.0013	.00
3	Long.	1	.0657	.0656	-.0001	.0015	.00
4	Long.	1	.0644	.0642	-.0002	.0014	.00
5	Long.	10	.0641	.0642	+.0001	.0015	.00
6	Long.	10	.0618	.0617	-.0001	.0013	.00
7	Long.	10	.0656	.0655	-.0001	.0013	.00
8	Long.	100	.0644	.0640	-.0004	.0013	.00
9	Long.	100	.0640	.0639	+.0001	.0014	.00
10	Long.	100	.0639	.0637	-.0002	.0013	.00
1	Trans	0	.0647	.0646	-.0001	.0013	.00
2	Trans.	1	.0627	.0625	-.0002	.0013	.00
3	Trans.	1	.0625	.0623	-.0002	.0012	.00
4	Trans.	4	.0649	.0647	-.0002	.0013	.00
5	Trans.	10	.0633	.0631	-.0002	.0013	.00
6	Trans.	10	.0650	.0649	-.0001	.0013	.00
7	Trans.	10	.0640	.0638	-.0002	.0013	.00
8	Trans.	100	.0639	.0637	-.0002	.0014	.00
9	Trans.	100	.0634	.0630	-.0004	.0015	.00
10	Trans.	100	.0624	.0620	-.0004	.0012	.00
11	Long.	500	.0622	.0628	+.0006	.0013	.00
12	Long.	500	.0640	.0630	-.0010	.0013	.001
13	Long.	500	.062[illegible]	.0642	+.0016	.0012	.001
11	Trans.	500	.0633	.0618	-.0015	.0015	.001
12	Trans.	500	.0635	.0636	+.0001	.0013	.001
13	Trans.	500	.0648	.0620	-.0028	.0013	.001

ne on Aluminized Tedlar

Δ t (in.)	Tensile Properties at Room Temp. Ult. Str (psi)	Yield Str (psi)	Elong. % in 1"	Modulus (psi)	REMARKS
0	12,000	5,600	85	151,000	Aluminum coating darkened
0	11,700	5,[illegible]	80	176,000	MMH remained colorless
-.0001	10,100	5,400	62	172,000	
-.0001	13,000	5,400	110	188,000	
-.0001	12,400	5,000	100	196,000	Aluminum coating appeared spotted
0	12,300	5,000	100	188,000	MMH remained colorless
0	11,000	5,400	72	156,000	
-.0001	12,850	5,400	115	148,000	Aluminum coating was powdery
-.0002	13,350	5,200	115	164,000	MMH remained colorless
0	12,70[illegible]	5,200	105	148,000	
0	11,000	4,800	115	172,000	Aluminum coating darkened
0	13,100	4,800	155	160,000	MMH remained colorless
-.0001	12,400	4,600	160	204,000	
0	11,300	4,800	120	208,000	
-.0001	12,080	4,800	130	154,000	Aluminum coating appeared spotted
-.0001	11,200	4,900	118	192,000	MMH remained colorless
-.000[illegible]	11,600	4,600	130	184,000	
-.0001	12,900	4,800	145	148,000	Aluminum coating was powdery
-.0002	10,700	4,600	115	184,000	MMH remained colorless
0	12,200	4,600	150	140,000	
-.0001	10,400	5,400	70	160,000	Aluminum coating completely stripped.
-.0001	9,500	5,200	60	156,000	MMH remained colorless
+.0001	9,400	5,200	60	180,000	
-.0002	10,700	4,800	105	160,000	Aluminum coating completely stripped
-.0001	10,600	4,800	100	160,000	MMH remained colorless
-.0001	10,300	4,800	90	144,000	

Table 29. Effect of Monomethylhydrazine on Nylo

Sample No.	Orient. of Tens.Con.	Exposure Time (hrs)	Coupon Weight (g) Before	Coupon Weight (g) After	Δ Wt. (g)	Coupon Thickness(in.) Before	Coupon Thickness(in.) After	
1	Random	0	.5564	.5680	+.0016	.0118	.0121	[illegible]
2		1	.4699	.4660	-.0039	.0086	.0096	+
3		1	.5178	.5160	-.0018	.0096	.0106	+
4		1	.5757	.5789	+.0032	.0106	.0117	+
5		10	.6100	.6056	-.0044	.0123	.0134	+
6		10	.4100	.3918	-.0182	.0075	.0084	+
7		10	.4400	.4188	-.0312	.0081	.0087	+
8		100	.3353	.3240	-.0113	.0072	.0078	+
9		100	.4719	.4472	-.0247	.0111	.0106	-
10		100	.4113	.3916	-.0197	.0093	.0093	
11		500	.4792	.4484	-.0308	.0093	.0093	
12		500	.5475	.5216	-.0259	.0107	.0105	-
13		500	.5051	.4955	-.0096	.0102	.0103	+

dhesive

Tensile Properties at Room Temp. Ult.Str. (psi)	Yield Str. (psi)	Elong. % in 1"	Modulus (psi)	REMARKS
3,450	1,300	180	32,000	MMH remained colorless
3,450	1,650	230	46,000	
3,650	1,500	210	51,000	
4,350	1,350	260	56,000	
5,575	3,500	220	96,000	MMH remained colorless
6,000	4,500	80	132,000	
4,250	-	4.0	120,000	MMH remained colorless
6,200	-	4.0	216,000	
5,840	-	3.75	186,000	
2,750	1,200	133	31,000	MMH remained colorless
2,370	1,250	55	28,000	Note the change in modulus and
2,400	1,400	20	46,000	elongation

Table 30. Effect of Monomethylh

Sample No.	Exposure Time (hrs)	Coupon Weight (g) Before	Coupon Weight (g) After	Δ Wt. (g)	Coupon Thickness (in.) Before	Coupon Thickness (in.) After	Δ (
1	0	2.1296	2.1308	+.0012	.0393	.0392	-.0
2	1	2.1772	2.1832	+.0060	.0392	.0394	+.0
3	1	2.1798	2.1852	+.0054	.0396	.0385	-.0
4	1	2.1773	2.1829	+.0056	.0398	.0392	-.0
5	10	2.2199	2.2064	-.0135	.0403	.0400	-.0
6	10	2.1831	2.1698	-.0133	.0394	.0392	-.0
7	10	2.1276	2.1133	-.0143	.0393	.0387	-.0
8	100	1.9974	1.9230	-.0744	.0374	.0356	-.0
9	100	1.9564	1.8903	-.0661	.0361	.0344	-.0
10	100	1.9801	1.9129	-.0672	.0380	.0368	-.1

e on Silicone Rubber

Tensile Properties at Room Temp. Ult.Str. (psi)	Yield Str. (psi)	Elong. % in 1"	Modulus (psi)		REMARKS		
1,440		840	233				
1,370		810	332				
1,280		750	306				
1,360		720	233				
1,250		630	280				
1,160		600	286				
700		330	280				
800		390	280				
680		350	318				

Table 31. Effect of Monomethy

Sample No.	Orient. of Tens.Cpn.	Exposure Time (hrs)	Coupon Weight (g) Before	Coupon Weight (g) After	Δ Wt. (g)	Coupon Thickness(in.) Before	Coupon Thickness(in.) After	Δ (
1	Trans.	0	.1628	.1627	-.0001	.0037	.0039	+.C
2	Trans.	1	.1621	.1619	-.0002	.0037	.0037	
3	Trans.	1	.1501	.1500	-.0001	.0034	.0034	
4	Trans.	1	.1626	.1624	-.0002	.0039	.0037	-.C
5	Long.	0	.1597	.1598	+.0001	.0037	.0038	+.C
6	Long.	1	.1620	.1620	0	.0037	.0040	+.C
7	Long.	1	.1723	.1722	-.0001	.0041	.0041	C
8	Long.	1	.1715	.1714	-.0001	.0040	.0041	+.C
9	Trans.	10	.1649	.1647	-.0002	.0037	.0037	
10	Trans.	10	.1702	.1700	-.0002	.0040	.0040	C
11	Trans.	10	.1777	.1774	-.0003	.0041	.0041	
12	Long.	10	.1754	.1752	-.0002	.0041	.0041	
13	Long.	10	.1752	.1750	-.0002	.0042	.0042	
14	Long.	10	.1676	.1675	-.0001	.0041	.0041	
15	Trans.	100	.1683	.1682	-.0001	.0039	.0039	
16	Trans.	100	.1484	.1484	0	.0034	.0034	
17	Trans.	100	.1644	.1642	-.0002	.0039	.0039	
18	Long.	100	.1498	.1494	-.0004	.0036	.0036	(
19	Long.	100	.1575	.1574	-.0001	.0037	.0037	(
20	Long.	100	.1414	.1412	-.0002	.0033	.0033	(

(1) 0.2% offset

ne on Polyethylene

Tensile Properties at Room Temp.				
Ult. Str. (psi)	Yield Str. (psi)	Elong. % in 1"	Modulus (psi)	REMARKS
1,380	650	560	16,150	MMH showed no discoloration
1,780	600	820	15,600	No apparent surface reaction
1,040	640	215	15,100	
1,280	650	180	12,800	
1,600	706	250	11,930	MMH showed no discoloration
1,730	680	303	12,900	No apparent surface reaction
2,640	750	722	13,300	
2,130	750	480	13,900	
1,930	720	920	16,600	MMH showed no discoloration
1,250	660	310	20,000	No apparent surface reaction
1,950	540	875	21,000	
2,840	720	780	16,700	MMH showed no discoloration
2,410	810	545	13,200	No apparent surface reaction
2,440	750	575	13,200	
1,820	-	782	-	MMH showed no discoloration
1,440	780	733	11,600	No apparent surface reaction
1,900	900	880	9,600	
1,840	640	210	11,200	MMH showed no discoloration
2,120	720	470	10,800	No apparent surface reaction
1,900	665	360	9,800	

Table 32. Effect of Monomethy

Sample No.	Orient. of Tens.Cpn.	Exposure Time (hrs)	Coupon Weight (g) Before	Coupon Weight (g) After	Δ Wt. (g)	Coupon Thickness Before	Coupon Thickness Af
1	Long.	0	.2234	.2230	-.0004	.0041	.0
2	Long.	1	.2266	.1879	-.0387	.0044	.0
3	Long.	1	.2481	.2102	-.0379	.0045	.0
4	Long.	1	.2112	.1748	-.0364	.0038	.0
5	Long.	10	.2167	.1759	-.0408	.0042	.0
6	Long.	10	.2080	.1705	-.0375	.0036	.0
7	Long.	10	.2064	.1673	-.0391	.0038	.0
8	Long.	100	.2411			.0047	
9	Long.	100	.2026			.0037	
10	Long.	100	.2135			.0043	
1	Trans.	0	.2338	.2339	+.0001	.0044	.0
2	Trans.	1	.2096	.1740	-.0356	.0042	.0
3	Trans.	1	.2328	.1945	-.0383	.0041	.0
4	Trans.	1	.2287	.1878	-.0409	.0043	.0
5	Trans.	10	.2319	.1878	-.0441	.0043	.0
6	Trans	10	.2081	.1675	-.0406	.0036	.0
7	Trans	10	.2098	.1669	-.0429	.0042	.0
8	Trans	100	.2018			.0036	
9	Trans	100	.2140			.0040	
10	Trans	100	.2352			.0042	

.zine on Polyvinyl Chloride

Δ t (in.)	Tensile Properties at Room Temp. Ult. Str. (psi)	Yield Str. (psi)	Elong. % in 1"	Modulus (psi)	REMARKS
+.0001	4,100	1,400	258	44,000	MMH turned yellowish
-.0002	6,390	6,000	30	200,000	Note significant weight loss
0	6,900	6,300	20	220,000	
0	5,400	5,200	10	194,000	
-.0003	5,375	4,600	20	178,000	Same as above
+.0002	4,800	4,500	15	156,000	
+.0001	5,300	5,000	15	190,000	
					MMH turned orange
					Coupon disintegrated
+.0001	2,900	1,080	220	49,000	MMH turned yellowish
-.0005	5,050		25		Note significant weight loss
-.0002	5,400	5,100	13	152,000	
-.0002	4,500	4,300	13	118,000	
-.0001	4,900	4,500	30	160,000	Same as above
-.0002	4,500	4,300	20	146,000	
-.0002	4,650	4,600	15	172,000	
					MMH turned orange
					Coupons disintegrated

Aluminized Mylar: A short time immersion of this material in MMH established that it behaves similarly to uncoated Mylar A. Hence, no further tests were performed.

Aluminized Tedlar (from table 28): After 1-hour exposure, the reflectivity of the aluminum coating decreased considerably. Longer exposure (10 hours) caused the aluminum to separate from the Tedlar film. However, the mechanical properties are affected only to a minor extent even after a 500-hour exposure.

Nylon Epoxy Adhesive (from table 29): All mechanical properties of nylon epoxy are affected significantly after exposure to MMH. Elastic modulus increases rapidly with time, while the ductility decreases. Specimens exposed for 100 hours exhibit no yield point. The elongation values drop from as high as 180 percent for unexposed specimens to 4 percent for exposed specimens.

Polyurethane Foam: Polyurethane foam did not exhibit sufficient compatibility with MMH to permit quantitative evaluation.

Silicone Rubber (from table 30): Ductility and ultimate tensile strength of this material are degraded extensively after 10- and 100-hour exposures. This is accompanied by an increase in elastic modulus. It should be mentioned here that silicone rubber was strained at a rate of 12 in/min as compared to the rest of the polymers which were tested at a crosshead speed of 0.05 in/min.

Polyethylene (from table 31): Polyethylene was found to remain essentially unaffected after exposure to MMH for periods up to 100 hours.

Polyvinyl Chloride (from table 32): Exposure to MMH for as little as 1 hour causes significant loss in weight. The degradation in mechanical properties of PVC is evident from the fact that ductility decreased by a factor of ten with attendant increase in modulus by a factor of approximately four. Ultimate tensile strength also increases. After 100-hour exposure, the specimen disintegrated, and the color the MMH solution changed to orange.

4.4 Stresses in Diaphragm Test Specimens

When the maximum axial deflection in a pressurized circular diaphragm exceeds approximately one-half the diaphragm thickness, the middle region becomes appreciably stressed. This stress, which is essentially biaxial, may be balanced by radial tension at the edges if the edges are held, or by circumferential compression if the edges are not horizontally restrained. The latter applies to the case of the proposed diaphragm tests.

When axial deflections exceeding one-half the specimen thickness are obtained, the shell appears stiffer than indicated by simple theory, and the load-deflection and load-stress relations are nonlinear.

The relationships for stress and axial deflection under three specific conditions of restraint are given below.

(1) Circular diaphragm, uniform load, edges fixed but not held (no edge tension).

t = thickness of diaphragm (inches)

α = radius of shell (inches)

p = pressure (psi)

δ = maximum deflection (inches)

σ_b = bending stress (psi)

σ_d = diaphragm stress (psi)

σ = $\sigma_b + \sigma_d$ = maximum stress (combined tension)

Max. δ at center,

$$\frac{p\alpha^4}{Et^4} = \frac{16}{3\,(1-\mu^2)} \left(\frac{\delta}{t}\right) + \frac{6}{7}\left(\frac{\delta}{t}\right)^3$$

Stress at center,

$$\sigma = \frac{Et^2}{\alpha^2} \left[\frac{2}{1-\mu} \left(\frac{\delta}{t}\right) + \frac{1}{2}\left(\frac{\delta}{t}\right)^2\right]$$

Stress at edge,

$$\sigma = \sigma_b = \frac{Et^2}{\alpha^2} \left[\frac{4}{1-\mu^2} \left(\frac{\delta}{t}\right)\right]$$

(2) Circular diaphragm, uniform loading, edges fixed and held:

Max. δ at center,

$$\frac{p\alpha^4}{Et^4} = \frac{16}{3\,(1-\mu^2)} \left[\frac{\delta}{t} + 0.488\left(\frac{\delta}{t}\right)^3\right]$$

Stress at center,

$$\sigma = \frac{Et^2}{\alpha^2} \left[\frac{2}{1-\mu} \left(\frac{\delta}{t}\right) + \frac{1}{2}\left(\frac{\delta}{t}\right)^2\right]$$

Stress at edge,

$$\sigma = \sigma_d + \sigma_b = \frac{Et^2}{\alpha^2} \left[\frac{4}{1-\mu^2} \left(\frac{\delta}{t}\right)\right] + 0.476\,E\left(\frac{\delta}{\alpha}\right)^2$$

(3) Circular diaphragm without flexural stiffness, uniform loading edges held,

$$\delta = 0.662\,\alpha\sqrt[3]{\frac{p\alpha}{Et}}$$

Stress at center,

$$\sigma_d = 0.423 \sqrt[3]{\frac{Ep^2\alpha^2}{t^2}}$$

Stress at edge,

$$\sigma_d = 0.328 \sqrt[3]{\frac{Ep^2\alpha^2}{t^2}}$$

In the case of two cases above where the diaphragm possesses bending rigidity, the maximum deflection, δ, must first be determined. If δ is known, then σ may be readily calculated.

While the stress distribution in circular diaphragms is nonuniform, the following advantages are readily apparent:

a. Relatively high stresses at the center may be attained at moderate hydraulic loads.

b. No molding or fabrication is required, thus preserving "as received" characteristics of sheet materials.

c. Stress measurement (through bulge height) is relatively simple.

Uniform Biaxial Tension: Two-dimensional tension, in which $\sigma_x = \sigma_y$, i.e., σ_d is constant over the entire specimen, may be achieved in a hydraulically-loaded hemispherical diaphragm. Variation of size and/or gauge section of such a diaphragm would permit relatively broad variation of stress at any given pressure differential across the diaphragm.

Uniaxial Tension: The most direct means of achieving uniaxial tensile stressing through hydraulic loading is by means of a hollow right cylinder, which is restrained along its axis. The size and/or gauge of such specimens would again be varied in order to achieve a broad range of hoop stresses at any given pressure differential. In practice, such specimens would have heavy gauge closures which could be restrained during testing without excessive deflection. Removal of the axial restraint would result in a biaxially-stressed cylinder, wherein $\sigma_x = 1/2\ \sigma_y$, where σ_x and σ_y are the axial and hoop stresses, respectively.

5. PERMEABILITY TESTS

5.1 Metal Diaphragms

5.1.1 Liquid Monomethylhydrazine Tests

Both a stainless steel and an aluminum diaphragm were mounted into the room temperature system and covered with approximately 3 liters of liquid MMH. The 8 mil stainless steel diaphragm was then loaded in increasing pressure steps to 97 psia with dry nitrogen gas with no indication of MMH or GN_2 permeation. That is, no change in the residual gas content, mainly nitrogen and water vapor, or the virtual leak rate of the system was observed at the several levels of overpressure applied.

T e 12 mil aluminum diaphragm covered with MMH was loaded in increasing pressure steps to 80 psia with dry nitrogen gas with no indication of MMH or GN_2 permeation. That is, no change in the residual gas content, mainly nitrogen and water vapor, or of the virtual leak rate of the system was observed at the several levels of overpressure applied.

In the above tests the stainless steel and aluminum diaphragms were stressed at the center to a calculated maximum 63.5% and 90.4%, respectively, of the materials' biaxial yield strengths. The permeation was calculated in terms of SPU. The results are presented in table 33. Permeability of liquid MMH through both materials at room temperature is less than the limiting values presented, based on the GN_2 sensitivity of the residual gas analyzer.

5.1.2 Liquid Nitrogen Tetroxide Tests

Both a stainless steel and an aluminum diaphragm were mounted in the room temperature system and covered with 3 liters of liquid N_2O_4. The 8 mil stainless steel diaphragm was then loaded in increasing pressure steps

Table 33. Permeability of Metal Diaphragms

Diaphragm Material	Thickness (inches)	Diameter (inches)	Test Fluid	Pressure Differential (psia)	Testing Time (sec)	SPU $\frac{cm^3 - cm}{cm^2 - cm\ Hg - sec}$	Calculated Stress*** (psi)
304 Stainless Steel	0.008	5.5	Liq MMH	97	7,200	$\leq 1.4 \times 10^{-18}$	1.27×10^5
2024-T6 Aluminum	0.012	5.5	Liq MMH	40	72,000	$\leq 5.0 \times 10^{-19}$	4.05×10^4
304 Stainless Steel	0.008	5.5	Liq N_2O_4	105	4,260	$\leq 2.1 \times 10^{-18}$	1.34×10^5
2024-T6 Aluminum	0.012	5.5	Liq N_2O_4	80	2,160	$\leq 3.3 \times 10^{-18}$	2.97×10^4
304 Stainless Steel*	0.008	5.5	LN_2	115	1	$\leq 8.4 \times 10^{-15}$	1.49×10^5
304 Stainless Steel*	0.008	5.5	LN_2	95	420	$\leq 1.9 \times 10^{-15}$	1.31×10^5
304 Stainless Steel**	0.008	2-5/8	LN_2	65	3,120	$\leq 2.1 \times 10^{-17}$	6.21×10^4
304 Stainless Steel**	0.008	2-5/8	LH_2	25	82	2.1×10^{-12}	3.31×10^4

*Diaphragm mechanically sealed to specimen mount

**Diaphragm weld sealed to specimen mount

***Stress at diaphragm center

to 105 psia with no indication of N_2O_4 permeation. At 105 psia, however, the high vacuum diaphragm seal slipped and a momentary passage of N_2O_4 occurred. This was indicated by the appearance of m/e 30 (NO) in the mass spectrometer output. Holding at 105 psia revealed no further seal slippage or N_2O_4 passage as indicated by rapid decay of the m/e 30 peak while the residual gas content, mainly nitrogen and water vapor, maintained the preburst level.

The 12 mil aluminum diaphragm covered with liquid N_2O_4 was loaded in increasing pressure steps to 80 psia with no indication of N_2O_4 permeation. At 80 psia, however, the high vacuum diaphragm seal slipped and a momentary passage of N_2O_4 occurred. This was indicated by the appearance of m/e 30 (NO) and m/e 46 (NO_2). The appearance of the latter, along with a large m/e 30 peak height as compared to the stainless steel diaphragm experiment, indicates the passage through the seal of a greater amount of N_2O_4 as compared to the stainless steel experiment. Holding at 80 psia revealed no further seal slippage or N_2O_4 passage as indicated by the rapid decay of the N_2O_4 products peaks while the residual gas content, mainly nitrogen and water vapor, maintained the preburst levels.

In the above tests the stainless steel and aluminum diaphragms were stressed to a calculated 67% and 44.3%, respectively, of the biaxial yield strength. The permeation was calculated in terms of SPU. The results are presented in table 33. Permeability of liquid N_2O_4 through both materials at room temperature is less than these limiting values based on the GN_2 sensitivity of the residual gas analyzer.

5.1.3 Liquid Nitrogen Tests

The determination of LN_2 permeation through metal diaphragms has followed the development of the mechanical seal for cryogenic permeation tests. Tests with both stainless steel and aluminum alloy diaphragms tightened with the high vacuum aluminum "O" ring seal to the specimen holder at room temperature have indicated a loss of the high vacuum seal at cryogenic temperature. With introduction of LN_2 into the system, the seal bolts tend to loosen as shown by retorquing after test. This results in loss of the high vacuum seal during cryogenic loading and/or system temperature reduction.

Precooling of the specimen holder, diaphragm and "O" ring seal assembly with LN_2 and torquing while cool showed promise. One stainless steel and one aluminum alloy diaphragm each maintained high vacuum to atmosphere while supporting several liters of LN_2. However, a second stainless steel diaphragm did not maintain the high vacuum seal during system LN_2 cool down and filling. This latter stainless steel diaphragm, however, was not precooled to the degree of the first. Both of the diaphragms that successfully held LN_2 at atmospheric pressure were pressurized. The stainless steel diaphragm was pressurized up to 65 psia. The aluminum alloy diaphragm held up to 40 psia at which point one of the seals ruptured. Both diaphragms exhibited increased nitrogen levels in the dutchman with increased pressure. These are believed to be due to leakage through the seal.

Review of the thermal expansion of the two diaphragm seal materials, the stainless steel of the bolts and the aluminum "O" ring, versus temperature[22] indicates that over the temperature range from room to cryogenic temperature, differential thermal expansion would cause the aluminum to contract faster than the stainless steel. This, in turn, would cause relaxation of the seal loading force as applied by the bolts. Typical room temperature values of the coefficient of thermal expansion for these materials is listed in table 34. To offset the aluminum-stainless steel differential thermal expansion, a washer made of a material having a smaller coefficient of thermal expansion than stainless steel was inserted on the bolts. The material used was tantalum. The thermal expansion coefficient for tantalum is listed in table 34. Calculations for the typical seal where the aluminum "O" ring has been compressed to about 20 mils in thickness indicate that 50 mils of tantalum would be required to maintain the seal loading force as applied at room temperature for a stainless steel diaphragm. An aluminum diaphragm would increase the amount of aluminum in the seal, requiring more tantalum for proper compensation. However, differential thermal expansion in the plane of the aluminum diaphragm would also require compensation.

To test the design, an 8 mil stainless steel diaphragm was mounted with 40 mils of tantalum, inserted on the bolts and the assembly torqued at room temperature.

Table 34. Seal Material Room Temperature Thermal Expansion

Material	Thermal Expansion Coefficient
304 Stainless Steel	8×10^{-6} in/in°F
Aluminum	12×10^{-6} in/in°F
Tantalum	2×10^{-6} in/in°F

The diaphragm was covered with approximately 6 liters of LN_2. No indications of seal leakage or diaphragm permeation were noted at atmospheric pressure. Overpressure was then increased in steps to 115 psia and, again, no indication of leakage or permeation was noted. However, at 115 psia, the seal slipped and the high vacuum was lost, terminating the test.

The above test stressed the 8 mil stainless steel diaphragm to approximately 50% of the material yield strength. Based upon the sensitivity of the detection apparatus as previously reported and the observed data, the numerical limit of permeation in terms of SPU was calculated. The result is presented in table 33. Permeability of LN_2 through a stainless steel diaphragm at cryogenic temperature is less than this limiting value based on the N_2 sensitivity of the residual gas analyzer.

Dimensional inspection of the diaphragm mounting assembly as torqued and after disassembly showed the bolt ring to have a 10-mil elastic set or taper along with a 1-mil machined taper on the top surface of the mount, both so aligned that a wedge-shaped space existed between the two surfaces when under torque at the aluminum O-ring position. The point of the wedge was toward the OD of the diaphragm assembly. Machining of both pieces was performed so that a taper with the point toward the center of the assembly existed under torque.

To test the design, an 8-mil stainless steel diaphragm was mounted with 60 mils of tantalum on the remachined pieces. An aluminum O-ring was used as before on previous tests. The diaphragm was covered with approximately 6 liters LN_2. No indication of seal leakage or diaphragm permeation was observed at atmospheric pressure, however, cryopumping was noted. Overpressure was then increased in steps to 95 psia with no noticeable change in the nitrogen peak height. However, a small improvement in vacuum was noted as each pressure step was applied. While increasing the overpressure to 115 psia, a rapid degradation in vacuum occurred and the test was terminated.

The modified diaphragm mount tested at the 95 psia pressure level resulted in stressing the 8-mil stainless steel diaphragm to 43.3% of the metal yield strength. The numerical limit of permeation in terms of SPU was calculated as before. The result is presented in table 33.

A third test was run using an 8-mil stainless steel diaphragm and 100 mil of tantalum spacer. However, high vacuum was lost during LN_2 filling. Analysis indicated that the exposure sequence to LN_2 and the thermal diffusivity of the diaphragm mount assembly components probably caused overcompression of the O-ring with initial contact of LN_2 on the bolt heads and tantalum washers which was followed by relaxation of the seal as the whole assembly cooled down.

As a background check of the LN_2 system operation and the diaphragm seal for subsequent LH_2 system checkout operations, an 8 mil stainless steel diaphragm, 2-5/8 inches in diameter, was weld-sealed to the diaphragm mount and assembled into the system. The weld-sealed diaphragm mount assembly is shown in figure 23. During initial LN_2 filling, high vacuum was lost which was traced to leakage past the O-ring seal between the dutchman and the bottom of the diaphragm mount assembly. Retightening the mounting bolts resealed the system. The diaphragm was covered with 13 liters of LN_2 and in

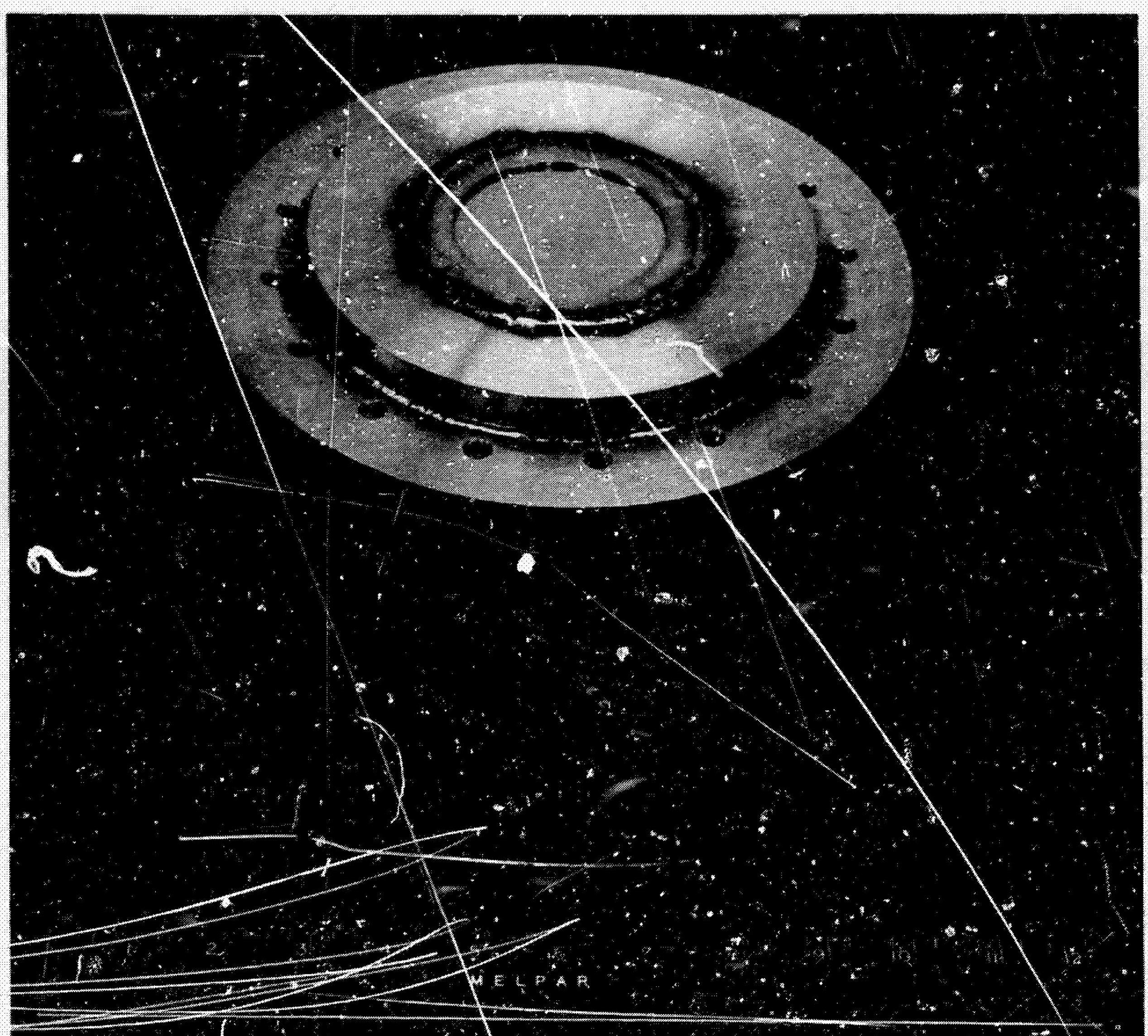

Figure 23. Weld-Sealed Diaphragm Mount Assembly

quick steps pressurized to 315 psia. However, abnormal behavior, i.e., a sporadic degradation of vacuum with time, precludes analysis of the data. On system warmup, the high vacuum was lost.

The system was restarted and high vacuum attained. The diaphragm was again covered with 13 liters of LN_2. At atmospheric overpressure the dutchman was cryopumped by the cold diaphragm and the surrounding mount. Pressure was increased to 65 psia by GN_2. Until a new system pressure-temperature equilibrium was re-established the cryopumping rate appeared to increase due to the higher fluid boiling point at the higher pressure. After a pressure surge, the vacuum system's mounting bolts were retorqued. As one of the bolts was retightened, the high vacuum was lost. The system was quickly restarted and high vacuum re-attained. LN_2 at 65 psia remained above the diaphragm while the vacuum was lost. Rechecking, the cryopumping rate was similar to that occurring prior to the loss in vacuum, indicating that any permeation of the diaphragm was below the detectable limits of the test equipment.

The weld-sealed diaphragm tested at the 65 psia pressure level was stressed to approximately 20.5% of the material yield strength. The numerical limit of permeation in terms of SPU was calculated. The result is presented in table 33.

5.1.4 Liquid Hydrogen Tests

Testing in the LH_2 system has been limited to the preliminary checkout of the system and its operation using the 8-mil stainless steel diaphragm weld sealed to the diaphragm mount (figure 23). The diaphragm was covered with approximately 10 liters of LH_2, but pressurization in excess of 40 psig could not be accomplished due to a faulty LH_2 fill solenoid valve. However, while holding the system at 25 psia, the operating characteristics and response of the cryogenic and vacuum system were explored. With the 6-inch gate valve open, both H_2 and N_2 were observed to increase with time and respond directly to the ion pump level and its fluctuations. Upon closure of the 6-inch gate valve, the N_2 peak remained constant while an increase in the H_2 level was noted. This increase in H_2 level is attributed to permeation.

In this test, the stainless steel weld-sealed diaphragm was loaded to a calculated 13% of the material's yield strength. As an approximation, the permeation was calculated in terms of SPU assuming the sensitivity of the detection equipment to be the same for H_2 as it is for N_2. The result may be found in table 33.

5.2 Polymeric Diaphragms

5.2.1 Coarse Screening Tests

The purpose of this experiment was to provide an indication of gross permeability rates of the propellants through the polymeric materials and to study the deformation characteristics of the polymer diaphragms when subjected to reduced pressures. Preliminary tests indicated that these functions would be achieved by the apparatus shown in figures 24 through 26. Functionally, the apparatus consists of two glass chambers which are separated from each other by the stainless steel polymer diaphragm holder. Silicone rubber gaskets are used at the ground glass joints to effect a vacuum seal on the bottom chamber and a leaktight seal on the top container. A capillary tube and overflow cup extend from the top container and its seal is effected through a standard taper joint. A filling tube also extends from the top container and is used to introduce and remove the liquid from the container. The bottom chamber contains a Hastings Raydist Thermocouple Tube for monitoring pressure, a stopcock for bringing the chamber back to atmosphere, and a trapped pumping tube. Using this apparatus, experiments were conducted to obtain gross permeation rates and to determine the presence of microporosity in the polymeric materials. The procedure is described below.

The test materials were cleaned thoroughly with methanol. After securing the polymeric sheet in the apparatus, the chamber below the diaphragm was evacuated until a terminal vacuum was attained. The stopcock at the trap was then closed, thus isolating the vacuum pump from the system. After a ten-minute period, the pressure was noted and the pressure change per

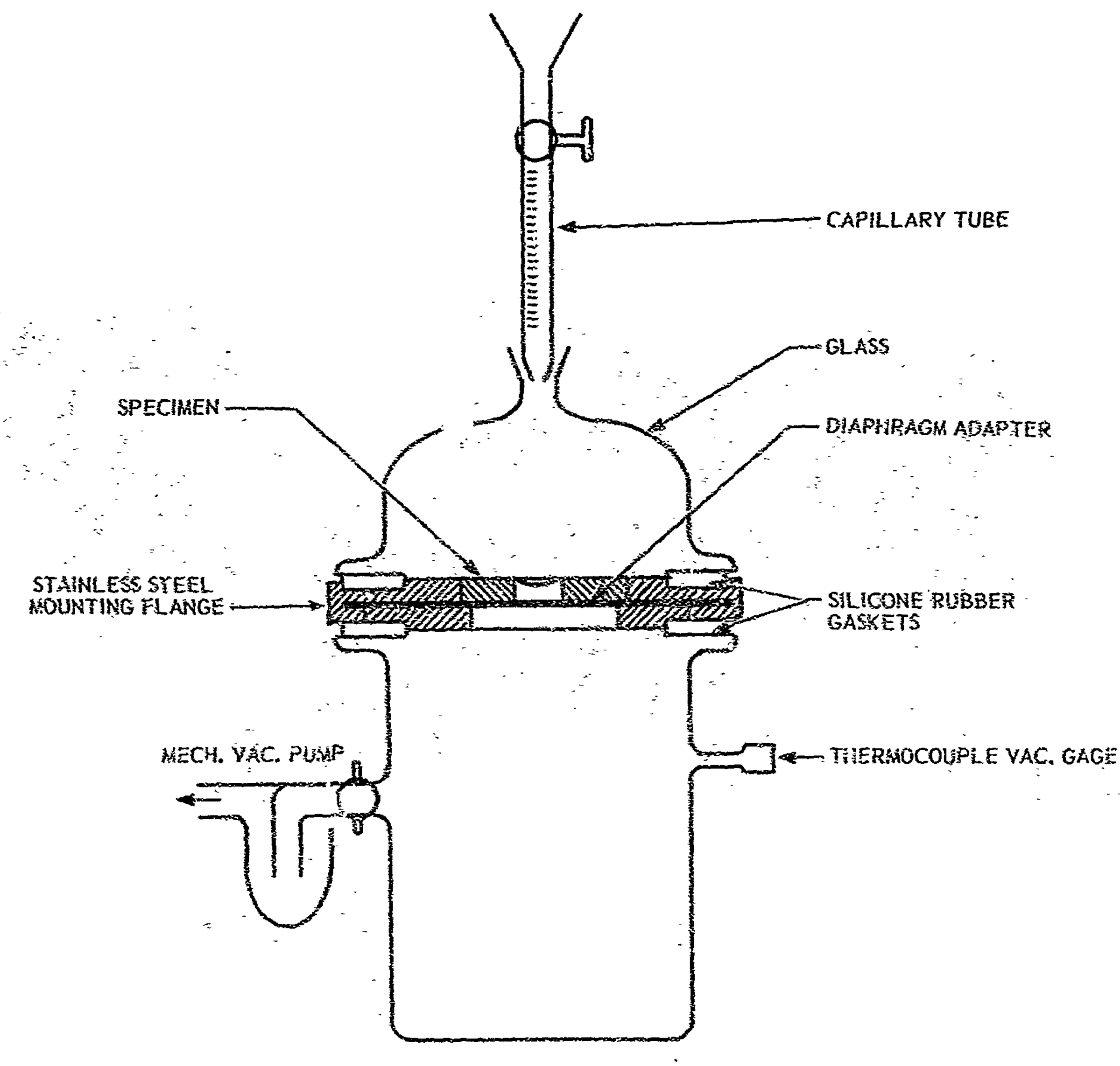

Figure 24. Coarse Screening Permeability Apparatus

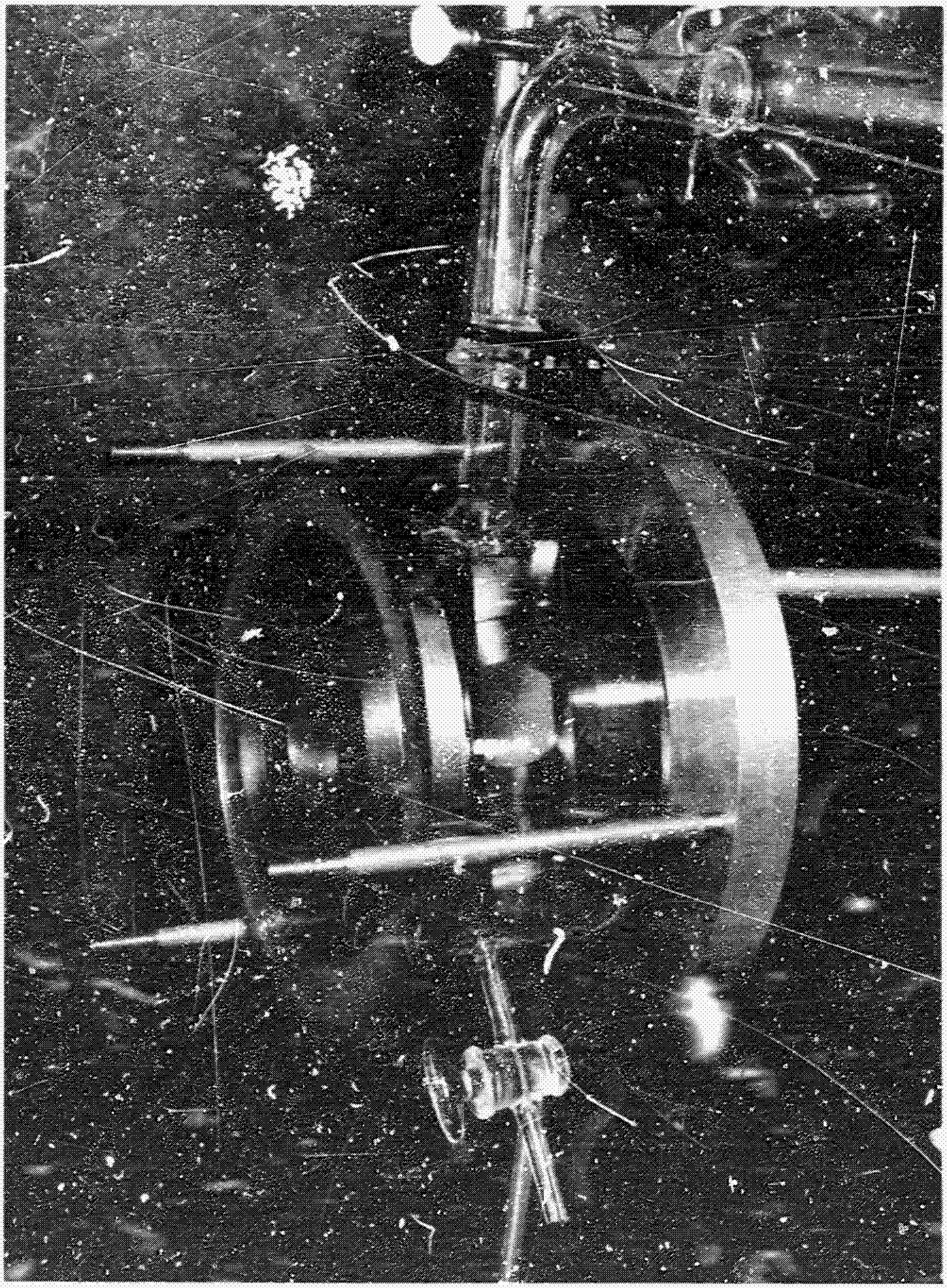

Figure 25. Close-up View of Diaphragm Mounting Apparatus

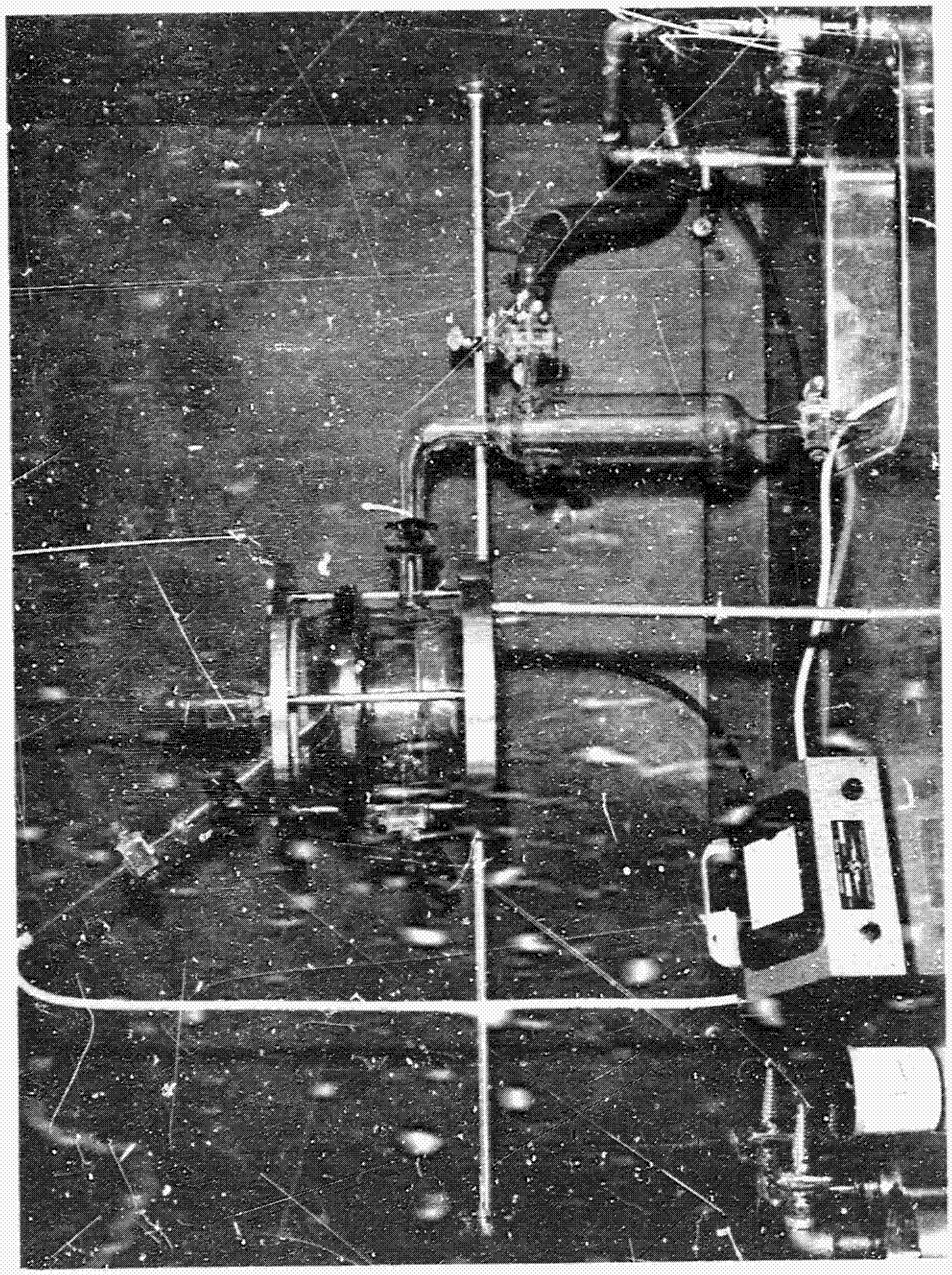

Figure 26. Coarse Screening Apparatus

minute determined. This value was taken as the natural drift of the system with one side of the diaphragm in air at atmospheric pressure. Two additional pressure change readings were taken for comparison. Keeping the bottom chamber under vacuum, the deflected diaphragm was filled with permeating fluid (water or MMH) and the procedure, as described above, repeated for three pressure change readings. The fluid was then removed from the deflected diaphragm and three pressure change readings taken to re-establish the natural leakage to air of the system with one side of the diaphragm in air at atmospheric pressure. Finally, the polymeric material was removed from the apparatus. Results of the preliminary tests are shown in tables 35 and 36.

Gross permeation rates of air and monomethylhydrazine through polyethylene diaphragms were determined on the Coarse Screening Apparatus for several thicknesses and diaphragm diameters. These results are presented in table 36. Summarizing these results, it can be seen that by keeping the diaphragm diameter constant and increasing the thickness of the polyethylene, thereby decreasing the level of strain in the diaphragm, the gross permeation rate of MMH generally decreases. Similarly, when the thickness of the polyethylene is held constant and the diameter of the diaphragm increased, thereby increasing the level of strain in the diaphragm, the gross permeation rate of MMH is shown to increase.

An explanation of these results is presented on the basis of physical imperfections in the polyethylene material. Examination of the polyethylene under polarized lighting clearly reveals that the density of physical imperfections not only increases as the thickness decreases, but varies within

Table 35. Gross Permeation Rates of Air and Water Th

Material	Thickness (in.)	Diaphragm Diameter (in.)	Initial Pressure (μ)	Final Pressure (μ)	Pressure Change (μ)	Time Inte: (mi
Polyethylene	.004	.729	9	64	55	10
	.004	.729	9	62	53	10
	.004	.729	9	63	54	10
	.004	.729	9	73	64	10
	.004	.729	10	77	67	10
	.004	.729	11	77	66	10
	.004	.729	10	72	62	10
	.004	.729	10	67	57	10
	.004	.729	9	66	57	10
	.004	1.050	10	75	65	10
	.004	1.050	10	71	61	10
	.004	1.050	9	68	59	10
	.004	1.050	8	72	64	10
	.004	1.050	10	82	72	10
	.004	1.050	11	81	70	10
	.004	1.050	10	70	60	10
	.004	1.050	10	66	56	10
	.004	1.050	*	*	*	*
Tedlar	.002	1.880	10	89	79	10
	.002	1.880	9	87	78	10
	.002	1.880	9	87	78	10
	.002	1.880	9	165	156	10
	.002	1.880	15	220	205	10
	.002	1.880	16	230	214	10
	.002	1.880	10	88	78	10
	.002	1.880	9	82	73	10
	.002	1.880	9	82	73	10
	.002	2.200	16	250	234	10
	.002	2.200	14	220	206	10
	.002	2.200	14	230	216	10
	.002	2.200	15	330	315	10
	.002	2.200	23	380	357	10
	.002	2.200	22	375	353	10
	.002	2.200	18	280	262	10
	.002	2.200	16	250	234	10
	.002	2.200	15	240	225	10

*Diaphragm ruptured during third evacuation

Selected Polymeric Diaphragms

Permeation Rate (μ/min.)	Calculated Stress (psi)	Diaphragm Environment
5.5		) Air at atmospheric pressure
5.3	$.671 \times 10^3$	)
5.4		)
6.4		)
6.7		) Diaphragm filled with water
6.6		)
6.2		)
5.7		) Water removed from diaphragm
5.7		) Air at atmospheric pressure
6.5	$.965 \times 10^3$	)
6.1		) Air at atmospheric pressure
5.9		)
6.4		)
7.2		) Diaphragm filled with water
7.0		)
6.0		)
5.6		) Water removed from diaphragm
*		) Air at atmospheric pressure
7.9	3.45×10^3	)
7.8		) Air at atmospheric pressure
7.8		)
15.6		)
20.5		) Diaphragm filled with water
21.4		)
7.8		)
7.3		) Water removed from diaphragm
7.3		)
23.4	4.04×10^3	)
20.6		) Air at atmospheric pressure
21.6		)
31.5		)
35.7		) Diaphragm filled with water
35.3		)
26.2		)
23.4		) Water removed from diaphragm
22.5		) Air at atmospheric pressure

Table 35. (Continued) Cross Permeation Rate

Material	Thickness (in.)	Diaphragm Diameter (in.)	Initial Pressure (μ)	Final Pressure (μ)	Pres Chan (μ
Teflon	.005	1.880	9	80	7
	.005	1.880	7	61	5
	.005	1.880	7	60	5
	.005	1.880	7	59	5
	.005	1.880	7	62	5
	.005	1.880	7	61	5
	.005	1.880	7	61	5
	.005	1.880	8	59	51
	.005	1.880	8	59	51
Polyethylene	.002	0.509	8	102	9
	.002	0.509	8	93	8
	.002	0.509	8	91	8
	.002	0.509	9	102	9
	.002	0.509	10	112	10
	.002	0.509	9	112	10
	.002	0.509	9	100	9
	.002	0.509	8	97	8
	.002	0.509	8	95	8
	.004	0.509	7	79	7
	.004	0.509	7	73	66
	.004	0.509	7	72	6
	.004	0.509	8	77	6
	.004	0.509	7	81	7
	.004	0.509	7	81	7
	.004	0.509	7	71	6
	.004	0.509	6	70	6
	.004	0.509	6	68	6
	.006	0.509	7	60	5
	.006	0.509	6	58	52
	.006	0.509	7	56	4
	.006	0.509	7	63	5
	.006	0.509	7	64	57
	.006	0.509	8	67	5
	.006	0.509	7	60	5
	.006	0.509	7	57	50
	.006	0.509	8	58	50

Air and Water Through Selected Polymeric Diaphragms

Time Interval (min.)	Permeation Rate (μ/min.)	Calculated Stress (psi)	Diaphragm Environment
10	7.1	1.38×10^3	)
10	5.4		) Air at atmospheric pressure
10	5.3		)
10	5.2		)
10	5.5		) Diaphragm filled with water
10	5.4		)
10	5.4		)
10	5.1		) Water removed from diaphragm
10	5.1		) Air at atmospheric pressure
10	9.4	$.938 \times 10^3$	)
10	8.5		) Air at atmospheric pressure
10	8.3		)
10	9.3		)
10	10.2		) Diaphragm filled with water
10	10.3		)
10	9.1		)
10	8.9		) Water removed from diaphragm
10	8.7		) Air at atmospheric pressure
10	7.2	$.468 \times 10^3$	)
10	6.6		) Air at atmospheric pressure
10	6.5		)
10	6.9		)
10	7.4		) Diaphragm filled with water
10	7.4		)
10	6.4		)
10	6.4		) Water removed from diaphragm
10	6.2		) Air at atmospheric pressure
10	5.3	$.312 \times 10^3$	)
10	5.2		) Air at atmospheric pressure
10	4.9		)
10	5.6		)
10	5.7		) Diaphragm filled with water
10	5.9		)
10	5.3		)
10	5.0		) Water removed from diaphragm
10	5.0		) Air at atmospheric pressure

Table 36. Gross Permeation Rates of Air and Monomethylhydrazine Thr

Material	Thickness (in.)	Diaphragm Diameter (in.)	Initial Pressure (μ)	Final Pressure (μ)	Pressure Change (μ)	Time Interval (min.)	Permea Rat (μ/min
Polyethylene	.002	0.509	7	112	105	10	10.
	.002	0.509	9	110	101	10	10.
	.002	0.509	9	110	101	10	10.
	.002	0.509	9	135	126	10	12.
	.002	0.509	11	148	137	10	13.
	.002	0.509	10	135	125	10	12.
	.002	0.509	10	125	115	10	11.
	.002	0.509	9	122	113	10	11.
	.002	0.509	9	115	106	10	10.
Polyethylene	.004	0.509	10	103	93	10	9.
	.004	0.509	8	86	78	10	7.
	.004	0.509	6	71	65	10	6.
	.004	0.509	6	71	65	10	6.
	.004	0.509	6	76	70	10	7.
	.004	0.509	6	75	69	10	6.
	.004	0.509	6	79	73	10	7.
	.004	0.509	6	73	67	10	6.
	.004	0.509	6	77	71	10	7.
Polyethylene	.006	0.509	8	66	58	10	5.
	.006	0.509	6	58	52	10	5.
	.006	0.509	6	58	52	10	5.
	.006	0.509	6	63	57	10	5.
	.006	0.509	5	61	56	10	5.
	.006	0.509	5	60	55	10	5.
Polyethylene	.004	0.729	7	87	80	10	8.
	.004	0.729	6	82	76	10	7.
	.004	0.729	6	80	74	10	7.
	.004	0.729	6	85	79	10	7.
	.004	0.729	10	132	122	10	12.
	.004	0.729	10	125	115	10	11.
	.004	0.729	10	104	94	10	9.
	.004	0.729	8	100	92	10	9.
	.004	0.729	6	95	89	10	8.

elected Polymeric Diaphragms

alculated Stress (psi)	Diaphragm Environment					
938 x 10^3	Air at atmospheric pressure					
	Diaphragm filled with MMH					
	MMH removed from diaphragm. Air at atmospheric pressure					
468 x 10^3						
	Air at atmospheric pressure					
	Diaphragm filled with MMH					
	MMH removed from diaphragm. Air at atmospheric pressure					
312 x 10^3						
	Air [illegible]ic pressure.					
	Diaphragm filled with MMH					
671 x 10^3						
	Air at atmospheric pressure.					
	Diaphragm filled with MMH					
	MMH removed from diaphragm. Air at atmospheric pressure					

Table 36. (Continued) Gross Permeation Rates of

Material	Thickness (in.)	Diaphragm Diameter (in.)	Initial Pressure (μ)	Final Pressure (μ)	Pres. Ch (
Polyethylene	.006	1.309	5	53	[illegible]
	.006	1.309	4	46	4
	.006	1.309	4	40	3
	.006	1.309	4	37	3
	.006	1.309	1	36	3
	.006	1.309	4	57	5
	.006	1.309	5	72	6
	.006	1.309	5	72	6
	.006	1.309	4	-	-

and Monomethylhydrazine Through Selected Polymeric Diaphragms

Time Interval (min.)	Permeation Rate (μ/min.)	Calculated Stress (psi)	Diaphragm Environment
10	4.8)	.803 x 10^3	
10	4.2)		Air at atmospheric pressure.
10	3.6)		
10	3.3)		
10	3.5)		Diaphragm filled with MMH
10	5.3)		
10	6.7)		
10	6.7)		
-	-		MMH removed from diaphragm. Diaphragm split along longitudinal lines during test.

each thickness of the film. These physical imperfections appear to be foreign particles that are imbedded in the film and may completely penetrate the film. These imperfections may act as stress concentrators and, during straining of the diaphragm, may completely separate, thereby forming micro-pores, or cause the material surrounding the imperfection to deform or "thin out" to the extent of forming micro-pores. Hence, as the strain level increases in any polyethylene diaphragm containing imperfections, the gross permeation rate of MMH increases correspondingly.

A particular type of diaphragm failure was noted during coarse screening testing of polyethylene, which is shown in figure 27. This type of failure occurred in the transverse direction along longitudinal lines. The lines were found in all the thicknesses of polyethylene tested and appear to be derived from extrusion. The effect of these lines on the tensile properties of polyethylene at room temperature becomes apparent after analysis of the data presented in section 4, table 22. The data shows that while the ultimate tensile strength in the transverse direction is less than that exhibited in the longitudinal and 45° direction, the tensile modulus and yield strength are correspondingly greater. This would seem to indicate that these lines locally reduce the effective cross-sectional area and also act as stress concentrators in the transverse direction. Similarly, the increased elongation in the transverse direction suggests that localized yielding occurs first at the region of minimum cross-sectional area and progresses locally along the entire gauge length.

While other polymeric materials showed some indication of directionality prior to failure under biaxial loading, polyethylene proved to be the most consistent.

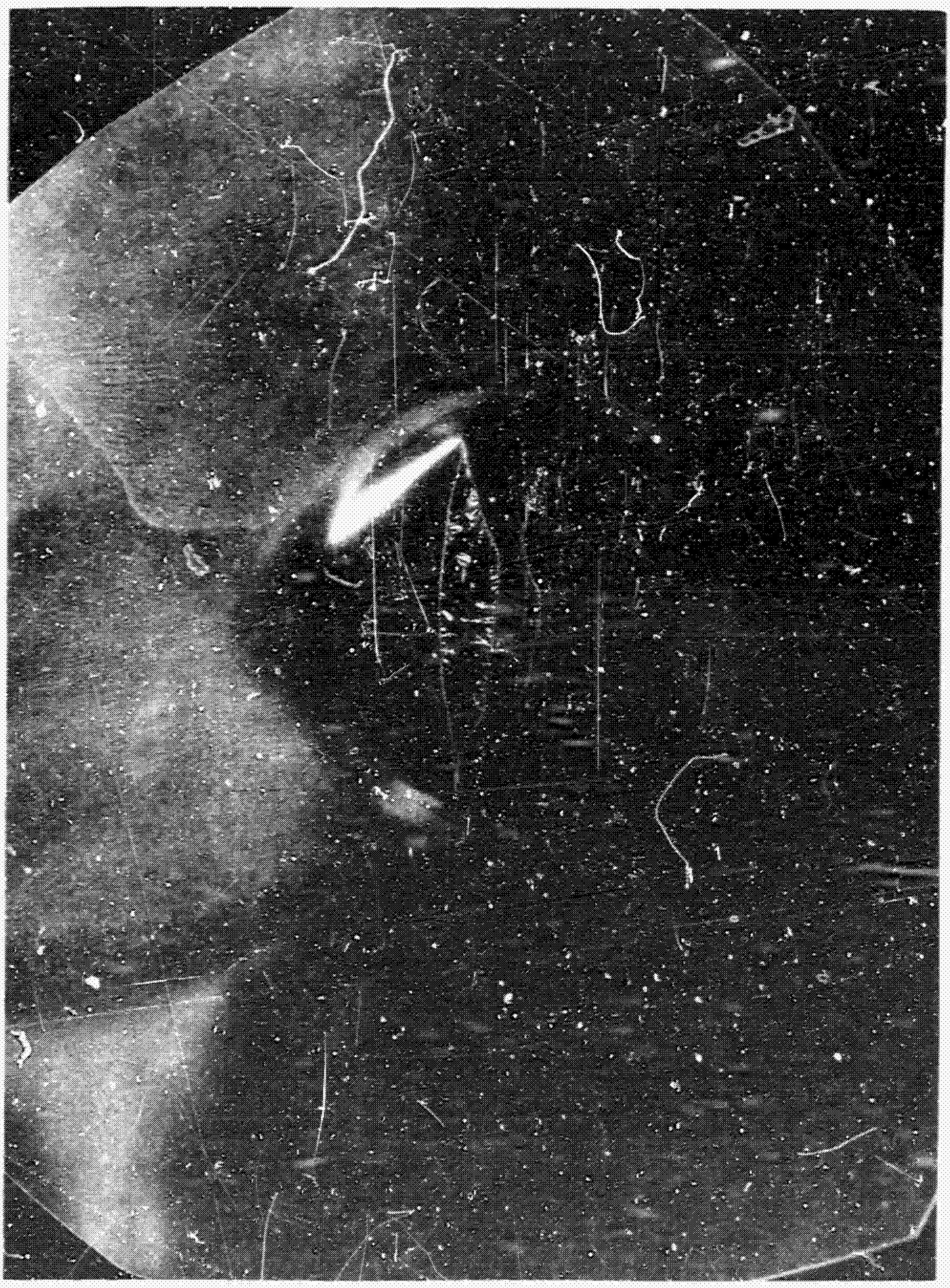

Figure 27. Polyethylene Failure

5.2.2 Polymeric Specimen Design

Preliminary evaluation of the polymeric specimen materials was performed to assist in determining diaphragm size and estimating expected stress levels. The mechanical properties used in the structural evaluation are summarized in table 37. The properties of the Tedlar and Nylon-epoxy were averaged from the tensile tests performed on representative samples selected for this program. The remaining materials were summarized from the literature survey.

The two major design variables which define the stress-pressure relationship for a circular diaphragm of a given material are thickness (t) and the radius (a). Since the plastic materials are available only in limited thicknesses, the diameter (d) or radius (a) is the only permissible variable. Theoretical relationships have been established to evaluate the effects of keeping one parameter constant while the other two vary. The effect of keeping the surface area constant is summarized in table 38. The relative diameters required for constant stress levels and constant pressure levels are shown in tables 39 through 41. For the test conditions where a constant stress level is desired, the required specimen diameter is obtained by reading horizontally in the tables. When constant pressure is desired, the diameters are read vertically from the tables.

The parametric study has indicated that the lower stress levels cannot be obtained by using a single specimen with a minimum surface area or 4.0 square inches (equivalent diameter of 2.257 inches). Table 41 shows that the diameter of the Tedlar specimens must be reduced to 1.4 inches to withstand 1 atmosphere at room temperature. By using a multiport specimen

Table 37. Summary of Mechanical Properties for Structural Study

Test	Properties	Mylar (Type A)	Teflon (FEP)	Tedlar (Type 40)	Poly-ethylene	Polyurethane Foam (H-602N)	Nylon-Epoxy (FM-1000)
Room	ult(psi)	21,000	2,000	7,780	2,000	35.0	6,200
	yld(psi)	--	--	5,666	1,300	--	--
	E (psi)	1.1×10^6	0.16×10^6	0.185×10^6	0.028×10^6	1600	0.041×10^6
	(in/in/°F)	20×10^{-6}					
-320°F	ult(psi)	31,000	14,000	24,000			19,000
	yld(psi	--	--	--			--
	E (psi)	1.9×10^6	1.04×10^6	$.684 \times 10^6$			0.99×10^6
	(in/in/°F)	20×10^{-6}					
-423°F	ult(psi)		20,200				
	yld(psi)		--				
	E (psi)		3.12×10^6				
	(in/in/°F)						
Available Thickness:		.002-.015 (.004)	.005-.040 (.040)	.002			(.006)

Table 38. Summary of Pressure-Stress Relationship for Plastic Specimen

Temp.	Mylar (Type A) t = .004 in. a = 2.0 in. radius			Teflon (FEP) t = .040 in. a = 2.0 in. radius			Tedlar (Type 40) t = .002 in. a = 1.13 in. radius			Nylor-Epoxy (FM-1000) t = .006 in. a = 2.0 in. radius		
	σ(psi)	ρ(psi)	δ(in)	σ(psi)	ρ(psi)	δ(in)	σ(psi)	ρ(psi)	δ(in)	σ(psi)	ρ(psi)	δ(in)
Room	1,000	0.22	.06	100	0.18	.05	100	0.015	-	100	0.054	-
	3,000	1.14	.11	200	0.54	.07	1,000	0.47	.01	1,000	1.70	.32
	5,000	2.45	.14	600	2.67	.12	2,000	1.34	.01	2,000	4.82	.45
	10,000	6.93	.19	1,000	5.75	.16	4,000	3.79	.02	4,000	13.62	.64
	15,000	12.73	.24	1,500	10.56	.20	6,000	6.96	.02	5,000	19.04	.71
	21,000	21.10	.28	2,000	16.25	.23	(7,780)	10.28	.02	6,200	26.29	.79
-320°F	1,000	0.17	.05	200	0.20	.02	200	0.022	-	200	0.03	-
	3,000	0.87	.08	1,000	2.25	.06	1,000	0.25	.04	1,000	0.35	.06
	5,000	1.86	.10	2,000	6.38	.09	3,000	1.28	.08	3,000	1.80	.11
	10,000	5.27	.15	5,000	25.21	.14	5,000	2.75	.10	5,000	3.87	.14
	15,000	9.69	.18	8,000	51.01	.18	10,000	7.78	.14	8,000	7.84	.18
	20,000	14.92	.20	10,000	71.28	.20	15,000	14.29	.17	10,000	10.96	.20
	25,000	20.85	.23	12,000	93.70	.22	20,000	22.00	.20	15,000	20.13	.25
	31,000	28.79	.26	14,000	118.08	.24	24,000	28.92	.22	19,000	28.70	.28
-423°F				1,000	1.30	.04						
				2,000	3.68	.05						
				5,000	14.55	.08						
				8,000	29.45	.10						
				10,000	41.156	.11						
				12,000	54.10	.13						
				15,000	75.62	.14						
				18,000	99.39	.15						
				20,200	113.15	.16						

Table 39. Specimen Diameter for Constant Pressure/Stress Ratio for Mylar

Material Thickness = 0.004 in.

	p psi / σ psi	Specimen Diameter (d) inches			
		14.7	20.0	30.0	50.0
Room Temp. $Pd = 27.7252 \times 10^{-6}\ \sigma^{3/2}$	5,000	.31	.23	.15	.09
	10,000	1.88	1.39	.92	.55
	15,000	3.46	2.55	1.70	1.02
	20,000	5.34	3.92	2.62	1.57
$-320^{\circ}F$ $Pd = 21.0957 \times 10^{-6}\ \sigma^{3/2}$	5,000	.51	.37	.25	.15
	10,000	1.44	1.05	.70	.42
	20,000	4.06	2.98	1.99	1.19
	31,000	7.84	5.76	3.84	2.30

Table 40. Specimen Diameter for Constant Pressure/Stress Ratio for Teflon

	$\frac{p\,psi}{\sigma\,psi}$	Material Thickness = 0.004 in. Specimen Diameter (d) inches		
		14.7	20.0	30.0
Room Temp. $Pd = 72.696 \times 10^{-5}\ \sigma^{3/2}$	600	0.073	0.053	0.036
	1,000	0.156	0.115	0.076
	1,500	0.288	0.212	0.141
	2,000	0.442	0.326	0.216
$-320^{\circ}F$ $Pd = 28.5136 \times 10^{-5}\ \sigma^{3/2}$	1,000	0.061	0.045	0.030
	5,000	0.686	0.504	0.336
	10,000	1.940	1.426	0.950
	14,000	3.214	2.362	1.574

Table 41. Specimen Diameter for Constant Pressure/Stress Ratio for Tedlar

		Material Thickness = 0.002 inches		
	ρ psi / σ psi	Specimen diameter (d) inches 14.7	20.0	30.0
Room Temp. $Pd = 33.85788 \times 10^{-6} \sigma^{3/2}$	1,000	.072	.054	.036
	2,000	.206	.142	.100
	4,000	.582	.428	.286
	(8,000)	1.426	1.212	.308
$-320^{\circ}F$ $Pd = 17.57974 \times 10^{-6} \sigma^{3/2}$	1,000	.038	.028	.018
	5,000	.422	.310	.208
	15,000	2.20	1.614	1.076
	20,000	3.38	2.48	1.658
	24,000	4.44	3.28	2.18

holder similar to figure 28, the material can be tested at the desired stress/pressure levels and still provide the required permeation surface area.

5.2.3 Liquid Monomethylhydrazine Tests

Preliminary testing of polymers with MMH was initiated with a 5 mil thick Teflon FEP diaphragm, using the multi-hole diaphragm mount described in section 3.4.2 without the compression ring. With MMH covering the specimen, the diaphragm was stressed to several levels with dry nitrogen gas. However, the results clearly indicated that gaseous nitrogen diffused rapidly into the high vacuum of the dutchman, indicating high liquid propellant permeability by nitrogen and leakage of the material and seal as discussed in section 5.2.5. Argon gas was substituted for nitrogen. Rapid diffusion of argon into the dutchman was also observed. This indicated that pressurization of the liquid propellant has to be done with a gas having a very large molecule, i.e., Freon 12.

No specific permeation values for MMH could be determined. However, no changes in the residual gas peaks could be attributed to MMH permeation nor were any new m/e peaks observed.

5.2.4 Liquid Nirtrogen Tetroxide Tests

Testing of N_2O_4 on Teflon FEP was conducted using 5, 10 and 20 mil thick material mounted on the polymeric diaphragm mount using the compression ring seal. Difficulties with the 5 and 10 mil material attributed to the imperfections proved uncontrollable and only some of the tests with 20 mil material yielded satisfactory results. The test results in terms of leak rates are presented in table 42. Permeation values in terms of SPU were

E0865

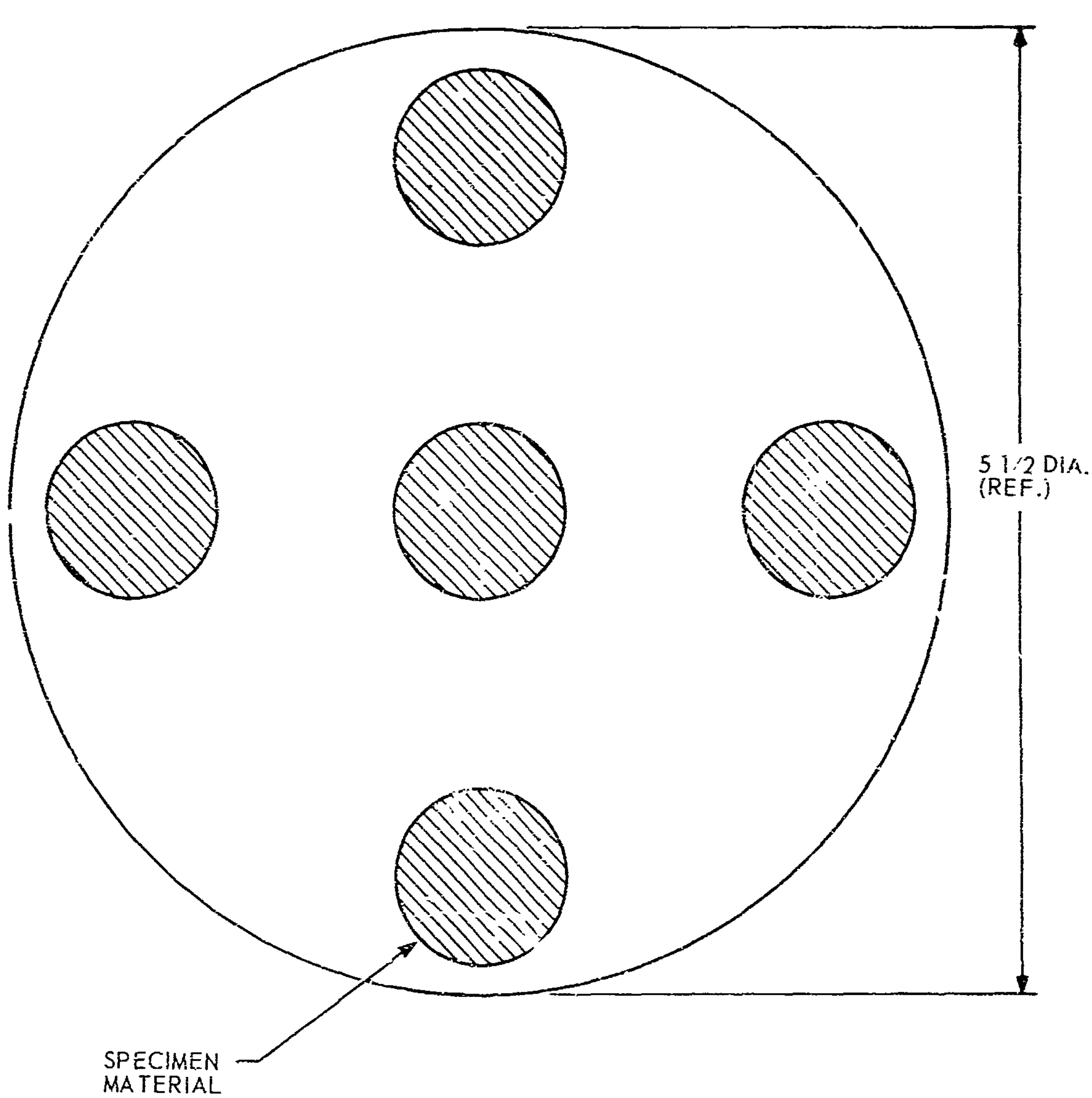

Figure 28. Typical Multi-Port Specimen

Table 42. N_2O_4-Teflon FEP Test Results

Overpressure*	m/e 30 Leak Rate** (cc/sec)	Permeation $\left(\frac{cc\text{-}cm}{cm^2\text{-}cm\ Hg\text{-}sec}\right)$	Calculated Stress (psi) σ_H***	σ_{SM}****
55 psia	2.66×10^{-8}	3.17×10^{-14}		
	3.17×10^{-8}	3.78×10^{-14}		
	3.92×10^{-8}	4.67×10^{-14}		
Avg.	3.25×10^{-8}	3.87×10^{-14}	172	9.1
75 psia	2.17×10^{-8}	1.90×10^{-14}		
	4.45×10^{-8}	3.89×10^{-14}		
Avg.	3.31×10^{-8}	2.89×10^{-14}	235	12.3

*Diaphragm
**Based on system sensitivity for m/e 28
***Stress in unsupported material holes
****Stress in supported material

calculated in terms of the total surface area exposed to the test fluid (see section 5.2.5). These values are presented in table 42. No significant change in permeation rate with increasing pressure is apparent. However, since the stresses introduced during test were very low (1% of yield), no conclusions regarding the effect of stress on permeation can be drawn.

5.2.5 Gaseous Nitrogen Tests

During the initial testing of polymeric diaphragms with N_2O_4 or MMH it was noted that seal leakage occurred, especially of nitrogen gas when used as the pressurizing medium. Using the high sensitivity for nitrogen, it was quickly shown that a compression ring had to be used for adequate sealing. The compression ring used was a previously-compressed aluminum O-ring which provided approximately 75% reduction in thickness of the diaphragm material. This sealing technique was developed using 15 mil Teflon TFE material to preclude the possibility of test material porosity obscuring the results.

The final tests on this material, Teflon TFE, not only showed seal adequacy but provided GN_2 permeation data through this material. The leak rates obtained are presented in table 43. Permeation values in terms of SPU were calculated in terms of both the area of the 26 1/4-inch diameter test holes of the diaphragm mount and of the total surface area within the compression ring seal. These values are presented in table 43. The permeation rates shown in the second column (based on total area) are believed to represent the true values. That is, the surface within the compression ring seal is uncompressed and the entire top surface is exposed to GN_2 while high vacuum is exposed to the entire lower surface. The compression ring seal acts as an edge clamp with the stress field existing over the entire specimen with some stress concentration in the material where it is unsupported over the holes.

Table 43. GN_2-Teflon TFE Test Results

Overpressure	Leak Rate* (cc/sec)	Permeation $\frac{cc\text{-}cm}{cm^2\text{-}cm\ Hg\text{-}sec}$ (1)	(2)	Calculated Stress (psi) σ_H**	σ_{SM}***
75μ	4.7×10^{-5}				
1 atoms.	8.7×10^{-5}	2.44×10^{-9}	1.31×10^{-10}	46.9	2.5
15 psig	1.3×10^{-4}	2.49×10^{-9}	1.34×10^{-10}	93.8	5.0
45 psig	2.1×10^{-4}	2.44×10^{-9}	1.31×10^{-10}	141.0	7.5
Extrapolated value	4.8×10^{-5}				

*Each entry, average of three values

(1) Based on area of 26 test holes only

(2) Based on area within seal compression ring

**Stress in unsupported material over holes

***Stress in supported material

Permeation values in terms of SPU based on the total area within the compression ring seal are compared with ΔP in figure 29. No significant change in permeation rate with increasing pressure is apparent. However, since the stresses introduced during test were very low (1% of yield), no conclusions regarding the effect of stress on permeation can be drawn.

Testing of Teflon FEP in thicknesses of 5, 10, and 20 mils using the developed sealing technique yielded erratic data. The thinner the material, the more erratic the data appeared. This behavior is describable in terms of variation in the degree of high vacuum obtainable, the variation in leak rates at a given condition, the observation of small random pressure bursts and in some cases high vacuum improvement on incremental pressure increases of GN_2. The latter is similar to observations made on diaphragms insufficiently compressed at the sealing surface.

Satisfactory test runs were performed using a 20-mil Teflon FEP sample. Permeation values in terms of SPU were calculated and are presented in figure 29 for comparison with Teflon TFE values. Stress in the material does not appear to effect the permeation rate. The permeation rate of GN_2 through Teflon FEP is somewhat higher than that through Teflon TFE.

The higher permeation rate and erratic performance of the Teflon FEP is attributed to the imperfections in the material. Figure 30 shows a typical specimen of 10-mil thick material after test, taken under polarized light. The lines are scratches in the polarizing film. Close examination reveals point-like imperfections similar to the one near the center of the specimen which is circled. Examination of this typical imperfection at high magnification (figures 31 and 32) reveals what appears to be a hole

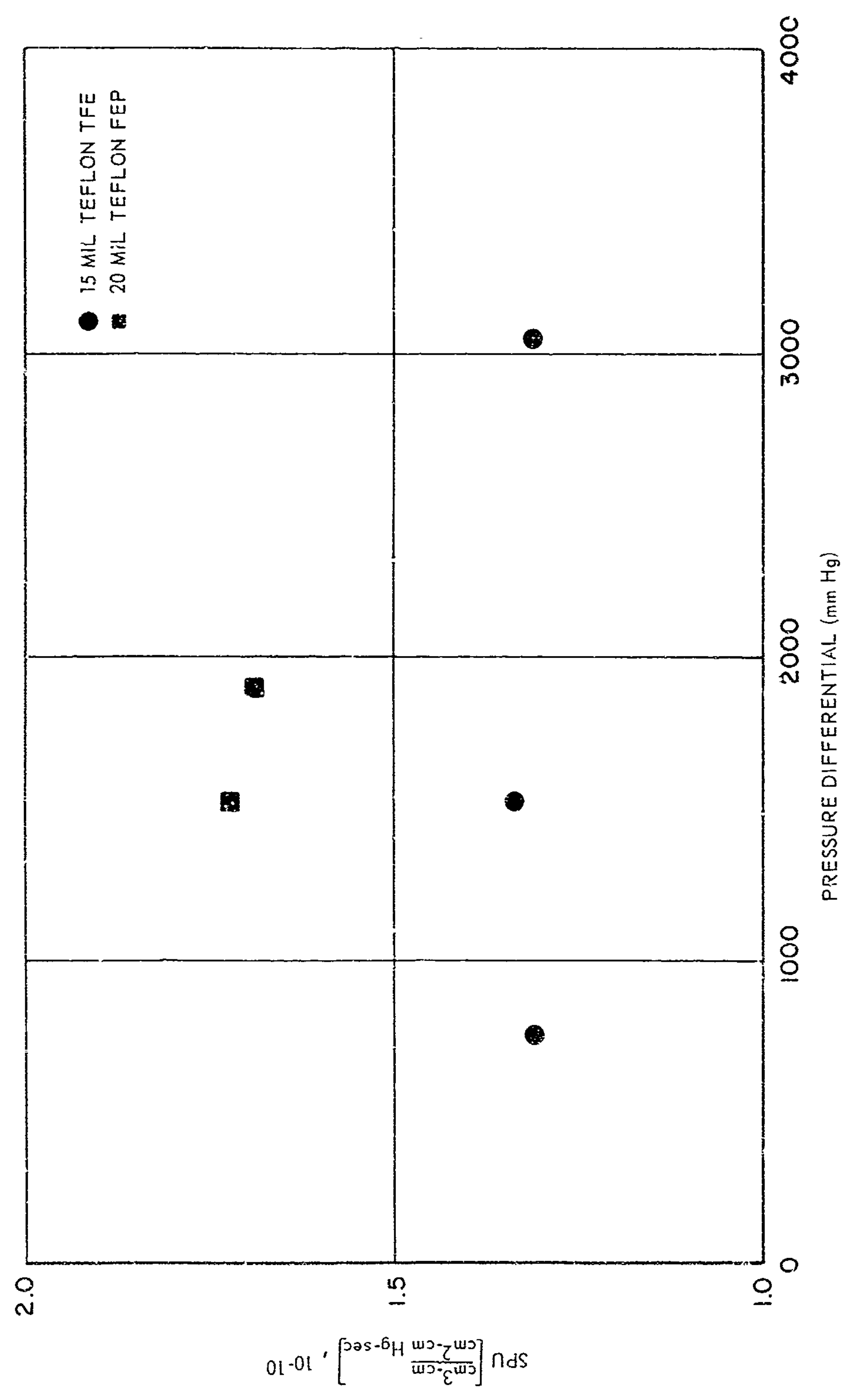

Figure 29. Permeability of GN_2 Through Teflon

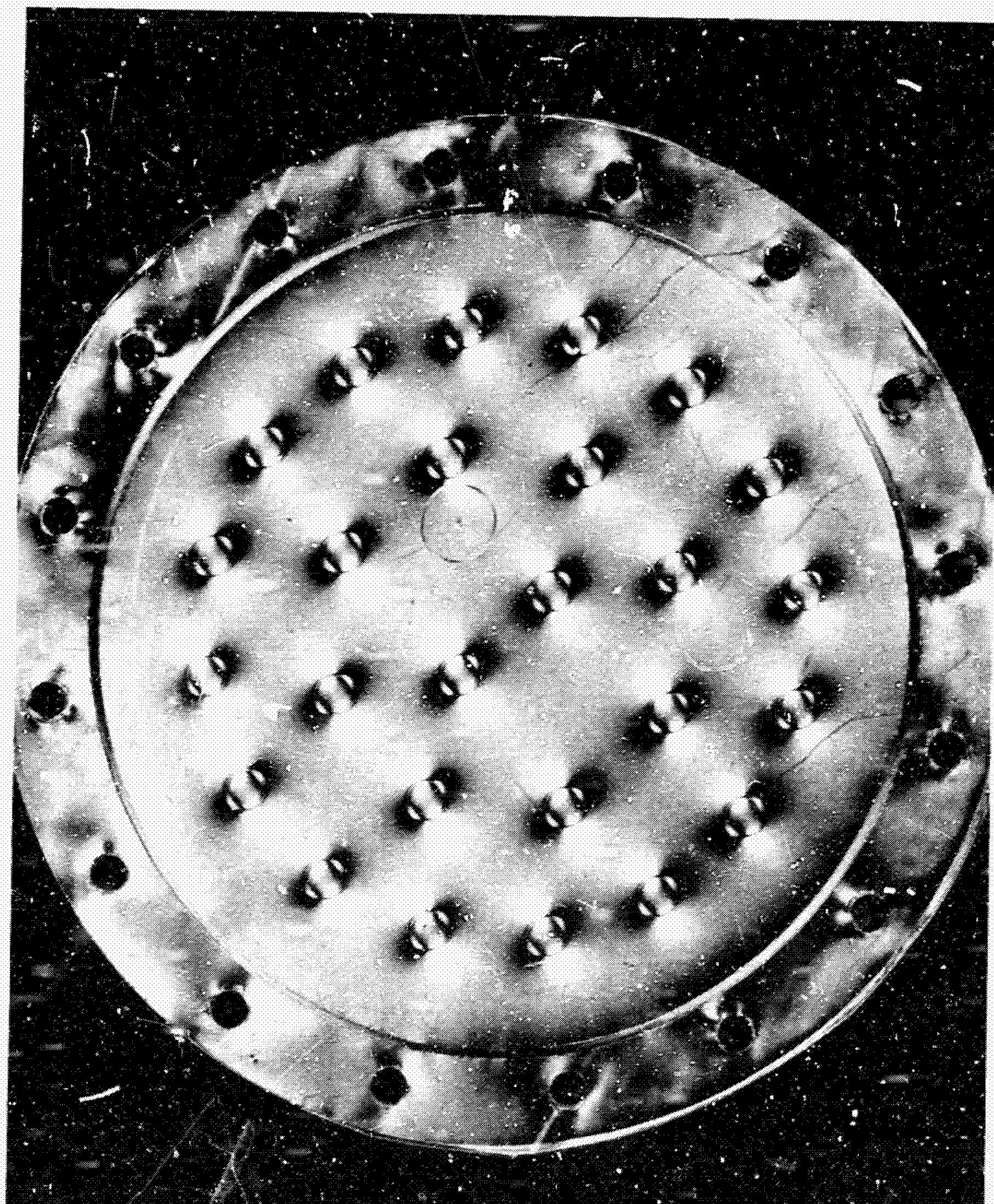

Figure 30. Typical Teflon FEP 10-mil-Thick Specimen After Testing With GN_2, Polarized Light

Figure 31. Selected Area of 10-mil Teflon FEP Diaphragm, 23X, Polarized Light

E2855

Figure 32. Selected Area of 10-mil Teflon FEP Diaphragm 112X, Polarized Light

or depression in the material, partially filled with a crystalline substance. This could be a dust particle embedded during manufacture, or residual, unreacted, or partially reacted catalyst used in the manufacture.

Random examination of the 5, 10 and 20 mil material, figures 33 through 35, shows the apparent density of the imperfections to increase slightly with thinner material. Approximately 50 such imperfections may be observed in any 5.5-inch diameter specimen. High magnification photomicrographs of one imperfection observed in 5-mil thick material is shown in figures 36 and 37 as viewed from either side of the material. Again, the crystalline appearance of the particle is apparent. Complete penetration of the hole through the material is questionable. Similar crystalline particles are observable in 10-mil material, figures 38 and 39.

Review of figure 31 shows short lines aligned about the imperfection which are related to the stress pattern. Comparison with "as received" material in figure 38 shows these short lines to result from stressing during testing and may possibly be induced local crystallinity in the material.

Figure 33. As-Received 5-mil Teflon FEP Sheet Polarized Light

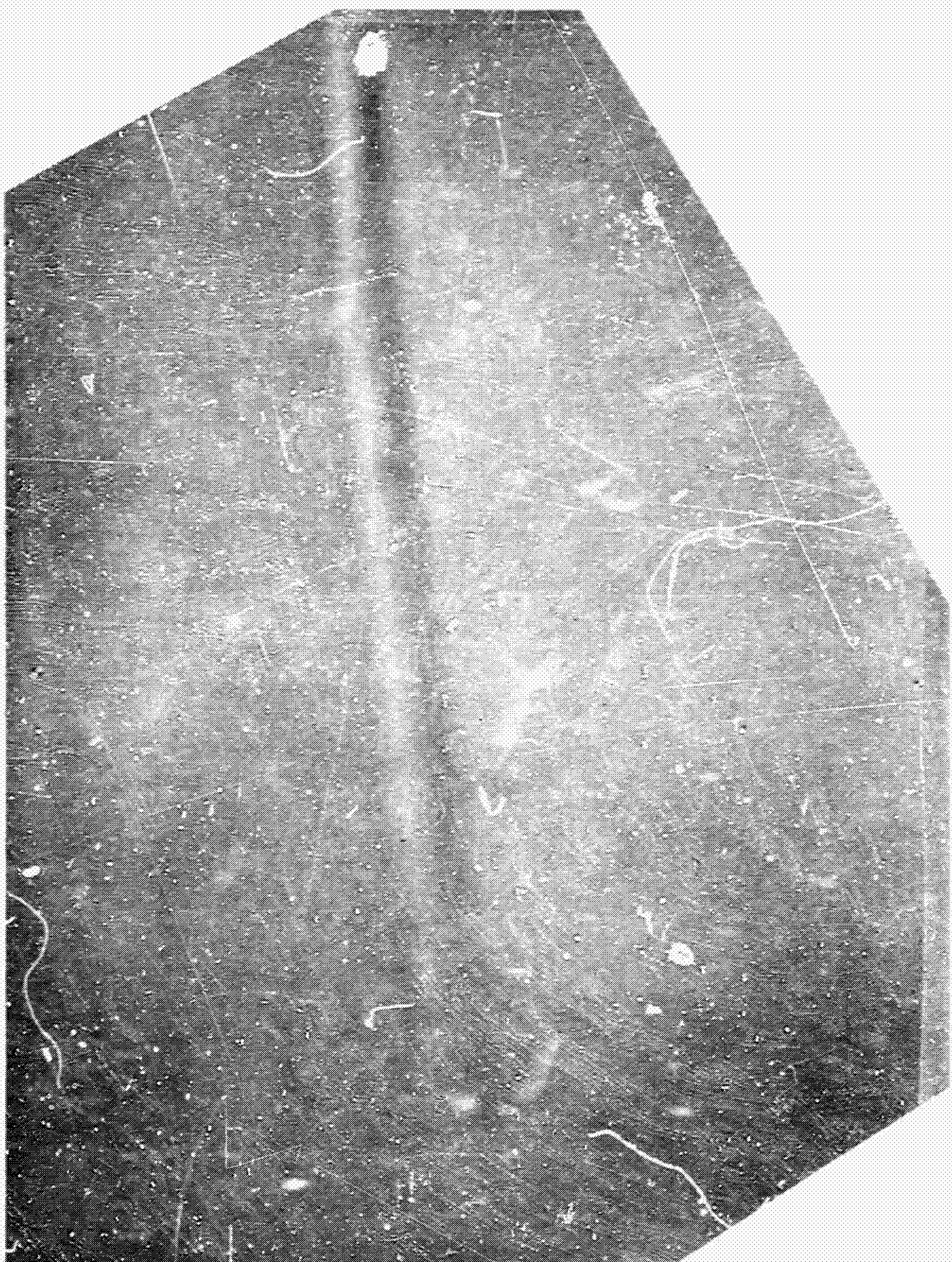

Figure 34. As-Received 10-mil Teflon FEP Sheet Polarized Light

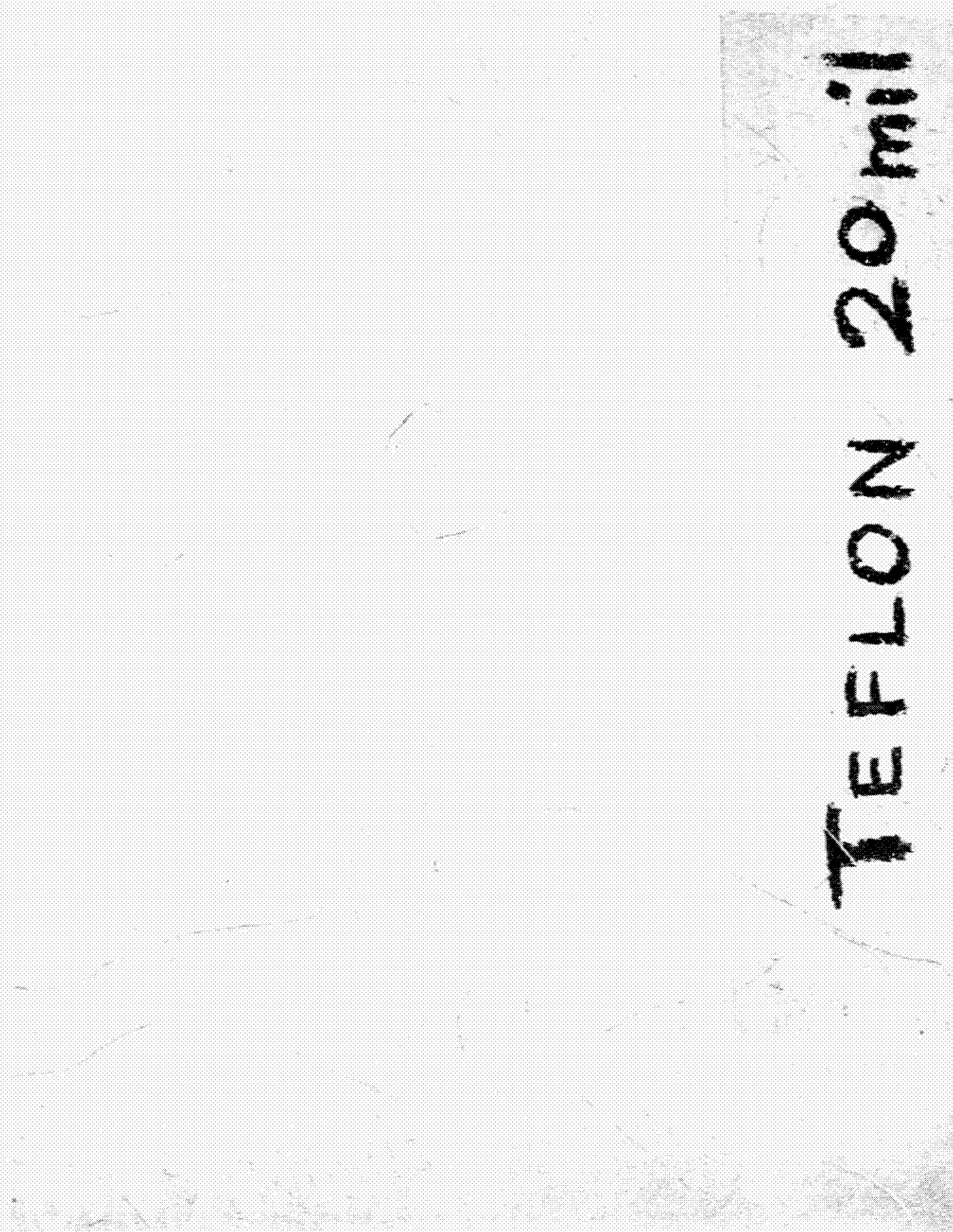

Figure 35. As-Received 20-mil Teflon FEP Sheet Polarized Light

Figure 36, Selected Area of 5-mil Teflon FEP as Received Sheet, 160X, Polarized Light

Figure 37. Reverse Side of Selected Area of 5-mil Teflon FEP As-Received Sheet, 160X, Polarized Light

E2858

Figure 38. Selected Area of 10-mil Teflon FEP As-Received Sheet, 31X, Polarized Light

E2859

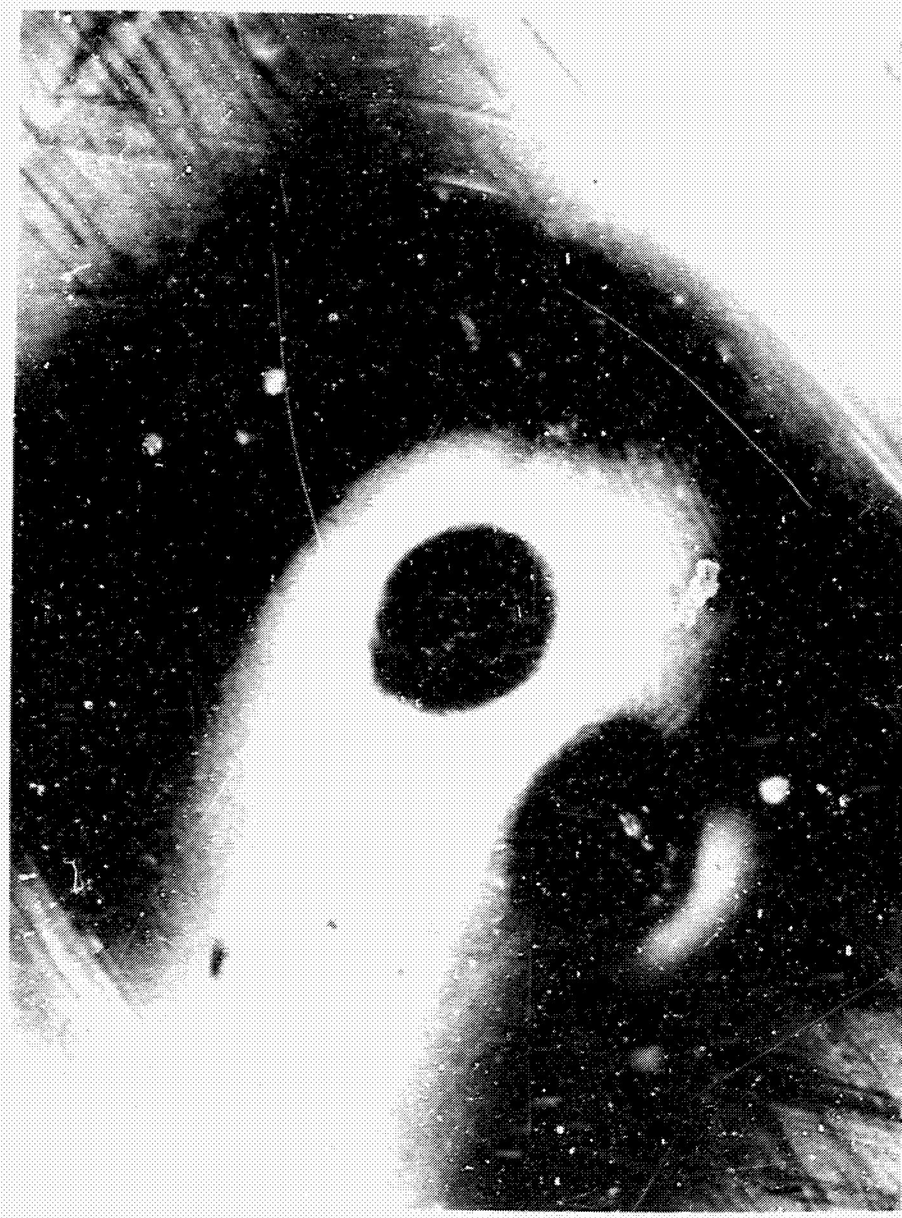

Figure 39. Selected Area of 10-mil Teflon FEP As-Received Sheet, 112X, Polarized Light

6. CONCLUSIONS

a. Apparatus and techniques evolved and currently in use are considered suitable for the measurement of permeability rates through highly stressed materials in the range of 10^{-10} to 10^{-17} SPU.

b. The chemical compatibility of Mylar, aluminized Mylar, aluminized Tedlar, nylon-based adhesive, polyurethane foam, silicon rubber, and polyvinyl chloride with monomethylhydrazine was found inadequate for uses involving prolonged exposure in terms of either dissolution, fluid discoloration, and/or degradation of mechanical properties.

c. Polymeric materials found most compatible with monomethylhydrazine included Teflon (FEP), Tedlar, and polyethylene.

d. The mechanical properties of metallic and polymeric materials both at room and cryogenic temperatures were evaluated and tabulated. In instances where vendor data exist, such data were correlated with obtained values.

e. Coarse permeability screening tests were found suitable in the identification of such limiting parameters as specimen dimensions and material imperfections.

f. All metallic diaphragms tested with MMH, N_2O_4, and LN_2 exhibited permeability rates of less than the detectable limits of the experimental apparatus while stresses to major fractions of their respective biaxial yield stresses.

g. Probable permeation of hydrogen through 0.008 inch stainless steel at liquid hydrogen temperature was observed during apparatus checkout.

h. The permeability of nitrogen tetroxide through Teflon was observed to be in the range of 1 to 4 x 10^{-14} SPU. The values observed did not appear to be affected by stress level.

i. The permeability of gaseous nitrogen through Teflon was observed to be in the range of 1.3 to 1.7 x 10^{-10} SPU. The values observed did not appear to be affected by stress level. Permeation rates for FEP Teflon were found to be higher than those for TFE Teflon.

j. The degree of permeability of the polymeric materials was observed to be related to imperfection density. Consequently, the predominant mechanism of permeation appears to be seepage through imperfections.

7. FUTURE WORK

Melpar's current effort will be extended to include studies of the permeability of stressed composite materials to certain propellants. These materials include reinforced polymeric materials, laminates, adhesives, and honeycomb structures which are more directly applicable to space vehicles. It is anticipated that the work will shed additional information on the complex problem of permeability wherein a basis for the selection and development of materials for use as aerospace hardware can be developed.

8. REFERENCES

1. R. M. Barrer, Transactions Faraday Society (London), 35, p. 628 (1939).

2. A. S. Michaels and H. J. Bixler, Journal of Polymer Science, 50, p. 393 and 413 (1951).

3. A. S. Michaels and R. B. Parker, Journal of Polymer Science, 41, p. 53 (1951).

4. S. B. Tuwiner, Diffusion and Membrane Technology, Reinhold Publishing Corporation (1962).

5. G. J. Van Amerogen, Journal of Polymer Science, 5, p. 307 (1950).

6. R. M. Barrer, Transactions Faraday Society (London), 35, p. 644 (1939).

7. D. W. Brubaker and K. Kammermayer, Industrial and Engineering Chemistry, 45, p. 1148 (1953).

8. J. M. Toth, Jr. and J. R. Barber, Cryogenic Engineering Conference held at Philadelphia, Pa. (August 1964).

9. W. Jost, Diffusion in Solids, Liquids and Gases, Academic Press, Inc. New York (1960).

10. C. Rogers, J. A. Meyer, V. Stannett, and M. Szwasc, Tappi, 39, 737 (1956).

11. A. W. Myers, C. Rogers, V. Stannett, and M. Szwasc, Tappi, 41, p. 716 (1958).

12. A. W. Myers, C. Rogers, V. Stannett, and M. Szwasc, Modern Plastics, 34, No. 9, 157 (1957).

13. C. H. Franklin, P. J. Klute, Journal of Polymer Science, 32, p. 161 (1958).

14. Harvey Alter, Journal of Polymer Science, 57, p. 925 (1962).

15. W. W. Brandt, Journal of Polymer Science, 41, p. 403 (1959).

16. R. Waack, N. H. Frisch, H. L. Stannett, and M. Szwasc, Industrial and Engineering Chemistry, 47, p. 2524 (1955).

17. C. D. Bailey et al, paper presented at National Aeronautic and Space Engineering and Manufacturing Meeting, Los Angeles, paper No. 746D (September 1963).

18. Boris Lavenetz, Lecture presented at University of California as a part of the course "Reinforced Plastics" (October 1963).

19. R. M. Basser, Diffusion in and Through Solids, Cambridge University Press, London (1951).

20. S. Dushman, Vacuum Technique, Wiley, New York (1949).

21. Von D. Jeschke and H. A. Stuart, Z. Naturfoeschg., 16a, pages 37-50 (1961).

22. A. Goldsmith, Hirschhom, and T. E. Waterman, WADC Technical Report 58-476 "Thermophysical Properties of Solid Materials."